UNIVERSITY OF BREMEN

MASTER THESIS

Benthic Soft-bottom Communities and Ecosystem Functions on the Northeast Greenland Shelf

Yasemin Bodur

1st Examiner:
Prof. Dr. Thomas Brey[1]

2nd Examiner:
Dr. Ulrike Braeckman[2]

[1] Alfred Wegener Institute, Helmholtz Centre for Polar and Marine Research, Germany
[2] Ghent University, Marine Biology Research Group, Belgium

A thesis submitted in fulfillment of the requirements for the degree of ***Master of Science***

September 25, 2018

"For the game of Western philosophy and science is to trap the universe in the networks of words and numbers, so that there is always the temptation to confuse the rules, or laws, of grammar and mathematics with the actual operations of nature. [...] every thing-event is what it is only in relation to all others. "

Alan Watts, Tao: The Watercourse Way

Contents

List of Figures

List of Tables

List of Abbreviations

79NG	79N Glacier; Nioghalvfjerdsbrae
ADCP	Acoustic Doppler Current Profiler
AIW	Atlantic Intermediate Water
AW	Atlantic Water
CA	Correspondence Analysis
CCA	Canonical Correspondence Analysis
Chl *a*	Chlorophyll *a*
CPE	Chloroplastic pigment equivalent (Chlorophyll *a* and Phaeopigments)
CTD	Conductivity, Temperature, Depth prolifer
DCA	Detrendend Correspondence Analysis
DIC	dissolved inorganic carbon
DOU	diffusive oxygen uptake
EGC	East Greenland Current
GAM	Generalized Additive Model
KW	Knee Water
mAIW	glacially modified Atlantic Intermediate Water
(TV-) MUC	(TV-) Multicorer
NEG	Northeast Greenland
NEGIS	Northeast Greenland Ice Sheet
NEW	Northeast Water
NØIB	Norske Øer Ice Barrier
nMDS	non-metric multidimensional scaling
OM	organic matter
PERMANOVA	permutational analysis of variance
pers. comm.	personal communication
PW	Polar Water
SCA	single cell abundance
SIMPROF	similarity profile routine analysis
TA	Total Alkalinity
TOU	total oxygen uptake

Abstract

Benthic communities regulate numerous ecosystem processes and rely almost exclusively on the sinking of organic matter from the pelagic. In association with climate change the Arctic sea ice is shrinking, glacial discharge is increasing and Arctic marine ecosystems are expected to become more Atlantic in character. For the last 20 years, these environmental changes were observed for the Northeast Greenland (NEG) shelf and might have altered benthic community structures and their function in this region. In September/October 2017, soft-bottom communities were sampled and oxygen consumption was measured ex situ over time at 13 stations on the NEG shelf. Sediment granulometry and porosity, pigment concentrations and porewater chemistry (DIC, nutrients, sulfate, chloride) were assessed to characterize the habitat. It was found that macrofauna communities did not separate among regions, while foraminifera communities (>500 μm) and polychaeta did distinguish the northern Westwind Trough from the southern Norske Trough and the 79N Glacier. Benthic pigment concentration was the most important predictor for the community structure. Total abundance and biomass of macrofauna, single cell abundances, porewater DIC and ammonia concentrations were highest in the Westwind Trough compared to all other regions, which suggests the highest benthic productivity in the Westwind Trough. Overall benthic pigment concentrations were up to sevenfold lower compared to the 1990s, accompanied by a fivefold lower total abundance of macrofauna. The present study confirms previous reports about a strong pelagic-benthic coupling on the NEG shelf which might have weakened since the 1990s, suggesting that this is a result of higher zooplankton grazing. Longer ice-free periods and higher inflow of warm Atlantic Water on the NEG shelf might have led to favourable conditions for zooplankton of Atlantic origin, increasing pelagic mineralization that would finally lead to a reductrion in the amount of organic matter reaching the sea floor.

Keywords: sediment, nutrients, infauna, NEW Polynya

1 Introduction

1.1 Climate change and Arctic benthos

As a result of climate change, polar regions are warming more than any other region on earth (Turner and Marshall, 2011). In the Arctic, the summer sea ice extent is declining at a rate that the region could be left ice-free in summer by the middle of this century (IPCC, 2013). Enhanced glacial melt, especially at Greenland's glaciers (Rignot and Kanagaratnam, 2006; Nick et al., 2013) and the shifting of warming water masses towards the high North (Beszczynska-Möller et al., 2012) are further effects that come along with climate change. This will most likely lead to drastic changes in Arctic ecosystems through all trophic levels.

Marine ecosystems in the Arctic are characterized by extreme seasonal changes in light availability and primary production due to seasonal sea ice dynamics (Leu et al., 2015). Pelagic mineralization patterns determine the amount of Organic Matter (OM) that sinks to the sea floor and ultimately serves as food for benthic communities (Graf, 1989; Wassmann and Reigstad, 2011). This has an impact on benthic functions and processes (Morata et al., 2015). A strong dependency of benthic ecosystems on pelagic processes in the Arctic (i.e. "pelagic-benthic coupling"; Fig. 1.1) has been documented for various fjord (e.g. McMahon et al., 2006) and shelf systems (Link et al., 2013; McTigue et al., 2015) as well as for the deep Arctic Ocean (Degen et al., 2015).

Several scenarios are discussed for the consequences of shrinking sea ice regarding primary production and with that on the fate of OM reaching the sea floor (Wassmann and Reigstad, 2011). A longer period of light availability might fuel more pelagic phytoplankton blooms (Arrigo et al., 2008), but the establishment of a bloom depends on multiple factors such as nutrient availability, vertical mixing and the amount of wind stress (Ardyna et al., 2014). These factors can be further influenced by sea ice loss and might affect primary production in a negative or positive way, depending on the region.

Moreover, primary production is determined by sea ice algae and pelagic phytoplankton in concert, whereby sea ice algae can contribute in a high amount to spring primary production (Horner and Schrader, 1982). Sea ice algae are regarded as a food source with higher nutritional value (Falk-Petersen et al., 1998). With a shorter sea ice season during the year, contribution to OM from both sources should shift towards phytoplankton, altering the quality and quantity of food reaching the benthos (Smith et al., 2013; Mäkelä et al., 2017b; Braeckman et al., 2018).

In the vicinity of glaciers, benthic communities are additionally influenced by glacial activity. Glacial meltwater input influences directly the physical dynamics of the water e.g. in terms of water column stratification, salinity and temperature as well as nearshore turbidity which in turn inhibits primary production at the surface due to the lower light availability (Görlich et al., 1987; Dierssen et al., 2002). Organisms at glacier proximities are subject to chronic physical disturbance and experience

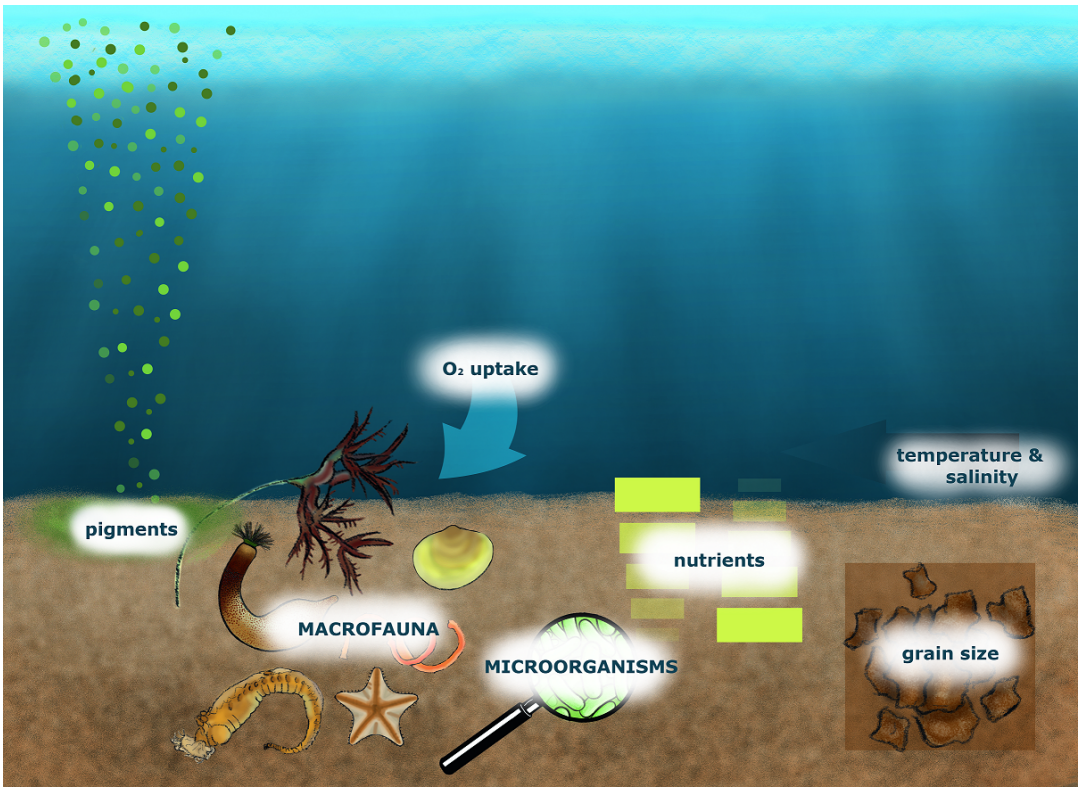

FIGURE 1.1: **Schematic illustration of pelagic-benthic coupling.** Organic matter sinking down from the upper water column, induced by primary production, determines the composition and amount of food (pigments) that is available for benthic communities. This study focused on macrofauna and microorganisms (single cell abundances) as components of the benthic community. They take up oxygen during the consumption of food. By their activity, nutrients get remineralized, which is an important function of the benthos. Environmental parameters, e.g. grain size and water properties (temperature & salinity) can influence the distribution and functioning of benthic comminities (M. Bodur).

low food input (Gutt, 2001; Włodarska-Kowalczuk and Pearson, 2004; Renaud et al., 2007b). Therefore, rather small and/or motile surface deposit-feeders or predators are mainly observed near glaciers (Włodarska-Kowalczuk et al., 2005; Renaud et al., 2007b; Pasotti et al., 2015) and species diversity is usually low (Włodarska-Kowalczuk et al., 2005; Renaud et al., 2007b; Pasotti et al., 2015).

Depending on wind and water circulation patterns, marine terminating glaciers may be important for marine productivity due to the initiation of nutrient upwelling (Meire et al., 2017; Hopwood et al., 2018), or may enhance stratification in fjords, counteracting primary production (van de Poll et al., 2018). Recently, the mass losses of the Greenland ice sheet quadrupled from 51 $\pm$ 65 $Gtyr^{-1}$ (1992-2000) to 211 $\pm$ 37 $Gtyr^{-1}$ (2000-2011; Shepherd et al., 2012). Especially the marine tidewater glaciers are subject to rapid retreats (Moon and Joughin, 2008), and their transformation into land-terminating glaciers is likely (Meire et al., 2017), which could have effects on the structure and functions of benthic communities (Pasotti et al., 2015).

Another important feature that may alter benthic communities in the Arctic is the flow of warm Atlantic water towards the Arctic Ocean (Ślubowska et al., 2005; Beszczynska-Möller et al., 2012). If Atlantic water will warm further, Arctic regimes may become more Atlantic in character (Cochrane et al., 2009). The introduction of species from the Atlantic can alter the benthic community composition, and finally the functioning of benthic ecosystems. A shift of Atlantic species further North is

ongoing across all trophic levels (e.g. Drinkwater, 2006; Fleischer et al., 2007; Hegseth and Sundfjord, 2008; Gregory et al., 2009; Kortsch et al., 2012; Braeckman et al., 2018). A "borealization" of Arctic benthic communities is seen in fjord systems around Svalbard (Kortsch et al., 2012) and in the Northern Bering Sea (Grebmeier et al., 2006). Predation pressure could change through the introduction of higher trophic animals. Zooplankton communities that are adapted to longer time of food availability might alter the tightness of the pelagic-benthic coupling through their grazing activities (Olli et al., 2007).

1.2 The importance of benthic communities in marine systems

The amount of OM that is exported vertically varies regionally. On average, only a small fraction of the primary production (< 5%) is settling to the sea floor, serving as food for the benthos (Schlüter et al., 2000). Pelagic processes, both biological (zooplankton grazing, microbial recycling) or physical (e.g. lateral advection) influence this export (Grebmeier and Barry, 1991). Microorganisms, single celled protists (especially foraminifera) and metazoans together constitute benthic communities. These are broadly distinguished according to their size (meiofauna, $0.02 - 1$ mm; macrofauna, $0.5 - 20$ mm and megafauna > 20 mm) and their ecological niche (infauna and epifauna). Benthic communities regulate numerous ecosystem processes such as carbon uptake, nutrient cycling (Link et al., 2013), oxygen respiration, organic matter decomposition, carbon burial and bioturbation (Clough et al., 1997). They deliver an important food source for e.g. marine mammals (Grebmeier et al., 2006). Opposing a common statement that the Arctic benthos is species-poor, it is, globally seen, rather characterized by intermediate diversity (Piepenburg et al., 2011).

In infaunal communities, polychaetes are usually the most abundant taxon (Hartmann-Schröder, 1996). They are regarded as good predictors of variability in Arctic macrobenthic communities (Włodarska-Kowalczuk and Kedra, 2007). The same was observed for foraminifera (Włodarska-Kowalczuk and Kedra, 2007; Mojtahid et al., 2008; Denoyelle et al., 2010). Foraminifera are important components of benthic communities and can account sometimes for 50 % or more of eukaryotic biomass (Gooday et al., 1992). Studies in polar regions that comprise several fractions of benthic communities and relate their distribution patterns to prevailing environmental drivers are rare (e.g. Piepenburg et al., 1997; Włodarska-Kowalczuk et al., 2013; Pasotti et al., 2015). Usually, investigations concentrate on only one fraction because the spanning of all size ranges is extremely elaborate, costly and time-consuming. However, it is necessary to get the full picture of the functioning of benthic communities.

1.3 The NE Greenland Shelf - case example for a changing Arctic

The Northeast Greenland Ice Sheet (NEGIS) is the largest part of the Greenland Ice Sheet. While the glaciers of Southeast and Northwest Greenland are subject to strong mass losses, the northern sector exhibited a small loss for a long time (Rignot and Kanagaratnam, 2006). However, starting between 2003 and 2006, glaciers around Northeast Greenland undergo sustained dynamic thinning (Khan et al., 2014). The

melting is probably triggered by increasing air temperature and the resulting reduced sea-ice concentration (Khan et al., 2014) which normally suppresses calving front retreat (Nick et al., 2012) and/or rising ocean temperatures (Mouginot et al., 2015).

The Northeast Greenland (NEG) shelf is located in the high Arctic between 77°and 81°N. Glacial melt, shrinking sea ice and stronger input of warm Atlantic Water are acting all at once in this region. Moreover, the NEW polynya, a conspicuous feature on the NEG shelf, is declining in size (ISSI, 2008). Therefore, it provides an interesting location for studying the effect of a changing Arctic on benthic ecosystems.

The NEG shelf has been studied intensively during the 1990s in terms of oceanography (Budéus and Schneider, 1995; Budéus et al., 1997; Schneider, 1997; Topp and Johnson, 1997), biogeochemistry (Lara et al., 1994; Kattner and Budéus, 1997) , biology (Ambrose and Renaud, 1995; Brandt, 1995; Piepenburg et al., 1997), and the formation of the NEW polynya (Smith et al., 1990; Schneider and Budéus, 1994, 1995; Schneider, 1997; Schneider and Budéus, 1997).

A tight pelagic-benthic coupling was reported for the region (Ambrose and Renaud, 1995; Hobson et al., 1996; Piepenburg et al., 1997; Rowe et al., 1997). Since then, no further biological studies have been carried out. Moreover, perennial fast ice cover had hindered investigations on benthic communities right in front of the 79N Glacier, the largest marine-terminating glacier on the NE Greenland shelf. Accordingly, this study represents a first assessment of benthic communities and their functions on the NEG shelf since the 1990s.

1.4 Hypotheses

Within the framework of this thesis, following hypotheses are tested:

1. *With respect to main environmental parameters, the NEG shelf is separated into distinct regions. This spatial pattern did not change between the 1990s and today.*

2. *The benthic soft-bottom communities and their functioning differs between these delineated regions.*

3. *Benthic soft-bottom communities and their functions have not changed since the 1990s.*

2 Material & Methods

2.1 Study site

2.1.1 The trough system on the NEG shelf

With an extent of more than 300 km from the coastline, the Northeast Greenland continental shelf (NEG) is the broadest shelf along the Greenland margin. Five cross-shelf troughs comprise more than 40% of the NEG (Fig. 2.1). The two most prominent ones, namely Westwind Trough in the North and Norske Trough in the South are located between 77°and 81°N and form a "C"-shaped trough system (Arndt et al., 2015; Schaffer et al., 2017), facing the Greenland coast with the Nioghalvjerdsbrae ("79N Glacier", hereafter referred to as 79NG) to the West and the Fram Strait with the southward-flowing East Greenland Current to the East. The north-eastern part of the Norske Trough is also referred to as Belgica Trough (e.g. Brandt, 1995; Budéus et al., 1997; Hughes et al., 2011), but in the present study the geographical names after Arndt et al. (2013) and Schaffer (2017) are used. The shelf area includes 3 shallow banks ($<$ 200 m) approximately located in the middle (Belgica Bank, Northwind Shoal and AWI Bank) that are half-encircled by the two troughs (Fig. 2.1).

At around 79°30'N, the Norske Øer Ice Barrier (NØIB), one of the largest areas of landfast ice on Earth, is present (Hughes et al., 2011). It is the southern barrier of the Northeast Water (NEW) Polynya which used to open in April or May and close in about September, and to last in a few occasions only until October or November (Schneider and Budéus, 1994). The Polynya varied in size, located within the area around 80°N in the Westwind Trough and was reported to at times covering 44.000 km^2 of area (Fig. A.5; Wadhams, 1981) which is approximately equivalent to the size of Denmark.

In 1992, ice concentrations were reported to be lowest in August with 20-40 % and increased to maximum concentrations in September/October until February with 95-100 %. Variable ice conditions were recorded until the end of March with a simultaneous increase of particle flux, indicating the formation and existence of the NEW Polynya during winter as well (Bauerfeind et al., 1997). Underneath first-year ice sheets, massive growth of assemblages of sub-ice algae was recorded, dominated by the diatom *Melosira arctica* (Gutt, 1995).

Sedimentation in the NEW Polynya was reported to increase from March onwards, with maximum sedimentation rates between August and October and lowest sedimentation during winter (Bauerfeind et al., 1997), in consistence with the prevailing ice cover conditions. Total sedimenting matter was 81 $mg\ m^2\ d^{-1}$ in September 1992, decreasing to 5.45 $mg\ m^2\ d^{-1}$ in December and January (Bauerfeind et al., 1997).

According to the ISSI (2008), the NEW Polynya is declining since these early investigations. In summer 2001, together with the declining sea ice in the Northeast Greenland Current it formed "what one could describe as an almost open continental shelf sea" (ISSI, 2008).

Previously, the NEG shelf was not easily accessible for investigations due to the permanent sea ice cover throughout the year. Since recently, the shrinking sea ice

(Stroeve et al., 2012) makes it possible to visit areas that have not been studied before.

The Norske Trough alone covers approximately 20% of the NEG continental shelf, with a length of about 350 km and a width of $35 - 90$ km. Its maximum depth is 560 m at the inner shelf, and its minimum depth is 320 m at the shelf edge. The Westwind Trough is about 300 km long and approximately 40 km wide. North to the 79NG and the Djmphna Sund, its maximum water depth is 300m at the shelf edge (Arndt et al., 2015). With a depth of 160, a sill at the entrance of the Djmphna Sund is the shallowest part of the Westwind Trough. The seafloor topography within the troughs is rather complex and reveals an undulating structure comprising sills, rises and ridges (Arndt et al., 2015). Generally said, the Westwind Trough is characterized by shallower water depths compared to Norske Trough (Arndt et al., 2015; Schaffer et al., 2017; Schaffer, 2017). It is suggested that the complex shape and bathymetry of the troughs upstream the 79NG were formed by glacial erosion by ice streams in full-glacial periods (Arndt et al., 2015; Callard et al., 2018). The sea-floor topography of the Norske Trough is characterized by bedrock hills and iceberg scour marks most probably from deglacial and Holocene (Roberts et al., 2017). Recent icebergs in this area have a rather shallow draft (pers. comm. D. Roberts), which is likely to result in no or few impact of ice-berg scouring on the NEG shelf on benthic communities.

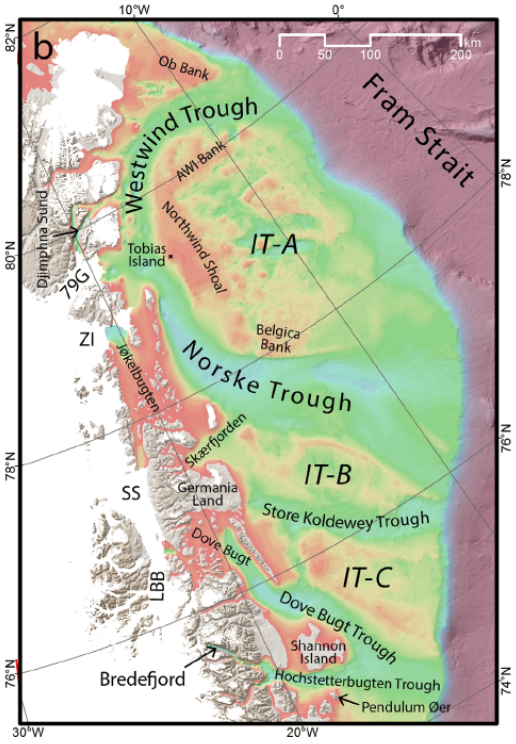

FIGURE 2.1: **Bathymetry and geographical names in the study area on the NEG shelf.** Figure adapted from Arndt et al. (2015).

As part of the Northeast Greenland Ice Shelf (NEGIS), the 79NG is the largest marine-terminating glacier on the NEG, leading to a large floating ice tongue that fills the entire interior of the 79N Fjord (Thomsen et al., 1997). It is located to the west of the trough system, embedded by land, with the Zachariae Isstrom to the south and the Djmphna Sund to the north. The glacier tongue is 80 km long and 20 km wide, and widens in a main calving front of approx. 30 km width towards the east. In front of its margin, several islands and seamounts are present and act as pinning points for the floating glacier (Schaffer, 2017). Additionally, it drains into the Djmphna Sund with an 8 km wide calving front (Schaffer et al., 2017). The speed of this floating tongue increased by more than 100 $m\ yr^{-1}$ in 2011 relative to winter 2000 - 2001 (Khan et al., 2014). Underneath, an overdeepened trough with a maximum depth of more than 900m below sea level is present, where subglacial melting takes place with a mean melt rate as fast as 8 $m\ yr^{-1}$ (Mayer et al., 2000). Water warmer than 1 °C (Wilson and Straneo, 2015) having the potential to cause basal melting is present in this cavity below the 79NG (Mayer et al., 2000; Straneo et al., 2012; Schaffer et al., 2017).

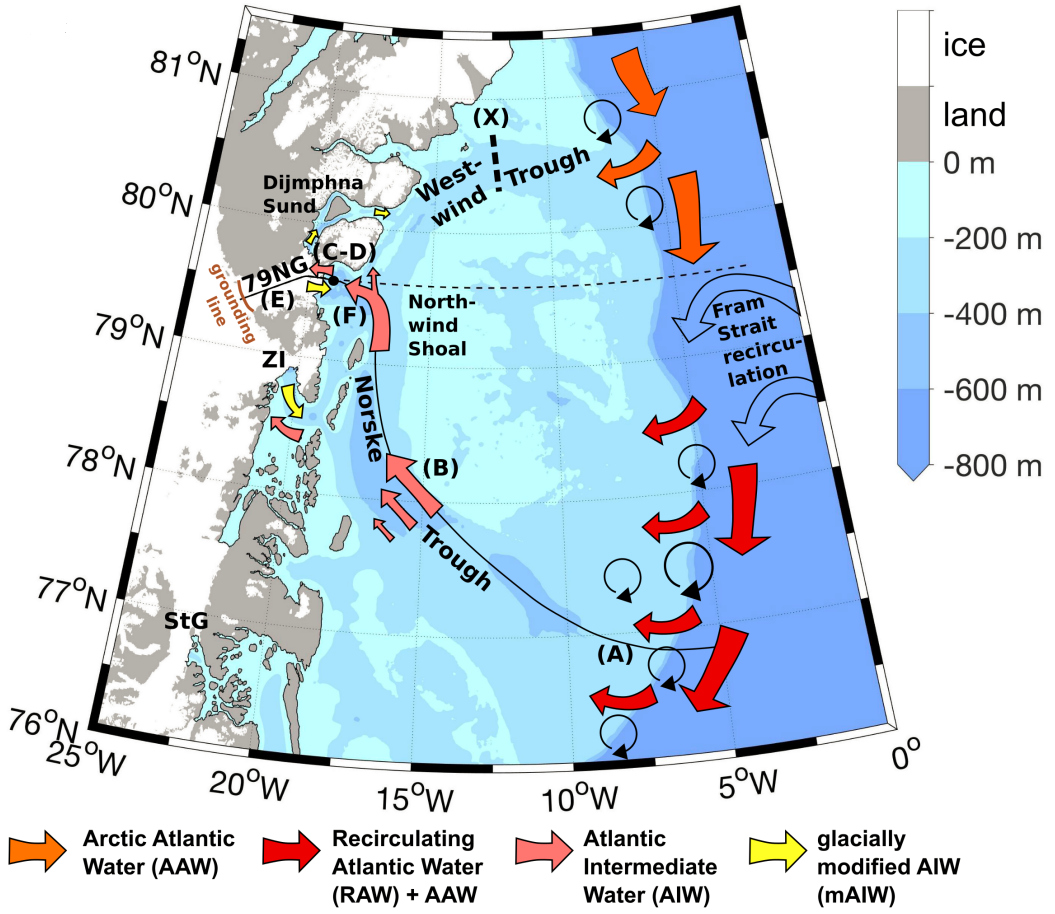

FIGURE 2.2: **Schematic illustration of inferred water mass pathways on the NEG shelf.** Figure adapted from Schaffer (2017).

2.1.2 Warm water circulation pathways

The bathymetry of the trough system provides a thalweg between the shelf break of the Norske Trough in the South and the shelf break of the Westwind Trough in the North (Arndt et al., 2015; Schaffer et al., 2017), allowing warm water of Atlantic origin in depths below $150 - 200\ m$ (subsurface Atlantic Intermediate Water, AIW) to circulate in an anticyclonic way (Bourke et al., 1987) across the shelf. The seaward inlets of both troughs are deep enough to allow the throughflow of AIW (Schaffer et al., 2017). While in the Westwind Trough the warmest waters are observed at depth, in the Norske Trough colder water has been detected below the AIW layer, which is trapped in the trough below sill depths and are indicative of old AIW (Schaffer, 2017). Polar Water (PW) occupies the upper water layer betweeen 80 to 150 m (Budéus and Schneider, 1995), circulating likewise anticyclonic as a gyre over the shallow banks (Bourke et al., 1987; Topp and Johnson, 1997) . Between the PW and the AIW, an intermediate water body called "knee water" (KW) is present in the Norske Trough, but absent in the Westwind Trough. It is likely advected from the Arctic Basin onto the NEG continental shelf (Budéus and Schneider, 1995).

AIW is transported through the Norske Trough toward the 79NG (Fig. 2.2, Schaffer, 2017) and does not enter the glacier cavity trough the Djmphna Sund as proposed by Mayer et al. (2000). It creates highest temperature differences at the ice grounding line (approximately 600 m) underneath the tongue (Wilson and Straneo, 2015) and

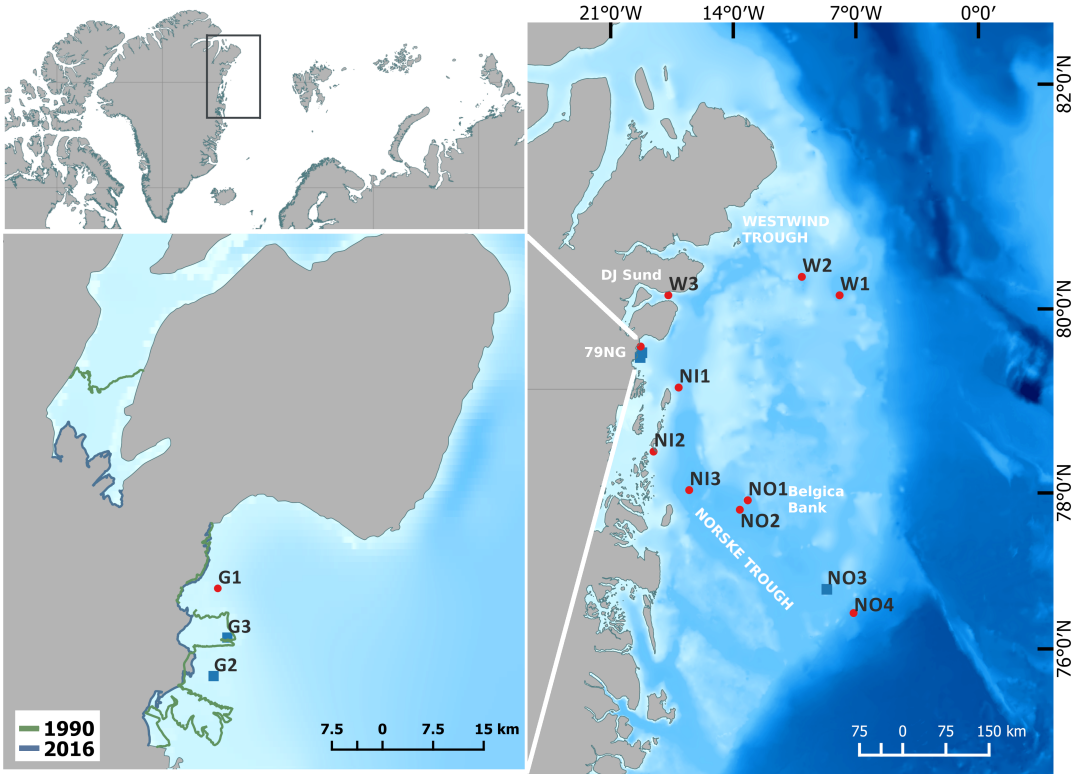

FIGURE 2.3: **Locations of sampling sites on the Northeast Greenland shelf during PS109 on *R/V* Polarstern.** Red circles indicate ex situ stations where sampling was performed with a multiple corer (MUC). Blue rectangles indicate sites where next to MUC sampling additional in situ sampling with a Lander was done. Bathymetric data were obtained from Jakobsson et al. (2012) and coastlines from Wessel and Smith (1996). Calving front data from 1990 (green line) and 2016 (blue line) were retrieved from ENVEO (2017).

potentially causing basal melting (Mayer et al., 2000; Schaffer et al., 2017). The outflowing glacially modified water (mAIW), formed by mixing of glacial meltwater and AIW inside the cavity is about 1 °C cooler and about 0.4 fresher, which makes it less dense (Schaffer, 2017). It results in a buoyant meltwater plume which rises along the 79NG base (Straneo et al., 2012; Schaffer, 2017), leaving the cavity towards the east via a pinned calving front (Schaffer, 2017) and towards the north via Djmphna Sund (Wilson and Straneo, 2015). The Djmphna Sund and the Norske Trough both are under influence of mAIW (Schaffer, 2017).

Very high bottom velocities of AIW with up to 30 $cm\ s^{-1}$ were revealed at the calving front of the 79NG (Schaffer, 2017). Current velocities of AIW in Westwind Trough were generally small, with values of less than 6 $cm\ s^{-1}$ below 200 m. In contrast, Norske Trough revealed higher current speeds with maximum of 16.5 $cm\ s^{-1}$. (Schaffer, 2017). Schaffer (2017) found that AIW throughout the whole trough system has warmed in the period between 2000 - 2016 relative to 1979-1999, with a warming of 0.5 °C throughout the Norske Trough.

2.2 Sampling and laboratory analyses

Samples were taken between September and October 2017 during PS109 with *RV* Polarstern at 13 stations at water depth between 139 and 645 m, with one shallow station of 69 m water depth and a station on the Greenland slope of 1200 m water depth. Bottom water temperatures and salinities ranged between -1.07 and 1.76 °C

TABLE 2.1: **Metadata for the benthic stations on the Northeast Greenland (NEG) shelf during PS109 on *R/V* Polarstern between September - October 2017.**

St ID	Location	Station	Gear	Date	Lat [°N]	Long [°W]	Depth [m]
W1	Westwind Trough	PS109/19-1	CTD	17.09.17	80° 8.9082	7° 56.7852	321
		PS109/19-2	TV-MUC	17.09.17	80° 8.839	7° 57.019	313
		PS109/19-4	TV-MUC	17.09.17	80° 8.049	7° 55.9038	315
W2	Westwind Trough	PS109/36-1	CTD	19.09.17	80° 19.596	9° 58.398	314
		PS109/36-2	TV-MUC	19.09.17	80°19.0579	10°01.9038	318
		PS109/36-3	TV-MUC	19.09.17	80° 18.779	10° 05.185	310
W3	Westwind Trough	PS109/45-1	CTD	20.09.17	80° 8.0928	17° 41.46	204
		PS109/45-3	TV-MUC	20.09.17	80° 08.057	10° 1.904	206
		PS109/45-4	TV-MUC	20.09.17	80° 08.062	17° 42.630	219
G1	79N Glacier	PS109/56 -1	CTD	22.09.17	79° 37.044	19° 17.256	352
		PS109/76-1	TV-MUC	24.09.17	79° 37.200	19° 17.488	366
		PS109/76-2	TV-MUC	24.09.17	79° 37.213	19° 17.323	367
G2	79N Glacier	PS109/82-1	CTD	24.09.17	79° 30.1242	19° 16.5462	333
		PS109/62-1	TV-MUC	22.09.17	79° 30.4002	19° 19.3152	301
		PS109/84-2	TV-MUC	24.09.17	79° 30.3762	19° 19.0962	309
		PS109/69-1	Lander	23.09.17	79° 30.316	19° 19.023	301
G3	79N Glacier	PS109/77-1	CTD	24.09.17	79° 33.998	19° 19.409	404
		PS109/61-1	TV-MUC	22.09.17	79° 33.393	19° 13.249	162
		PS109/85-1	TV-MUC	25.09.17	79° 33.996	19° 19.41	156
		PS109/68-1	Lander	23.09.17	79° 33.371	19° 13.186	169
NI1	Norske Trough (inner)	PS109/93-1	CTD	26.09.17	79° 11.676	17° 5.574	390
		PS109/93-2	TV-MUC	26.09.17	79° 11.349	17° 7.199	386
		PS109/93-3	TV-MUC	26.09.17	79° 11.045	17° 08.791	389
NI2	Norske Trough (inner)	PS109/101-1	CTD	28.09.17	78° 28.782	18° 33.36	439
		PS109/105-1	TV-MUC	28.09.17	78° 28.088	18° 33.371	440
		PS109/105-2	TV-MUC	28.09.17	78° 28.865	18° 33.312	441
NI3	Norske Trough (inner)	PS109/115-1	CTD	29.09.17	78° 1.872	16° 34.278	509
		PS109/115-2	TV-MUC	29.09.17	78° 01.969	16° 32.436	503
		PS109/115-3	TV_MUC	29.09.17	78° 01.989	16° 31.017	502
NO1	Norske Trough (outer)	PS109/128-1	CTD	03.10.17	77° 54.45	13° 16.362	142
		PS109/122-1	TV-MUC	02.10.17	77° 54.688	13° 10.456	140
		PS109/129-1	TV-MUC	03.10.17	77° 54.753	13° 10.630	139
NO2	Norske Trough (outer)	PS109/125-4	CTD	03.10.17	77° 47.748	13° 38.244	389
		PS109/125-2	TV-MUC	03.10.17	77° 47.918	13° 37.667	391
		PS109/125-3	TV-MUC	03.10.17	77° 47.747	13° 37.530	392
NO3	Norske Trough (outer)	PS109/140-1	CTD	05.10.17	76° 50.574	8° 52.524	355
		PS109/139-2	TV-MUC	04.10.17	76° 47.945	8° 39.624	354
		PS109/139-3	Lander	04.10.17	76° 48.046	8° 38.232	357
		PS109/139-4	TV-MUC	04.10.17	76°48.1068	8°37.5114	357
NO4	Norske Trough (outer)	PS109/142	CTD	05.10.17	76° 29.262	7° 8.286	1163
		PS109/154-1	TV-MUC	07.10.17	76° 29.214	7° 07.921	1177
		PS109/154-2	TV-MUC	07.10.17	76° 29.182	7° 06.561	1200

and 33.96 - 34.94 psu. 3 stations were located in the Westwind Trough, 7 stations in the Norske Trough, and 3 stations close to the 79NG (Fig. 2.3, Table 2.1). At each station, a camera-equipped multiple corer (TV-MUC, core diameter 0.007 m^2) was used for *ex situ* measurements and sediment sampling. Additional samples for *in situ* measurements were taken with an autonomous benthic lander at 3 of these stations (one at the outer Norske Trough (Station 139) and two at the margin of the 79NG (Stations 68 and 69).

2.2.1 Sediment solid-phase parameters

Upon arrival on deck, 3 of the MUC cores were directly subsampled for different sediment depth intervals ($0-1$, $1-2$, $2-3$, $4-5$ cm) for granulometry, porosity, Chlorophyll *a* (Chl *a*) and phaeopigments (phaeophorbid and phaeophytin).

Porosity samples were stored in 5 ml cut-off syringes wrapped in aluminium foil. In the home lab, the samples were sliced in 0.5 cm sediment depth intervals and the wet mass of the sediment samples was measured and then dried at 60 °C in a drying oven. Porosity was calculated by the difference between the wet and dried mass of the samples after Dalsgaard et al. (2000).

Porosity ϕ characterizes the relative amount of pore space within a sample volume (Breitzke, 2006) and is determined after Wolff (2008) by the equation

$$\phi = \frac{m_w/\rho_w}{m_w/\rho_w + m_d - (S * m_w))/\rho_s^2} \tag{2.1}$$

where

m_w = mass of evaporated water
ρ_w = density of the evaporated water
m_d = mass of dried sediment, including salt
S = salinity of the overlying water
ρ_s = density of the sediment

Unfortunately, porosity was not available for all stations and sediment depths due to analytical difficulties. Therefore, porosity was modelled for the stations lacking data by linear regression with silt fraction (fraction of grain size below 63μm). The used equation for the calculation of the porosity was

$$porosity = 0.0048 \cdot silt\ fraction + 0.2745 \tag{2.2}$$

with an adjusted R^2 of 0.33 and a p-value <0.001. Due to the low fit, porosity was excluded from the analyses but used for the calculation of pigment concentrations expressed in $mg\ m^{-2}$ for comparative purpose with other studies only.

For granulometry, the sediment was sliced in 1 cm intervals and stored in $2-5$ ml scintillation vials or plastic bags. Grain size spectra were assessed by laser diffraction (Malvern Instruments, Malvern, UK).

Chl *a* and phaeopigments were subsampled in three replicates with 10 ml cut-off syringes which were gently pushed until 5 cm sediment depth and stored at -80 °C. In the home laboratory, the samples were analysed using high performance liquid chromatography (HPLC) after Wright et al. (2005). Quantities are expressed as microgram pigment per gram of dry sediment $[\mu g\ g^{-1}]$. The chloroplastic pigment equivalent (CPE) was calculated as the sum of Chl *a* and Phaeopigments. The ratio of Chl *a* to phaeopigments (Chl *a*-Phaeopigments ratio) was used as an indicator for

the relative freshness of food, while the ratio of Chl *a* to CPE (Chl *a*-CPE ratio) was calculated as an indicator for the amount of fresh food relative to all food available.

Only for comparative purpose with other studies, the amount of benthic Chl *a* and phaeopigments in $\mu\ m^{-2}$ was calculated from the modelled porosity using following equation

$$\frac{\mu\ g}{g\ (dry\ sediment)} \cdot (1 - porosity) \cdot 2.55 \frac{g}{cm^3} \cdot 1\ cm \cdot 10000 \tag{2.3}$$

2.2.2 Sediment porewater parameters

At each station, two MUC cores with pre-drilled holes were mounted additionally on the MUC for porewater extractions. Samples for measuring porewater chemistry (DIC, nutrients, sulfate, sulfide and chloride concentrations) were collected with Rhizon samplers (pore size 0.2 μm, Rhizosphere, Wageningen, Netherlands) by inserting them carefully into the predrilled holes on the retrieved MUC cores with depth intervals of 1 *cm* until 10 *cm* sediment depth, and 2 *cm* intervals until 20 *cm* sediment depth. A total of 9 *ml* porewater for each depth interval was retrieved in this manner.

To determine dissolved inorganic carbon (DIC) and total alkalinity (TA), 2 *ml* porewater was sampled in glass vials pretreated with $HgCl_2$ and stored at 4 °C. DIC concentrations were measured using a flow injection system equipped with the Spark Optimas auto-sampler (model 820, Ambacht, Netherlands). TA was determined by titration using the Titrino analyzer (Methrom, Germany) and calculated following Dickson (1981).

For the analysis of porewater nutrients, 15 *ml* of porewater was transferred to acid-washed Sarstedt Vials, stored at -20 °C and further subsampled in the home lab before analysis (4 *ml* for phosphate, silicate and ammonium, 1 *ml* for nitrate and nitrite). Analysis of the samples was done with a Continuous Segmented Flow Analyser (QuAAtro39, SEAL Analytical, Norderstedt, Germany).

Approximately 1 *ml* volume was retrieved from the porewater and stored in pre-weighted Eppendorf tubes with 500 μm 2% ZnAc at 4 °C for subsequent analysis of sulfate, sulfide and chloride. Sulfate and chloride were analyzed by non-suppressed ion chromatography (761 Compact IC, Metrohm using 838 Advanced Sample Processor Metrohm) with 3.2 mM Na_2CO_3 and 1 mM $NaHCO_3$ as eluent. The detection limit of sulfate in the porewater was 50 μM. Sulfide was determined using the photometric methylene blue method after Cline (1969) with a Shimadzu UV120 spectrophotometer (detection limit 2 μM). Sulfate was not detected and is therefore not further treated in this work.

2.2.3 Sediment oxygen profiles and oxygen fluxes at the sediment-water interface

For the assessment of *ex situ* fluxes at the sediment water interface, part of the overlying water from three cores was removed and stored separately, while the height of the remaining water above the sediment was adjusted to 10 *cm* by pushing the sediment gently vertically upwards from beneath without disturbing the surface sediment layer. The cores were transferred into a dark-room with a temperature-controlled water bath where the temperature had been adjusted to the *in situ* values in the bottom water at the respective station (information retrieved from ship-board sensors) right before the incubation. The overlying water was homogenised with a magnetic stirrer and the water surface was gently streamed with a soft air stream to aerate the overlying water.

For the quantification of diffusive oxygen uptake (DOU), two oxygen microprofiles were measured simultaneously in the ideal case within 2 h after sampling (in some cases >24 h) and for each sediment core with 2 oxygen optodes (tip size 50 μm) mounted on an autonomous x-y-z microprofiler module. The sensors were two-point calibrated using on-board signals recorded in air saturated surface sea water and anoxic, dithionite-spiked bottom water at in situ temperature.

Total oxygen uptake (TOU) was assessed by measuring oxygen concentration in the overlying water over time for approx. 48 h (at least 36 h). For this, after microprofiling the cores were closed airtight with no air bubbles in the overlying water. Magnetic stirrers ensured the homogenisation of the overlying water. At three time points, an oxygen optode measured the oxygen concentration in the overlying water Total sediment oxygen flux was determined as the decrease in oxygen concentration in the water phase. The incubation was terminated at 80 % [O_2] or less.

To quantify *in situ* fluxes at the sediment-water interface, additional samples were taken with an autonomous benthic lander equipped with three benthic chambers (diameter 0.4 m^2), a sediment profiler and a Niskin bottle. Upon arrival at the sea floor, the lander chambers were driven into the sediment 4 h after the lander deployment to allow resuspended matter to settle down on beforehand. The lander chambers enclosed about $20x20\ cm$ of sediment and $10 - 15\ cm$ of overlying water (depending on the final orientation of the lander). The overlying water was gently stirred to avoid stagnation. A syringe sampler collected nutrient and DIC samples from the overlying water at regular times, while an Aanderaa optode (4330, Aanderaa Instruments, Norway, two-point calibrated as described above) continuously measured the oxygen concentration in the overlying water at an interval of 10 min during over a total incubation time of around 48 h. At the same time, electrochemical oxygen microsensors (adapted and customized after Revsbech (1989) and calibrated with a two-point calibration) measured DOU profiles at 3-5 points. The bottom water oxygen concentration (taken from the Niskin bottle and estimated by Winkler titration) was used as the first calibration point. When the sensor had reached the anoxic zone of the sediment, the sensor signal at this point was taken as the second calibration point. Otherwise, the sensor signal in an anoxic solution of sodium dithionite was used. The maximum penetration depth of the profiler during in situ profiling was 180 mm, depth resolution was 100 μm.

At the end of the incubation, a blind closed the chambers at the bottom to retrieve the incubated sediment together with the Lander from the seafloor. On board, the height of the overlying water body was measured with a ruler at 6 to 8 positions within each chamber and subsampled for the above-mentioned measurements.

Both *ex situ* and *in situ* DOU fluxes across the sediment-water interface obtained by MUC core incubations and Lander chambers were calculated from running average smoothed oxygen profiles using Fick's first law

$$DOU = -[\frac{\Delta O_2}{\Delta z}]_{z=O<2} \tag{2.4}$$

where

$[\frac{\Delta O_2}{\Delta z}]_{z=O<2}$ = oxygen gradient at the sediment-seawater interface, obtained by linear regression from the first alteration in the oxygen concentration profile across a maximum depth of 1 mm.

TOU fluxes were calculated as

$$TOU = \frac{\delta O_2 \cdot V}{\delta t \cdot A} \tag{2.5}$$

where

δO_2 = difference in oxygen concentration
V = volume of the overlying water
δt = difference in time
A = enclosed surface area

2.2.4 Benthic community parameters

Single cell abundances

For single cell abundance estimations, depth intervals of $0-1$, $1-2$, $2-3$, $4-5$ cm were sampled with a 10 ml cut-off syringe. 2 ml of each slice was transferred into a scintillation vial and fixed with 2 % filtered formaldehyde-seawater solution. Afterwards, the samples were diluted, filtered through Polycarbonate filters (0.2μm, Whatman Nucleopore Track-Etch Membrane) and stained with a 0.001 % Acridine Orange solution after Hobbie et al. (1977). At least 30 grids were counted for 2 replicate filters per sample each with a Zeiss Axiophot microscope (Germany) and a 100x oil immersion objective lens (Zeiss Plan-Apochromat, Germany). Quantities are expressed in $cells\ ml^{-1}$.

Macrofauna communities

At the end of the *in situ* (or *ex situ*) incubations, the MUC cores (or Lander chambers upon arrival on deck) were opened and sampled for the assessment of soft bottom communities by slicing them into $0-5$ cm, $5-10$ cm and $10-20$ cm, sieving over a 500 μm mesh and storing in 4 % formaldehyde in Kautex bottles at room temperature. In this study, only the $0-5$ cm interval was considered.

In the lab, the samples were stained with Rose Bengal. Macrofauna, including foraminifera, were identified to the lowest possible taxon using a range of different literature sources, and the wet formalin weight of macrofauna was determined after drying shortly on a paper towel with a DeltaRange XP56 or AX205 precision balance (Mettler Toledo, Ohio, USA), depending on the organism size and weight. It should be noted that, because of the extremely small size of the specimen, the evaporation of water led to a steady decrease of weight on the precision balance. Polychaetes were taken out of their tubes before weighting, molluscs were weighted with their shells. Other encrusting and calcifying organisms such as bryozoans were also weighted with their tests, noting their biomass is most likely overestimated. Colonial animals such as Bryozoa and Hydrozoa were weighted for biomass estimations but excluded from the total number of individuals. When no head was present in the sample but body segments were, polychaete taxa were counted as one specimen. Nematoda were excluded from the biomass and density calculations since they are usually regarded as meiofauna.

Usually, foraminifera are sieved through much smaller sieve fractions (> 45 μm, > 63 μm and > 150 μm) and dry-picked (e.g. Corliss and Emerson, 1990; Murray and Alve, 2000). In the present study, only the foraminifera of the fraction > 500 μm as

components of the macrofaunal community were considered. Appropriate methods for quantifying living foraminifera have been discussed in several studies (Jorissen et al., 1995; Bernhard, 2000; Murray and Alve, 2000). The most commonly used staining method with Rose Bengal was criticised especially by Bernhard (1992). Proteins adsorb Rose Bengal, which gives the cytoplasm a brilliant rose color (Walton, 1952). Bernhard (2000) state that even cytoplasm of organisms that have been dead for weeks or months can be stained. On the other hand, Corliss and Emerson (1990) assume that stained specimens with Rose Bengal reflect protoplasm-containg tests which were either alive during collection or in the "recent" past. Here, we decided for this most commonly used staining method ($2g$ dye in 1 l Methanol) after Lutze and Altenbach (1991) to distinguish living from dead foraminifera.

Accordingly, after the extraction of macrofauna, the samples were stained once again in the above mentioned way and stored between a couple of days and 3 weeks before wet-picking of foraminifera. Only foraminifera from MUC stations were counted. In case the staining inside the test was not clearly visible, the foraminifera were gently broken to see if organic material was present. For larger samples, a subsample was taken by distributing the sediment homogenously in a 200 x 15 mm petri dish and splitting it into four fractions, counting the foraminfera for only one or two fractions and the standing crop numbers calculated for the whole sample. Worms that were inhabiting foraminifera tests (Nematoda, small Nemertea) were excluded, since they were not part of the macrofauna communities.

Since weighting the foraminifera with their tests would lead to a high overestimation of the organic biomass, the ZooScan scanner system (HYDROPTIC, L'Isle Jourdain, France) was used to determine their body mass. Foraminifera were extracted from the original sample, sorted and stored in Ethanol until scanning them with the ZooScan. The dimensions of every particle on the scan were calculated via the image processing software ImageJ. Afterwards the pictures were sorted using the software PlanktonIdentifier (Gasparini and Antajan, 2007) and the dimensions for every individual foraminifera was calculated. Their dimensions were then used to calculate their biomass, following methods from (Murray and Alve, 2000). Biomass estimations were only done for MUC stations. For every station, the samples of one or two replicates were scanned, and the biomass for the remaining replicates was calculated using the biomass per individual calculated from the scanned samples. This was possible, since very few differences in size within one species in this size fraction (> 500 μm) were observed. Tubular foraminifera (e.g. belonging to the genera *Astrorhiza*, *Hyperammina* or *Rhabdammina*) made for a large proportion from the entire foraminifera biomass (personal observation), but were excluded from the abundance and biomass analyses since they are easily fragmented (Licari, 2004), and the biomass could not be assessed from one sample for the others because of the pronounced differences in sizes between samples. Results from foraminifera biomass are not further treated in this master thesis.

Densities for macrofauna and macrofauna including foraminifera are expressed in $ind\ m^{-2}$, biomasses for macrofauna only in $g\ m^{-2}$. For the representation of total biomass, *Priapulus bicaudatus* and *Ctenodiscus crispatus* were removed from W2 (original biomass: 147.6 g) and NO2 (original biomass: 277.9 g), respectively, since otherwise the data was skewed.

5 diversity indices were calculated for all ex situ stations (excluding Lander stations) for macrofauna and macrofauna + foraminifera densities, respectively.

Shannon-Weaver taxonomic diversity H'

$$H' = -\sum_{i=l}^{R} p_i \, ln \, p_i \tag{2.6}$$

is the most widely used diversity index in ecology. Pielou's index J'

$$J' = \frac{H'}{H_{max}} \tag{2.7}$$

is a measure for how even the species are distributed at each station. Taxonomic diversity Δ

$$\Delta = \frac{\sum\sum i < j \, \omega_{ij} x_i x_j}{\frac{N(N-1}{2}} \tag{2.8}$$

is expressed as the average taxonomic "distance" between any two organisms, and taxonomic distinctness Δ^*

$$\Delta^* = \frac{\sum\sum i < j \, \omega_{ij} X_i X_j}{\sum\sum i < j \, X_i X_j} \tag{2.9}$$

is expressed as the average path length between any two randomly chosen individuals, conditional on them being from different species. While taxonomic distinctness can be seen as a measure of pure taxonomic relatedness, taxonomic diversity mixes taxonomic relatedness with the evenness properties of the abundance distribution. Species richness S is defined as the number of species per station.

All data acquired for the project were published on PANGAEA and are accessible through https://doi.pangaea.de/10.1594/PANGAEA.894658 (after asking for permission).

2.2.5 Data obtained from other sources

Physical oceanography data (salinity and temperature) from spring and summer 1993 (expeditions PS25 and PS26) were taken from shipboard CTD measurements (Budéus and Schneider, 2010a,b).

Since data for attenuation were not available for the PS109 campaign, attenuation in the water column from summer 2016 (uncalibrated, PS100, (Kanzow et al., 2017)) from the closest stations to the complementary PS109 stations were taken as a proxy for turbidity. The values at the deepest measuring point was compared with the depth at the complementary PS109 station and taken as "bottom water attenuation". Bottom current velocities during PS109 in autumn 2017 were acquired with a moored Acoustic Doppler Current Profiler (ADCP) to assess possible influence of bottom currents on the biota. Data were provided by Janin Schaffer (pers. comm.).

Polychaeta density data were available from campaigns of the US Coast Guard vessel Polar Sea between July 18 and August 1, 1992 and from R/V Polarstern during PS25 and PS26 between May and August 1993 (Paul Renaud, pers. comm.). Data were previously published in Ambrose and Renaud (1995) and Piepenburg et al. (1997). CPE concentrations and total macrofauna densities were taken from Ambrose and Renaud (1995). It should be noted that sampling procedures during these campaigns differed from the sampling procedures in the present study in the in the way that box cores (diameter 0.25 m^2) with 2 to 7 replicates were used, from which 3 to 5 replicate subcores of 0.008 m diameter and 0.0015 m depth were taken.

2.3 Statistical analyses

2.3.1 Univariate measures and analyses

For the representation of univariate measures, dotplots were used because of the low sample size per group (3-4 stations as representatives per site) and the high variation within groups. Station NO4 as the only station off the shelf is presented in the dotplots, but excluded from all statistical analyses since it was the only deep station at the slope and under influence of different environmental drivers compared to all other stations. NO4 was correlating strongly with water depth and shaded the influencing patterns on the shelf (not shown).

For all subsequent statistical analyses, environmental variables were used in the following way: depth values were taken from the benthic MUC stations. Values for bottom water temperature and salinity were taken from the deepest point measured by the ship-board CTD. The same was done for current velocity data, where values were taken from the deepest point measured by the moored ADCP. Here it should be noted that CTD and ADCP bottom depths did vary from the depths measured at benthic MUC stations. Especially current velocity data from the ADCP might not represent accurately the conditions on the sea floor, since velocities were often measured much higher above the bottom. For the pigment concentrations, median grain size and silt fraction at each station, the mean value across all sediment depths (0-1, 1-2, 2-3, 3-4, 4-5 cm) was taken. For single cell abundances, the mean from 0-1 and 4-5 cm sediment depth was used. Bottom water nutrient concentrations, DIC, alkalinity and sulfate concentrations were taken from the concentrations measured for the sediment profiles from the water above the sediment (bottom water). Measurements of environmental parameters and single cell abundances obtained by landers were takes as additional station data replicates, when available, since the subsampling from ex situ and in situ samples occured in the same way and was therefore not influenced by the differing surface area between MUC and Lander.

On the contrary, oxygen fluxes and community measures (densities and biomass) were down-scaled by the larger sampling area covered by the Lander (MUC stations represent a much larger overestimate than the Lander samples). Species density is very sensitive to the area covered by the sampling method (Gotelli and Colwell, 2011). With their larger surface area in situ data provide a much better resolution for these parameters, but since more ex situ data were available, these were used for all community analyses. Therefore, oxygen fluxes and community measures from in situ stations are presented together with ex situ stations in univariate dotplots (for the differentiation indicated by dots and triangles, respectively), but excluded from all statistical analyses. Diffusive Oxygen Uptake (DOU) fluxes were not included in the mutlivariate analyses (but shown in dotplots) due to the low number of replicates per site.

Species accumulation curves were plotted for ex situ data as the mean from random permutations of the data and their standard deviations. They represent the accumulation rates of new species with every MUC sample added. Ideally, the curve should rise steeply first and approach an asymptote as more samples are added to the curve. If this is the case, it indicates a good representation for the sampled communities by the sampling effort.

Environmental variables, bottom water nutrients, total oxygen uptake and single cell abundances were tested for correlations across stations. All variables were

standardized by scaling the values of each variable to zero mean and unit variance and tested for normal distribution with the Shapiro-Wilk Test prior to analysis. Transformation did not lead to normal distribution for following variables: Salinity, Phaeopigments, CPE, Ammonia and Nitrite. Therefore, a non-parametric Spearman rank correlation test was applied on transformed variables and raw variables in cases where a transformation was not possible. Spearman rank correlation coefficient ρ between each pair of environmental variables is represented by a number between -1 (perfect negative correlation) and +1 (perfect positive correlation). The corresponding p-value for each correlation is given.

2.3.2 Multivariate analyses

To delineate the different environmental influences on the regions in an exploratory approach, unconstrained principal component analysis (PCA) was performed on standardised environmental parameters. PCA assumes normal distribution of the variables and a linear relationship among variables (Buttigieg and Ramette, 2014). Therefore, prior to analysis, environmental variables were deselected when their correlation was high based on the Spearman rank correlation and variables that were not following a normal distribution were transformed. PCA uses Euclidian distances between stations based on the environmental parameters to project the arrangement of stations in reduced dimensions. The first component (or first axis) of the PCA accounts for as much of the variability in the data as possible, followed by the second component and so on.

Two similarity profile routine (SIMPROF) analyses were performed on Bray-Curtis distance based raw (untransformed) community density data (macrofauna only and macrofauna + foraminifera, respectively) to test how many station groups based on the community structure are delineated significantly when foraminifera are included and excluded from the total macrofauna community.

A detrendend correspondence analysis (DCA) was used to decide if a linear (principal component analysis, PCA) or unimodal response model (CA) should be applied to identify spatial patterns in species abundance. In a linear response, the variable (i.e. species abundance) displays a linear shape along an environmental gradient, while in the latter case, the species composition data shows a unimodal response along the environmental gradient (Paliy and Shankar, 2016). The axis length of the first DCA axis (scaled in units of standard deviation) was >4, which indicated a heterogenous dataset on which unimodal methods should be used (CA and CCA).

Correspondence analysis (CA) was performed on Hellinger-transformed species densities (macrofauna + foraminifera). CA is based on a χ^2 distance matrix which is not always appropriate for the analysis of community composition data (Legendre and Gallagher, 2001). Therefore the Hellinger transformation was applied to the density data prior to analysis. It is particularly suited to species abundance data, since it gives low weights to variables with low counts and many zeros (Buttigieg and Ramette, 2014). Analysis on untransformed data showed differences mainly between the stations at the Westwind Trough and all others (not shown); by transformation, the patterns of the other stations were distinguishable as well. Standardized environmental variables were fitted on top of the species abundance ordination to delineate which variables contribute the most to the observed patterns in species abundance.

Non-metric multidimensional scaling (nMDS) was applied on a Bray-Curtis distance based matrix of squareroot-transformed polychaeta densities to display ranks of pairwise dissimilarities among samples to see if sites can be distinguished based on polychaete families. Environmental drivers might influence the distribution of polychaete families, which usually represent different functional groups. nMDS uses a distance matrix (sample-sample symmetric matrix of distances between stations) to display ranks of pairwise dissimilarities among objects. The lack of fit between object distances in the nMDS ordination space and the calculated dissimilarities among objects is expressed by a "stress" value (Paliy and Shankar, 2016). If the stress value is < 0.2, the ordination can be considered as a valid representation for the community patterns (Clarke, 1993).

To test if there is a significant influence of the factor "site" (factor with 4 levels: Westwind Trough, 79N Glacier, inner Norske Trough, outer Norske Trough) on the communities delineated by the CA, PERMANOVAs were applied on Bray-Curtis distance based community abundance data for macrofauna density, macrofauna + foraminifera density, polychaeta density and macrofauna biomass. PERMANOVAs were performed on raw (untransformed) and Hellinger-transformed data for each analysis, respectively to check if the patterns in the community structure were related to the dominant species (revealed by untransformed data) or the entire community (transformed data). Afterwards, a pairwise multilevel comparison after Arbizu (2018) was performed to check for the significance of the differences among each pair of site.

To understand which set of environmental variables were the most important drivers for community densities, a stepwise sequential test was performed on Bray-Curtis distance based community densities (macrofauna + foraminifera) against environmental drivers.

CPE concentrations and total macrofauna densities from this study were compared to patterns in 1992 with a two-way ANOVA among regions (Westwind, inner Norske Trough, outer Norske Trough) and time (1992, 2017). Glacier stations were excluded since these were not present in 1992 (Ambrose and Renaud, 1995). Data was tested previously for normality with the Shapiro-Wilkinson Test and for homogeneity of variances by means of the Levene Test. To discover *post hoc* the variables that accounted for the differences among regions, a pairwise Tukey Honestly Significant Difference (HSD) test was conducted.

All statistical analyses were performed by means of the computing environment R (R Core Team, 2018) using the packages *vegan* Oksanen et al. (2018), *corrplot* (Wei et al., 2017) and *clustsig* (Christman, 2014).

3 Results

3.1 Environmental characteristics on the NEG shelf

Water depth of the sampled stations ranged between 140 (NO1) and 1177 m. NO1 was located on the shallow Belgica Bank, NO4 on the slope outside the mouth of Norske Trough. All other stations varied between 156 and 502 m depth (Fig. 3.2). In general stations at the glacier and in the Westwind Trough were shallower than Norske Trough stations. Station W3, which is located in Djmphna Sund north to the glacier was the shallowest station in the Westwind Trough. G3 was much shallower than the other two glacier stations (156 m). In 1992, this station was still covered by the glacier (Fig. 2.3). In Fig. A.1 it is visible that this station was located on a shoal right in front of the glacier margin, peaking out of a 300 to 500 m deep area.

Bottom water salinity and temperature, proxies for distinguishing different water masses, differed strongly between the stations in front of the 79NG where warmest water was present, the stations in the Westwind Trough with cooler and fresher water, and most of the Norske Trough stations, with values in between the Westwind Trough and glacier in terms of temperature, but with the highest salinities (Fig. 3.3). The coolest and freshest station was NO1, which was also the shallowest station. NO4 as the deepest station was the second coldest station. Salinity at W3 in the Djmphna Sund was lower than at the other stations in the Westwind Trough.

Highest current velocities were present at the glacier (especially high at shallow G3), while lowest were present in the inner and outer Norske Trough. W3 in the Djmphna Sund had especially high current velocities compared to W1 and W2. Within the outer Norske Trough stations, NO4 as the deep slope station had highest current velocities compared to the other stations.

Attenuation in the bottom water was lowest at the glacier stations. A low attenuation indicates high turbidity. G3 had a much higher attenuation than the other two stations, similar to the values in the Westwind Trough and in the Norske Trough. The attenuation in the Westwind through lies between the values at the glacier and in the Norske Trough. These turbidity patterns were also observable trough the entire water column (Fig. 3.4). Especially close to the glacier, the attenuation drops drastically at depth and reveals much higher turbidity. Turbidity was highest in both surface and bottom water at all stations.

Median grain size was lowest at all glacier stations and highest in the outer Norske Trough (Fig. 3.2), with very high variability. The highest grain size was observed at the shallow station NO1. In the Westwind Trough, much lower grain sizes were present in the Djmphna Sund at Station W3 compared to W1 and W2. The stations in the inner Norske Trough had generally lower grain sizes. This pattern was also reflected in the silt content (% fraction of the grain size smaller than 63 μm), with highest silt content at the glacier and in the inner Norske Trough and lowest values in the outer Norske Trough. In general, the silt content was extremely high with values of around 95% at the glacier stations and of about 80% at the other stations. With 56.19%, NO1 had the lowest silt content, followed by NO4 with 73.1%.

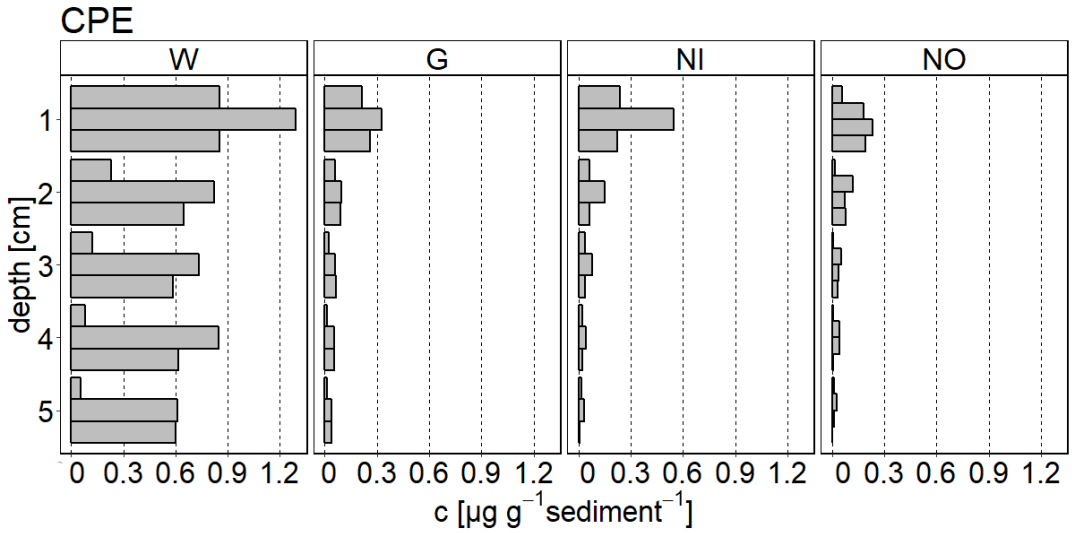

FIGURE 3.1: **Variation of CPE (chloroplastic pigment equivalent) with sediment depth at each site on the NEG shelf during PS109**. Barplots of 3 replicates for each sampled sediment depth are shown. W = Westwind Trough, G = 79N Glacier, NI = inner Norske Trough, NO = outer Norske Trough.

Average concentrations of all pigment compounds (CPE, Chl *a*, Phaeopigments and Fucoxanthin) were highest in the Westwind Trough, where W3 had lower pigment concentrations than W1 and W2. At all other sites, pigment concentrations were much lower, with similar ranges at the glacier stations compared to the Norske Trough. Chl *a*-Phaeopigments ratio as an indicator for the relative freshness of food and Chl *a*-CPE ratio as an indicator for the amount of fresh food relative to all food available revealed slightly different patterns. Both were highest in the Westwind Trough and at stations NO1 and NO2 in the Norske Trough, and much lower at all other sites. When looking at the variation of the CPE with sediment depth, it is clear that pigments were depleted with depth at all stations except for the stations in the Westwind trough (Fig.3.1). Particularly low values were present in the outer Norske trough.

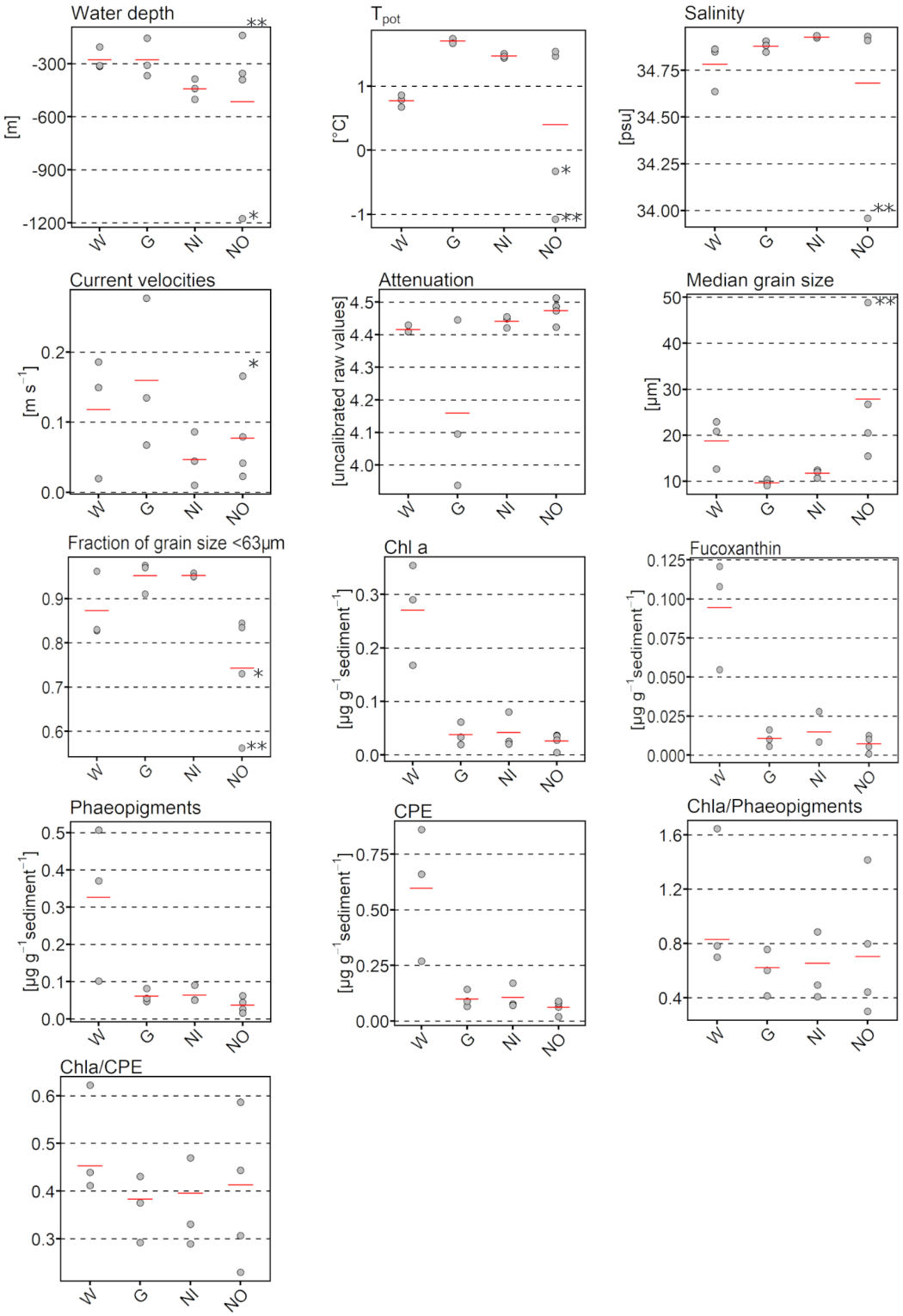

FIGURE 3.2: **Dotplots of environmental parameters on the NEG shelf from ex situ and in situ samples during PS109.** Dots represent values at stations, red lines represent means. Outliers are indicated by ** (Station NO1) and * (Station NO4). CPE = Chloroplastic pigment equivalent. T_{pot} = potential temperature.

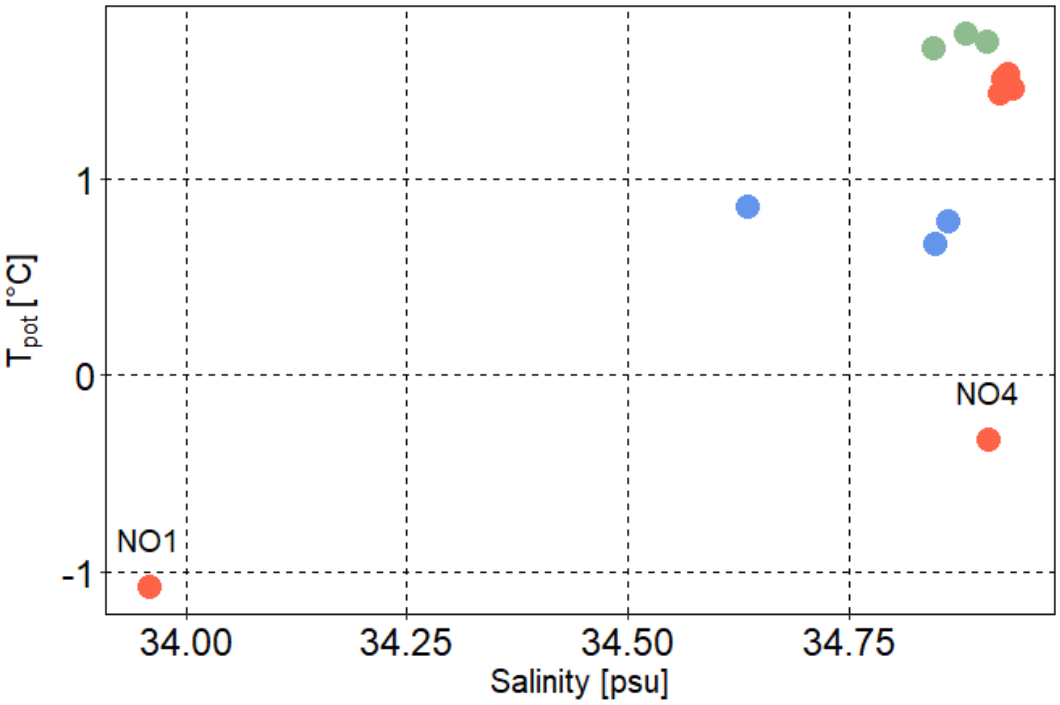

FIGURE 3.3: **Bottom water potential temperature and salinity at benthic stations on the NEG shelf during PS109.** Dots represent stations. Green = 79N Glacier, blue = Westwind Trough, lightred = inner Norske Trough, darkred = outer Norske Trough.

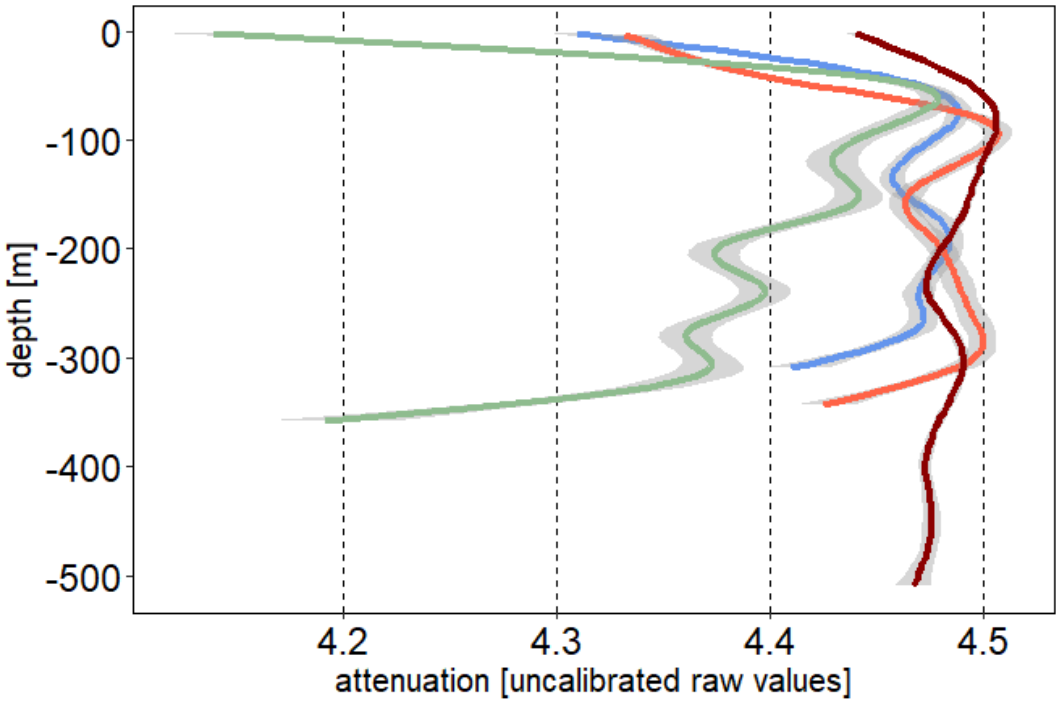

FIGURE 3.4: **GAM-smoothed attenuation profiles as a proxy for turbidity for each site on the NEG shelf during PS100.** NO4 as the only station off the shelf was excluded from the plot, since attenuation was much higher here than at all other stations. Green= 79N Glacier, blue = Westwind Trough, lightred = inner, darkred = outer Norske Trough.

3.2 Oxygen fluxes and porewater nutrients

Total oxygen uptake (TOU) was extremely low across all sites (Fig. 3.5). Highest uptakes were measured in the Westwind Trough, and lowest at the glacier, with few differences compared to the other sites. Diffusive oxygen uptake (DOU) was not available for all stations, but it is visible that at all sites except for one station in the outer Norske, DOU was higher than TOU. Lowest DOU was measured in the inner Norske Trough.

Porewater nutrient concentrations were generally low (Fig. 3.6). Sulfate and sulfide were not detected in the sampled cores. Overall, the Westwind Trough revealed contrasting nutrient profiles compared with all other stations.

Ammonia concentrations were highest in the Westwind Trough, with increasing values with sediment depth. At all other stations, concentrations were close to 0. An increase of Ammonia with sediment depth was measured at W2.

Nitrate concentrations decreased with sediment depth in the Westwind Trough, while at the glacier and in the Norske Trough higher values were observed. In the Westwind Trough, Nitrate concentrations peaked between 0 and 5 cm sediment depth, especially at W3 with values of around 20 μM, and rapidly decreased again.

Nitrite concentrations were extremely low at all stations. In the Norske Trough and at the glacier, concentrations were very close to 0, while in the Westwind Trough a slight increase in concentrations with sediment depth was measured. At around 20 cm sediment depth, the concentration was around 1 μM at W1 and W2. At W3, a peak of Nitrite occured at around -10 cm sediment depth. After 15 cm sediment depth values dropped down to 0.

Phosphate was present in overall low concentrations between $2.5 - 5$ μM in the Norske Trough, except for NO3 where a slight peak occurred between 9 to 12 cm sediment depth. Concentrations were lowest at the glacier with <2.5 μM. At W1 and W2, the concentrations were slightly increasing with depth and were highest at maximum values of around 7.5 μM at W1 and W2. Concentrations at W3 were similar to the values in the Norske Trough.

DIC concentrations did not differ much across sites; nevertheless highest values exceeding 2.5 μM were present in the Westwind and the outer Norske Trough, whereas the inner Norske and the glacier stations showed lower DIC values.

Silicate as a proxy for biogenic compounds originating from diatoms was present with highest concentrations in the Westwind Trough, with double and triple values compared to the concentrations at all other sites.

When looking at the nutrient concentrations in the bottom water only, it is only Ammonia that is present in higher concentrations in the Westwind Trough compared to the other stations (Fig. 3.5). Nitrate concentrations were highest in the inner and outer Norske Trough and lowest in the Westwind Trough and at the glacier. Nitrite was absent in the bottom water in the Norske Trough but present in the Westwind Trough and at the glacier, the latter with highest values. Silicate was highest in the inner Norske Trough. Phosphate and DIC values did vary less than 0.1 μM among all sites.

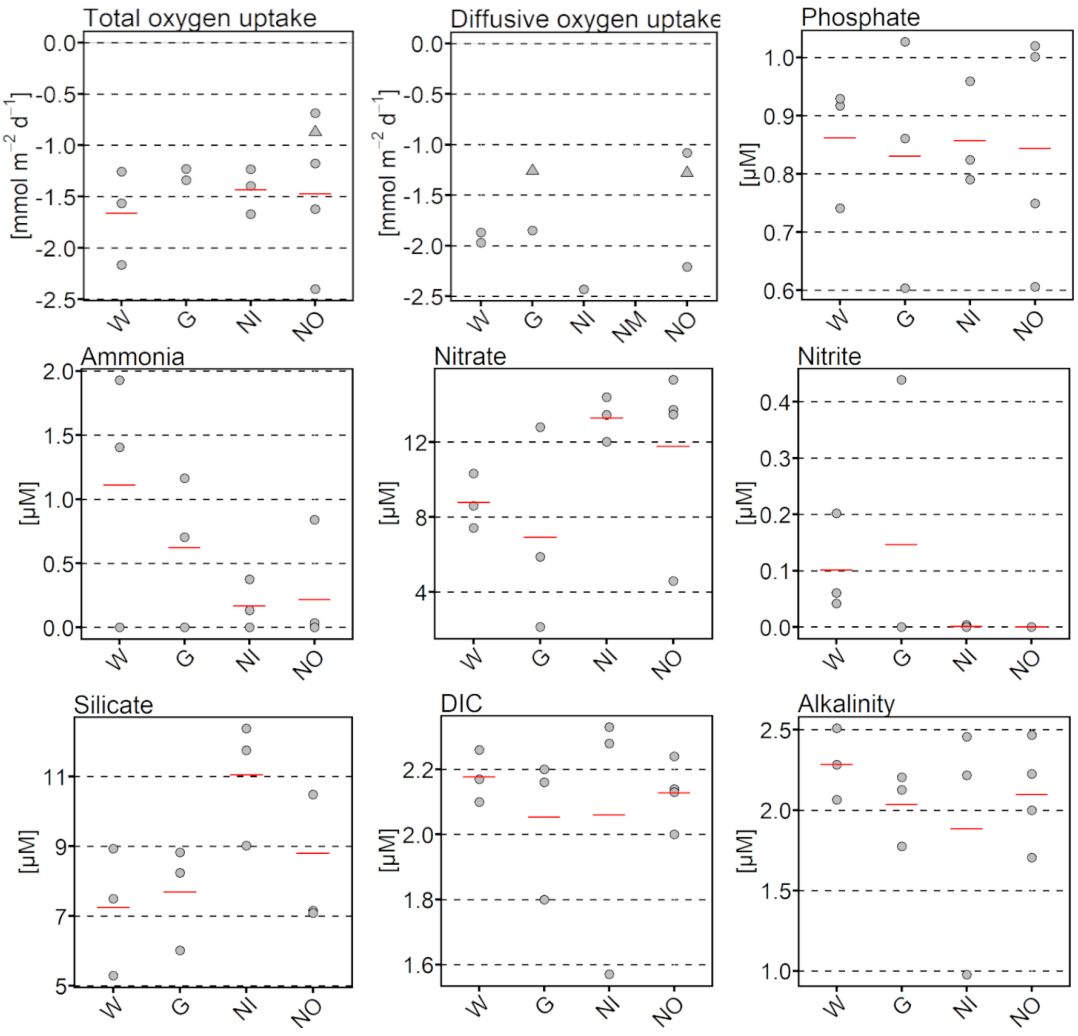

FIGURE 3.5: **Dotplots for oxygen fluxes and bottom water nutrient concentrations on the NEG shelf during PS109.** Dots represent ex situ values at stations and red lines the respective means. Triangles indicate in situ values (not included in the means). Means for DOU are not shown due to the low sample sizes.

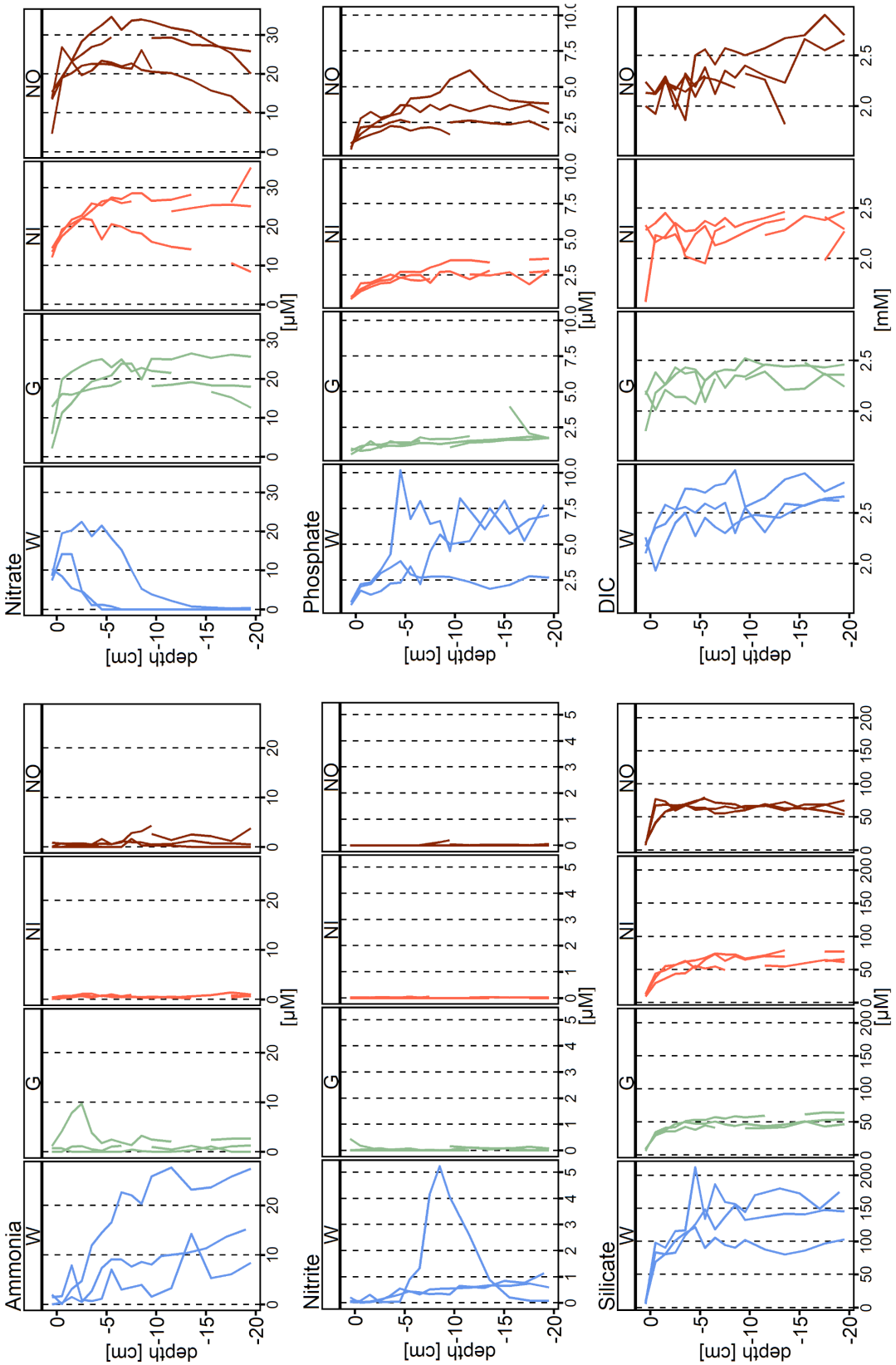

FIGURE 3.6: **Sediment nutrient and DIC profiles for each site on the NEG shelf during PS109 across -0.5 cm (bottom water) and 20 cm sediment depth.** DIC = Dissolved inorganic carbon.

3.3 Environmental drivers

Table 3.1 and Fig. 3.7 show Spearman rank correlations of all measured environmental parameters, biogenic compounds, bottom water nutrients, TOU and single cell abundances. Fig. 3.7 shows the significance of each corresponding correlation (p-values indicated by asterisks).

Salinity was strongly positively correlated with depth. Current velocities were not significantly correlated with any of the other parameters. Temperature was negatively correlated with grain size, pigments and single cell abundances. Grain size was positively correlated with single cell abundances. As expected, a high negative correlation occurred between the silt fraction and median grain size. Pigments (Chl *a*, Fucoxanthin, Phaeopigments, Chl *a*-CPE and Chl *a*-Phaeo ratios) were mostly highly positively correlated to each other. Chl *a*-CPE and Chl *a*-Phaeopigments ratios were negatively correlated to temperature, salinity and depth, with Chl *a*-Phaeopigments ratio being significantly negatively correlated. Surprisingly, pigments were significantly negatively correlated with attenuation; the opposite was expected. Highest attenuation was present at the Norske Trough, where also lowest values of pigments were detected. Nitrate was positively correlated with depth and salinity. Alkalinity was positively correlated with DIC.

The PCA in Fig. 3.8 shows how the stations are separated based on the environmental variables. Based on the correlations outlined in Fig. 3.7, only one pigment parameter was chosen (Chl *a*), since all of them correlated strongly with each other. Temperature was selected for salinity, and median grain size for the silt fraction. 74% of the total variance between sites are explained by the first two axes of the PCA (Table 3.2). Temperature was most correlated with the first PC axis, current velocities with the second PC axis.

Variance was high between the shallow glacier station G3 and all other stations. The Westwind Trough stations and the cold shallow NO1 are seperated from all other stations (glacier and Norske Trough) along the first axis, correlating highly negatively with temperature. Stations with higher current velocities (Westwind and glacier stations) are separated from stations with lower current velocities (Norske Trough stations) along the second axis. Westwind stations correlated positively with Chl *a* concentrations and negatively with depth. Glacier stations correlated negatively with attenuation and grain size, while NO1 correlated positively with grain size.

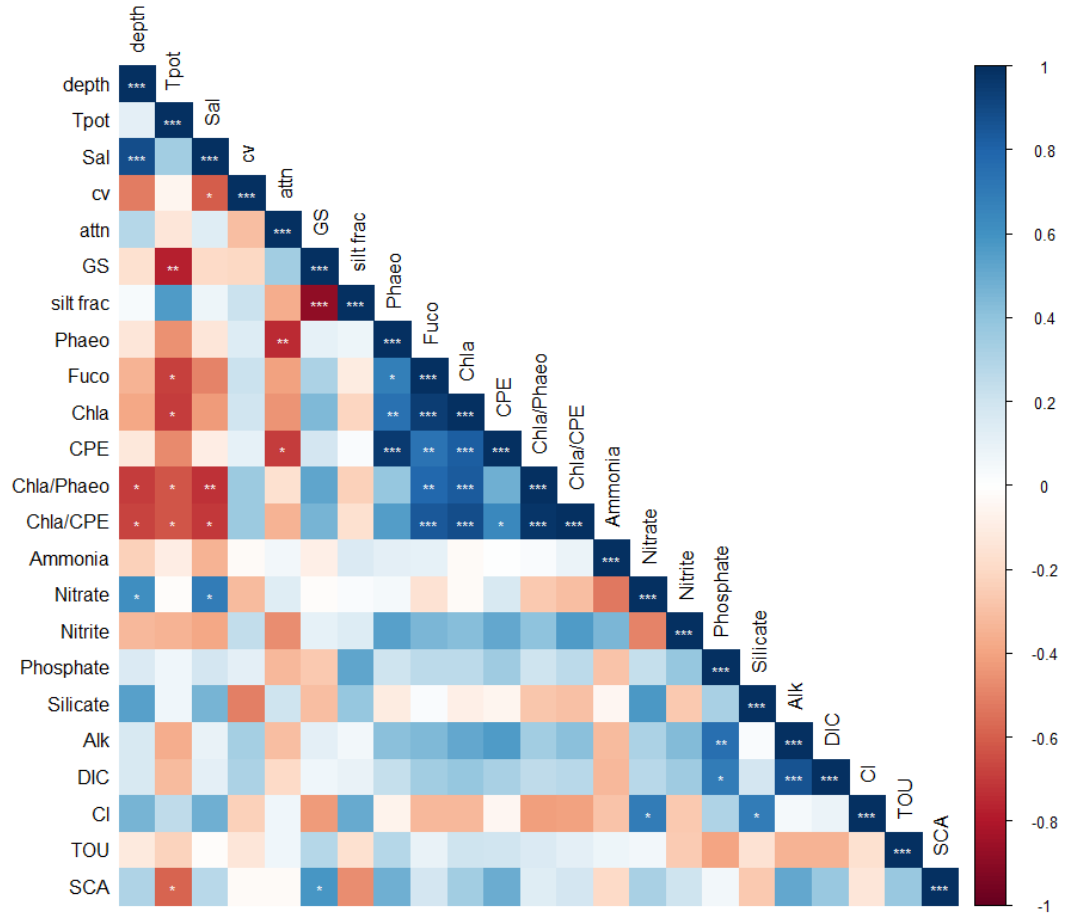

FIGURE 3.7: **Correlation plot of Spearman-rank correlations between environmental parameters, bottom water nutrients, total oxygen uptake (TOU) and single cell abundances (SCA) on the NEG shelf during PS109.** Station NO4 was excluded from the analysis because it is the only deep station at the slope and under influence of different environmental drivers compared to all other stations on the shelf. If correlations were significant, asterisks indicate p-values of $p < 0.05$ (*), 0.01 (**), 0.001 (***). Fuco = Fucoxanthin, CPE = chloroplastic pigment equivalent, Phaeo = Phaeopigments, silt frac = silt fraction <63 µm, GS = median grain size, TOU = total oxygen uptake, SCA = single cell abundance, Alk = Alkalinity, Cl = Chloride, Sal = Salinity, attn = attenuation.

TABLE 3.1: **Correlation coefficients for Spearman rank correlations for environmental parameters, bottom water nutrients, total oxygen uptake (TOU) and single cell abundances (SCA) during PS109 on the NEG shelf.** Station NO4 was excluded from the analysis because it is the only deep station at the slope and under influence of different environmental drivers compared to all other stations on the shelf. Fuco = Fucoxanthin, CPE = chloroplastic pigment equivalent, Phaeo = Phaeopigments, silt frac = silt fraction <63 µm, GS = median grain size, TOU = total oxygen uptake, SCA = single cell abundance, Alk = Alkalinity, Cl = Chloride, Sal = Salinity, attn = attenuation. For p-values of the correlations, see Fig.3.7.

	depth	Tpot	Sal	cv	attn	GS	silt frac	Phaeo	Fuco	Chla	CPE	Chla/ Phaeo	Chla/ CPE	Ammonia	Nitrate	Nitrite	Phosphate	Silicate	Alk	DIC	Cl	TOU
depth																						
Tpot	0.11																					
Sal	0.89	0.34																				
cv	-0.51	-0.06	-0.61																			
attn	0.29	-0.13	0.14	-0.30																		
GS	-0.16	-0.78	-0.20	-0.20	0.34																	
silt frac	0.03	0.57	0.08	0.22	-0.36	-0.88																
Phaeo	-0.14	-0.45	-0.14	0.15	-0.74	0.10	0.08															
Fuco	-0.34	-0.68	-0.50	0.22	-0.41	0.32	-0.11	0.69														
Chla	-0.38	-0.70	-0.43	0.20	-0.45	0.45	-0.22	0.74	0.95													
CPE	-0.13	-0.48	-0.10	0.10	-0.70	0.18	0.03	0.96	0.74	0.83												
Chla/Phaeo	-0.70	-0.63	-0.73	0.36	-0.17	0.52	-0.23	0.38	0.78	0.83	0.49											
Chla/CPE	-0.68	-0.63	-0.71	0.36	-0.35	0.46	-0.16	0.56	0.84	0.89	0.64	0.97										
Ammonia	-0.23	-0.09	-0.35	-0.02	0.06	-0.09	0.16	0.12	0.10	-0.03	0.00	0.02	0.09									
Nitrate	0.62	-0.01	0.69	-0.31	0.14	-0.01	0.02	0.04	-0.15	-0.02	0.16	-0.27	-0.30	-0.53								
Nitrite	-0.33	-0.34	-0.39	0.24	-0.47	0.11	0.14	0.55	0.45	0.42	0.51	0.41	0.56	0.45	-0.49							
Phosphate	0.15	0.07	0.19	0.11	-0.32	-0.27	0.52	0.21	0.26	0.27	0.36	0.21	0.27	-0.28	0.24	0.39						
Silicate	0.55	0.06	0.47	-0.50	0.21	-0.31	0.38	-0.10	0.02	-0.08	-0.06	-0.27	-0.29	-0.04	0.57	-0.27	0.33					
Alk	0.17	-0.36	0.10	0.34	-0.30	0.12	0.06	0.42	0.45	0.51	0.57	0.35	0.41	-0.31	0.31	0.44	0.76	0.03				
DIC	0.17	-0.31	0.11	0.31	-0.20	0.06	0.09	0.24	0.35	0.38	0.33	0.25	0.27	-0.33	0.28	0.35	0.70	0.18	0.87			
Cl	0.47	0.25	0.49	-0.23	0.06	-0.43	0.50	-0.06	-0.32	-0.32	-0.05	-0.41	-0.41	-0.28	0.70	-0.27	0.31	0.70	0.05	0.08		
TOU	-0.12	-0.22	-0.01	-0.14	0.06	0.29	-0.17	0.29	0.09	0.20	0.20	0.15	0.12	0.08	0.06	-0.26	-0.40	-0.15	-0.35	-0.35	-0.17	
SCA	0.30	-0.59	0.28	-0.02	-0.02	0.58	-0.46	0.48	0.18	0.35	0.50	0.13	0.18	-0.20	0.32	0.20	0.06	-0.27	0.51	0.38	-0.13	0.38

TABLE 3.2: **Principal Component Analysis results of standardized and transformed environmental variables on the NEG shelf.** Correlating variables were deselected when Spearman-rank correlations were high (Fig. 3.7, Table 3.1). Station NO4 was excluded from the analysis because it is the only deep station at the slope and under influence of different environmental drivers compared to all other stations on the shelf. Eigenvalues and the proportion explained by the 4 ordination axes and linear coefficients (Eigenvectors) are given. T_{pot} = potential temperature, cv = current velocities, attn= attenuation, GS = median grain size.

	PC1	PC2	PC3	PC4
Eigenvalue	2.41	2.06	0.97	0.43
Proportion explained	0.40	0.34	0.16	0.07
Cumulative proportion	0.40	0.74	0.91	0.98
Eigenvector				
Depth	0.57	0.74	-0.64	0.17
T_{pot}	1.10	-0.08	0.29	-0.16
cv	-0.09	-1.03	0.25	0.45
attn	-0.38	0.92	0.33	0.48
GS	-0.92	0.43	0.41	-0.31
Chl a	-0.85	-0.39	-0.69	-0.02

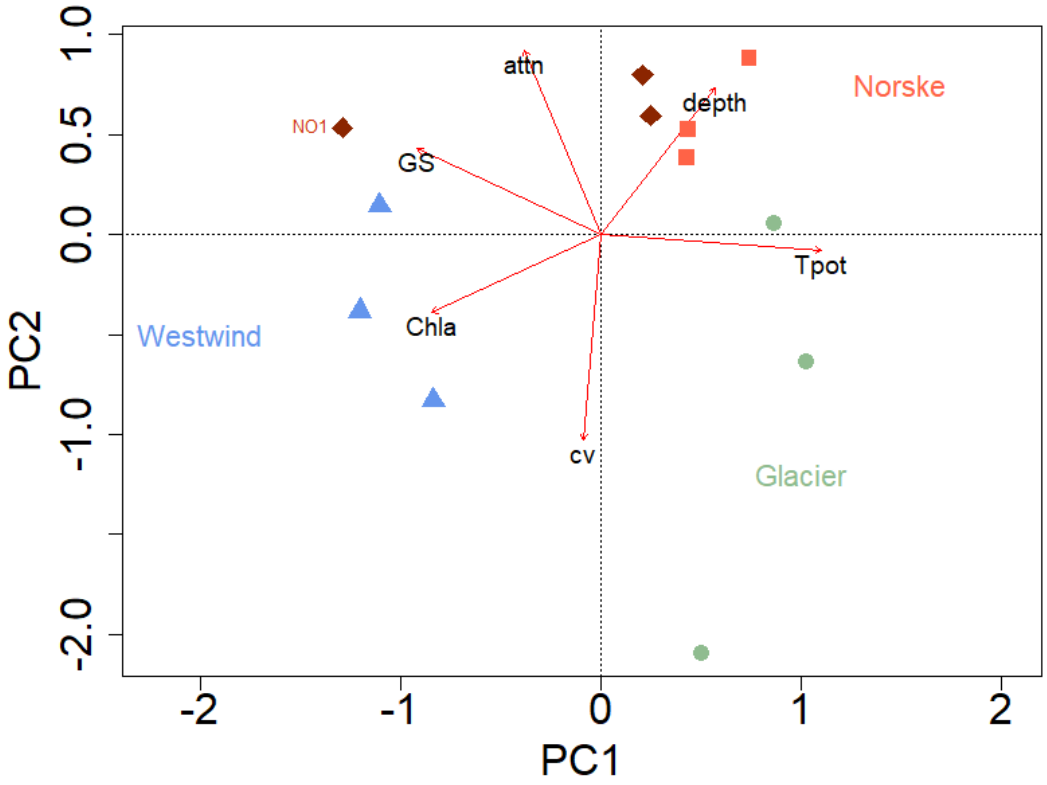

FIGURE 3.8: **Principal component analysis (PCA) showing similarity among stations based on standardized and transformed environmental variables on the NEG shelf during PS109.** Correlating variables were deselected when Spearman-rank correlations were high (Fig. 3.7, Table 3.1). Vectors indicate the direction and strength for the contribution of each parameter to the overall distribution. Coloured symbols indicate stations. Station NO4 was excluded from the analysis because it is the only deep station at the slope and under influence of different environmental drivers compared to all other stations on the shelf. Blue downward triangles = Westwind Trough, green circles = 79N Glacier, lightred quadrangles = inner, darkred rhombi = outer Norske Trough. CPE = chloroplastic pigment equivalent, GS = median grain size, cv = bottom water current velocities, attn = attenuation, T_{pot} = potential temperature.

3.4 Community characteristics

In total, 4263 individuals were identified, which belonged to 236 distinct taxa, of which 3697 individuals and 35 species were foraminifera. Total macrofauna species numbers in the samples ranged from 1 at several stations (G3, NO3, NI3) to 20 (W2). The steep slope of the species accumulation curves (ex situ stations only, excluding foraminifera) demonstrates that the used sampling effort was not sufficient to cover the communities. Even when taking all sampling sites into account, the curve still revealed a steep slope (Fig. 3.9).

The most abundant macrofauna species was *Boltenia ovifera* (Ascidiacea) with 5.33 *ind* 0.007 m^{-2} at NO2, followed by juvenile Bivalvia at W1 and *Nothria conchylega* at NO1 with an average number of 4 *ind* 0.007 m^{-2} each. All other macrofauna taxa occurred with average densities lower than 4.

Foraminifera species occurred in much higher densities at all stations. The most abundant species was *Labrospira crassimargo* with an average density of 195.5 *ind* 0.007 m^{-2} at W3, followed by *Cribrostomoides subglobosum* at NO3 (49.7 *ind* 0.007m^{-2}). *Quinqueloculina sp.* was the most abundant species at G3 and G2 with 41.67 and 9.33 *ind* 0.007 m^{-2}, respectively. This species was also most abundant at NI2 with an average of 10 *ind* 0.007 m^{-2}. In contrast, at G1 *Cuneata arctica* was the most abundant species. Komokioidea were most abundant at W1 and W2 with 13.3 *ind* 0.007 m^{-2} and 9.67 *ind* 0.007 m^{-2}, respectively (Table 3.3).

In situ samples from Landers and ex situ samples from MUC revealed different patterns in the representation of abundance and biomass per m^2 (Fig. 3.3). While total density estimated by the calculation as *ind* m^{-2} was much higher for all ex situ stations, for in situ stations much lower densities were estimated. By contrast, all in situ stations had a higher biomass compared to ex situ. Excluding foraminifera, total densities of macrofauna were highest in the Westwind Trough and at the stations NO1 and NO2, while at the glacier, the inner Norske Trough and at the stations NO3 and NO4 lowest densities were recorded (Fig. 3.10). This pattern was similar when foraminifera abundances were included, although the tendency was weakened (Fig. 3.10). The high variation of the densities in the Westwind Trough results from the low numbers of foraminifera found at W1 and W2 (with average total densities of 13.67 and 16.33 individuals 0.007 m^{-2}), while W3 had high numbers of foraminifera (270.25 *ind* 0.007 m^{-2}, Fig. 3.3). One sample at the glacier station G1 (85-1, Table 2.1) did not contain any macrofauna individuals except for a colonial Bryozoan specimen (*Escharella sp.*), which could not be weighted due to its small individual size and fragility.

Similar to density, total biomass was highest in the Westwind Trough with values between 8.4 and 22.3 $g\ m^{-2}$ and in the outer Norske Trough ($1.2 - 80.0\ g\ m^{-2}$), and lowest at the glacier ($0.5 - 2.1\ g\ m^{-2}$) (Fig. 3.10). The high value at NO1 originates from the high density of large *Nothria conchylega* individuals.

Total single cell abundances in 0-1 *cm* sediment depth ranged from $4 \cdot 10^{08}$ to $2.61 \cdot 10^{09}$ *cells* ml^{-1} with lowest values at all glacier stations ($4 \cdot 10^{08} - 1.59 \cdot 10^{09}$ *cells* ml^{-1}), and highest values in the Westwind Trough ($1.60 \cdot 10^{09}$ - $2.61 \cdot 10^{09}$ *cells* ml^{-1}). In $4 - 5$ *cm* depth, cell abundances were in average lower than in 0-1 *cm* across all sites except at the outer Norske Trough, where $1.86 \cdot 10^{09}$ *cells* ml^{-1} were counted (Fig. 3.10). The differences between sites observed in the single cell abundances of 0-1 *cm* was reflected in the average values in the 4-5 *cm* sediment layer, except for the high cell abundances at the outer Norske (NO3 and NO4) and the much lower values at NO1 and NO2. Station W1 in the Westwind Trough had higher cell abundances in 4 - 5 *cm* than in 0-1 *cm* ($2.70 \cdot 10^{09}$ and $1.60 \cdot 10^{09}$ *cells* ml^{-1}, respectively).

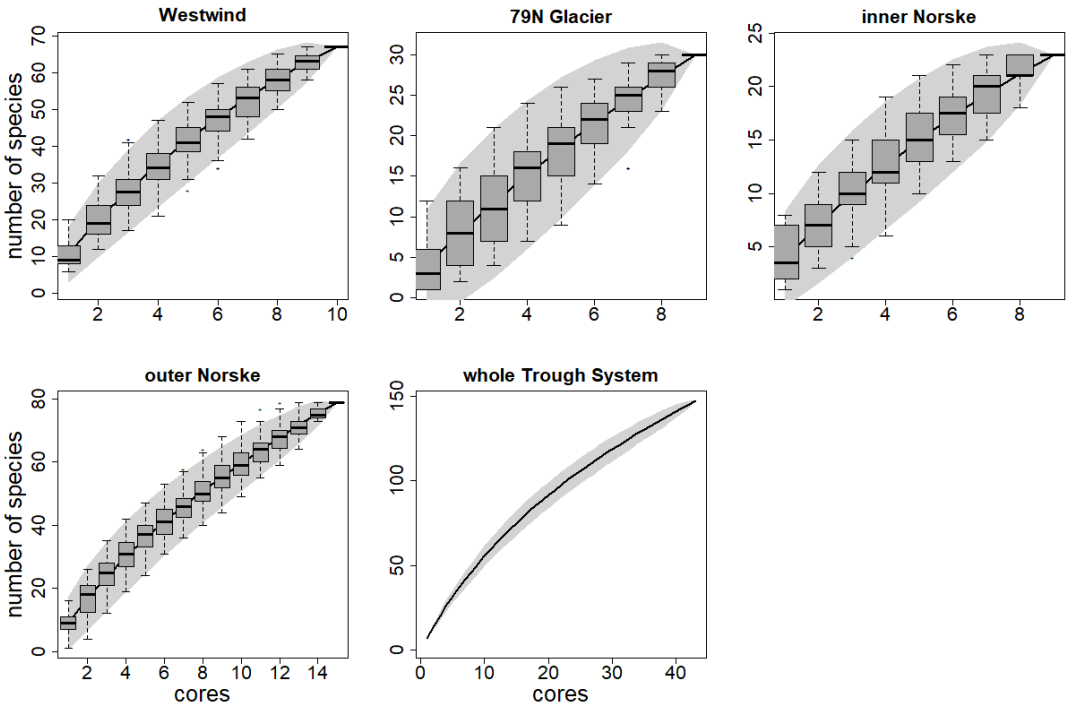

FIGURE 3.9: **Species accumulation curves for macrofauna species from ex situ samples on the NEG shelf during PS109.** Colonial taxa are included, foraminifera are excluded. Boxplots represent single samples.

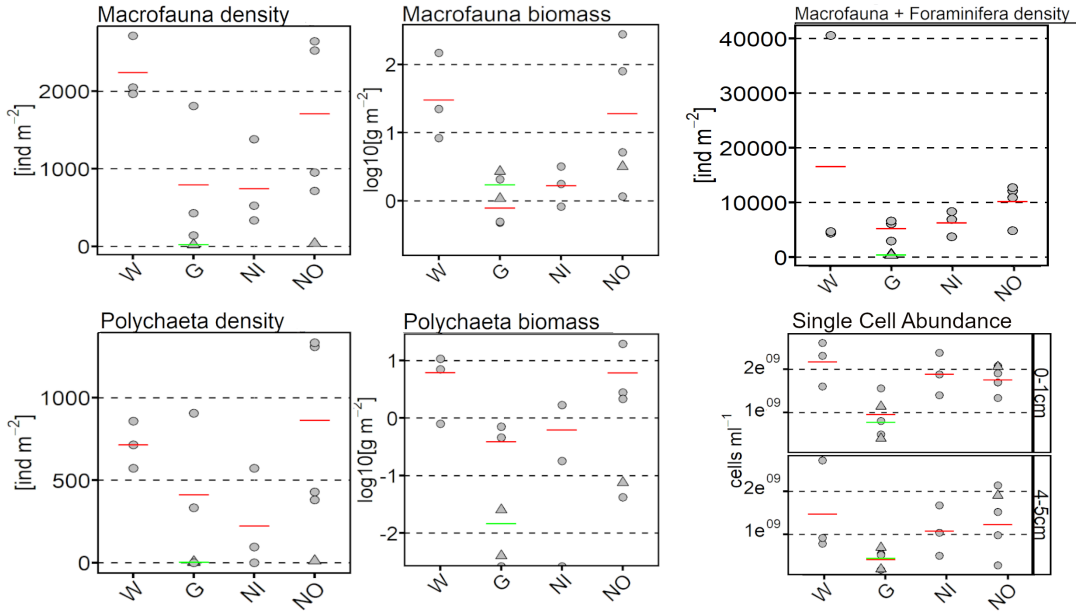

FIGURE 3.10: **Dotplots for community parameters and single cell abundances per station for each site on the NEG shelf during PS109.** Dots represent ex situ, triangles represent in situ stations. Red lines indicate for averages taken from ex situ stations, green lines for averages taken from in situ stations. Macrofauna densities only, macrofauna + foraminifera densities, Polychaeta densities, log10-transformed polychaeta biomass, log10-transformed macrofauna biomass, prokaryotic single cell abundances for sediment depths of 0-1 cm and 4-5 cm are shown. Biomasses at W2 and NO1 were highly skewed due to the presence of a single individual of *Priapulus bicaudatus* at W2 and *Ctenodiscus crispatus* at NO1, each (Table 3.3), therefore their body mass was subtracted. W= Westwind Trough, G = 79N Glacier, NI = inner, NO = outer Norske Trough.

TABLE 3.3: **Benthic community parameters for all stations on the NEG shelf during PS109.** Foraminifera data were not available for the in situ station NO1. Most abundant taxa are nor reported for macrofauna species, since no dominant species were present in samples. Sampling area for in situ (Lander) samples was 0.4 m^2, for ex situ (MUC) samples 0.007 m^2. Numbers in red: For total biomass at W2 the body mass of one large specimen of *Priapulus bicaudatus* was subtracted (original total biomass: 147.6 g), while for total biomass at NO2, the body mass of *Ctenodiscus crispatus* was subtracted (original biomass: 277.9 g) since otherwise the data was skewed.

		DENSITY								BIOMASS		SINGLE CELL ABUNDANCE			
		Macrofauna			Foraminifera					Macrofauna		0-1cm		4-5cm	
Gear	**St**	**total nr of ind per sampling area**	**total nr of ind per m^2**	**sd ind per m^2**	**total nr of ind per sampling area**	**total nr of ind per m^2**	**sd ind per m^2**	**most abundant taxon**	**total nr of ind per sampling area**	**total biomass $g\ m^{-2}$**	**sd $g\ m^{-2}$**	*cells* m^{-1}	**sd**	*cells* m^{-1}	**sd**
MUC	W1	14.3	2047.6	659.8	16.3	2333.3	1.95×10^3	Komokioidea	13.3	8.4	5.3	1.60×10^9	3.08×10^8	2.71×10^9	3.09×10^8
	W2	19.0	2714.3	1984.6	13.7	1952.4	1.84×10^3	Komokioidea	9.7	12.0	11.9	2.31×10^9	5.43×10^8	7.86×10^8	1.23×10^8
	W3	13.8	1964.3	713.1	270.3	38607.1	1.50×10^4	*Labrospira crassimargo*	195.5	22.3	13.6	2.61×10^9	4.68×10^8	9.19×10^8	1.36×10^8
	G1	12.7	1809.5	540.8	30.3	4333.3	1.74×10^3	*Cuneata arctica*	7.3	2.1	1.3	4.95×10^8	1.11×10^8	1.86×10^8	9.32×10^7
	G2	3.0	428.6	142.9	17.7	2523.8	1.70×10^3	*Quinqueloculina sp.*	9.3	0.5	0.4	8.05×10^8	4.44×10^6	5.28×10^8	1.38×10^8
	G3	1.5	214.3	1.5	45.3	6476.2	5.77×10^2	*Quinqueloculina sp.*	41.7	0.7	0.6	1.56×10^9	7.52×10^8	5.49×10^8	7.52×10^7
	NI1	9.7	1381.0	9.7	38.7	5523.8	8.73×10^2	*Rhabdammina sp.*	14.7	3.2	1.6	2.38×10^9	5.64×10^8	1.04×10^9	1.18×10^8
	NI2	3.7	523.8	3.7	54.7	7809.5	7.05×10^2	*Quinqueloculina sp.*	10.0	1.8	1.7	1.40×10^9	3.85×10^7	5.07×10^8	6.28×10^7
	NI3	2.3	333.3	2.3	23.7	3381.0	1.25×10^3	*Cribrostomoides subglobosum*	10.3	0.8	0.2	1.88×10^9	6.95×10^7	1.68×10^9	5.22×10^8
	NO1	18.5	2642.9	18.5	66.5	9500.0	2.88×10^3	*Cibicidoides lobatulus*	16.3	80.0	96.3	1.70×10^9	2.53×10^8	2.84×10^8	9.77×10^6
	NO2	17.7	2523.8	17.7	58.7	8381.0	2.84×10^3	*Cuneata arctica*	16.0	5.1	2.6	2.08×10^9	7.40×10^8	9.84×10^8	1.13×10^8
	NO3	5.0	714.3	5.0	84.3	12047.6	3.64×10^3	*Cribrostomoides subglobosum*	49.7	3.0	2.9	1.91×10^9	2.12×10^8	2.14×10^9	7.06×10^8
	NO4	6.7	952.4	6.7	27.3	3904.8	1.49×10^3	*Cuneata arctica*	11.0	1.2	1.6	1.33×10^9	2.16×10^8	1.52×10^9	4.14×10^8
Lander	G2	8.0	20.0	8.0	182.0	455.0	3.53×10^2	*Quinqueloculina sp.*	102.3	1.1	0.8	4.00×10^8	7.73×10^7	6.99×10^8	1.96×10^8
	G3	9.0	22.5	9.0	140.3	350.8	2.75×10^2	*Quinqueloculina sp.*	126.7	2.7	4.4	1.14×10^9	4.51×10^7	2.02×10^8	4.09×10^7
	NO3	16	40	16.0	-	-	-	-	-	3.2	4.4	2.06×10^9	3.85×10^8	1.90×10^9	3.78×10^8

When looking at the 9 most important phyla across all sites in terms of densities, the most abundant phylum was Annelida, represented by polychaeta exclusively and accounting for the high numbers (Fig. 3.11). They were especially abundant in the outer Norske and in the Westwind Trough; lowest numbers were observed in the inner Norske Trough. Ampharetidae was the most represented family, followed by Maldanidae. Crustacea was the second most abundant phylum, with Isopoda being the most abundant order, followed by Cumacea, Ostracoda and Tanaidacea. Among the molluscs, the genus *Yoldiella* was most abundant, being represented by five different species across the NEG shelf. *Bathyarca pectunculoides* and *Dacrydeum vitreum* were the second and third most abundant mollusc species. Small individuals of the ascidian *Boltenia ovifera* accounted for the high numbers of tunicates in the inner and outer Norske Trough. Surprisingly, Sipuncula occurred in high densities relative to the small sample sizes, being most abundant in the Westwind and outer Norske trough, and mostly represented by *Nephasoma diaphanes*. Echinodermata were present in low densities but in generally large individual sizes and high body mass.

If foraminifera were excluded, all diversity indices for ex situ stations were highest in the Westwind and the outer Norske Trough. Species numbers S were especially low at the glacier and inner Norske Trough. When foraminifera were taken into account, values for indices shifted. All values for the diversity indices decreased in the Westwind Trough and increased at the glacier stations. Taxonomic distinctness Δ^* was highest at the glacier stations. H' and species evenness J' were still lowest for the glacier, but highest in the inner Norske Trough and much lower in the Westwind Trough. Although all values increased for the glacier and inner Norske Trough, total number of species was still lower at these sites than at the Westwind and outer Norske Trough.

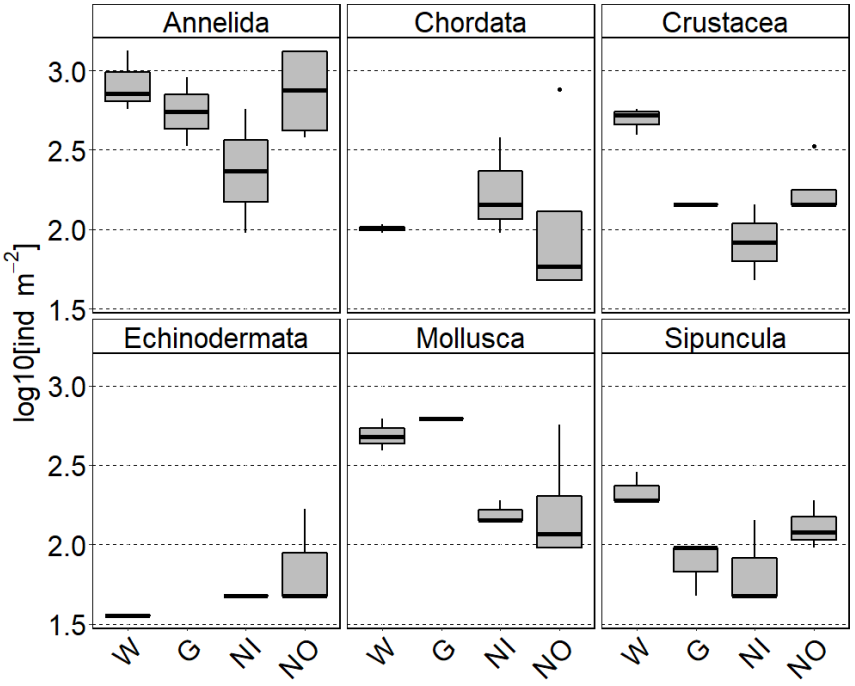

FIGURE 3.11: **The most important phyla sampled at each site on the NEG shelf during PS109.** W= Westwind Trough, G = 79N Glacier, NI = inner, NO = outer Norske Trough.

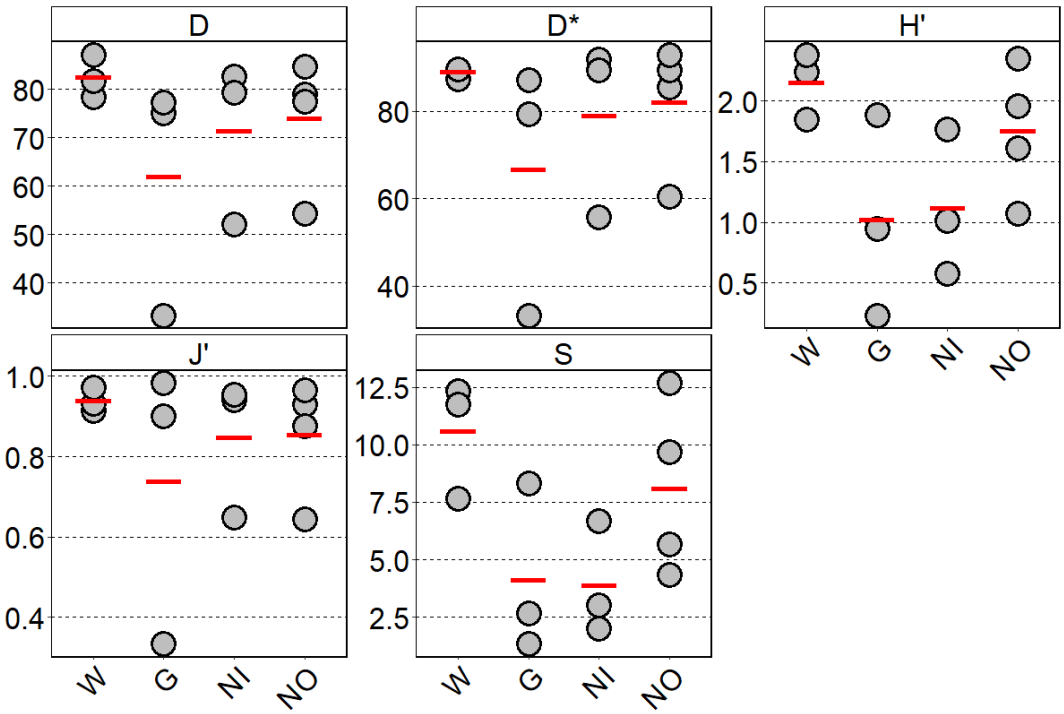

(A)

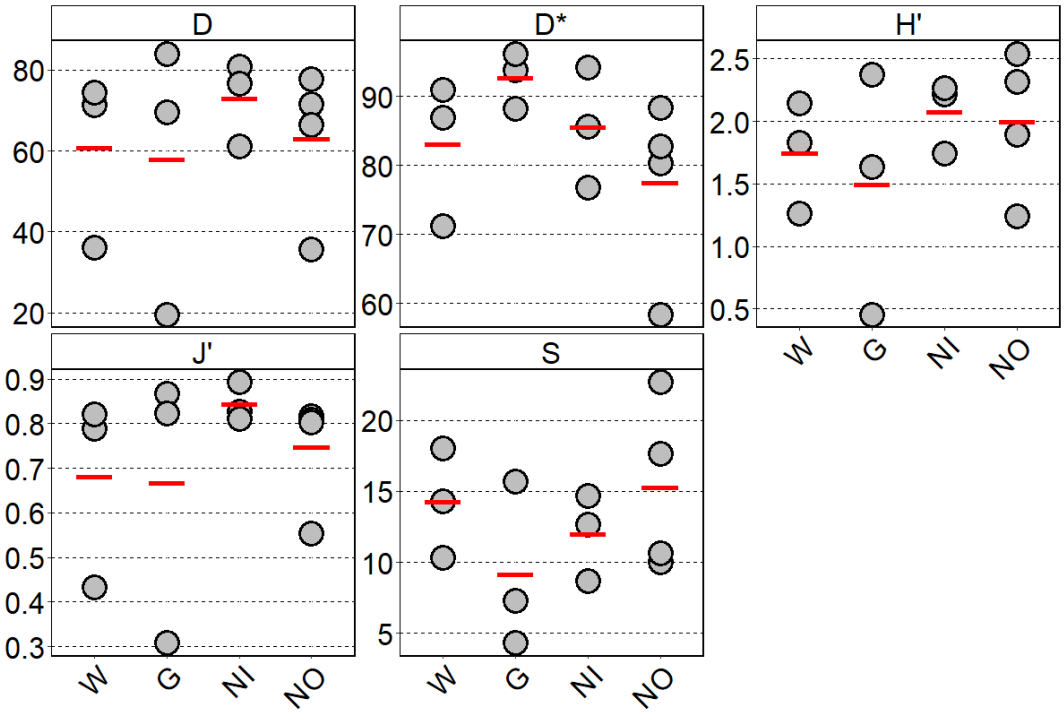

(B)

FIGURE 3.12: **Diversity indices based on community abundances for each site on the NEG shelf during PS109** (A) for macrofauna taxa and (B) macrofauna + foraminifera. Ex situ samples are excluded. D = taxonomic diversity, D* = taxonomic distinctness, H' = Shannon-Wiener diversity, J' = Pielou's evenness, S = total species number per MUC station. W= Westwind Trough, G = 79N Glacier, NI = inner, NO = outer Norske Trough.

Table 3.4 shows the results of the similarity profile routine (SIMPROF) analysis for all ex situ stations. The analysis reveals 3 statistically distinct groups based on community density on the NEG shelf when foraminifera are excluded. One group consists of all Westwind stations, another of one glacier and one inner Norske trough station, while all other stations cluster together in a third group. If foraminifera are taken into account, 6 distinct groups can be distinguished. The Westwind stations are divided into 2 groups but still cluster together. Most of the outer Norske stations cluster together, while most of the glacier stations group together with the inner Norske stations. NO4 and G3 cluster by themselves, respectively and do not group with the other stations. Based on these results and the differing environmental variables at Station NO4, this station was excluded from all subsequent analyses to focus on the driving factors on the NEG shelf.

TABLE 3.4: **Results of Bray-Curtis distances-based SIMPROF analysis for non-transformed community density data.** Ex situ stations are excluded. Analyses were performed for macrofauna and macrofauna + foraminifera, respectively. The analysis identified 3 and 6 statistically distinct groups, respectively.

	Macrofauna		Macrofauna + Foraminifera	
Significant cluster	1	NO1, NO3, G2, NO4, NO2, NI2, G1, NI1	1	G3
	2	G3, NI3	2	NO2
	3	W3, W1, W2	3	G2, G1, NI3, NI1, NI2
			4	NO3, NO1, NO2
			5	W3
			6	W1, W2

If squareroot-transformed polychaeta densities from all ex situ stations (except for Station NO4) as the most abundant taxon were considered only, the sites could be mainly distinguished between the Westwind Trough and all other stations (Fig. 3.14). The glacier station G3 and the inner Norske Trough Station NI1 needed to be excluded from the analysis, because no polychaeta were present at these stations. Generally, less polychaete families were represented in the inner Norske Trough and at the glacier. Sedentarian filter-feeding Sabellidae and surface deposit-feeding Ampharetidae correlated well with the Norske and one glacier station, and tube dwelling (Maldanidae, Oweniidae), burrowing (Capitellidae, Cirratulidae) deposit-feeders and the small free-living Pholoid *Pholoe sp.* were mainly present in the outer Norske Trough. Mobile, free-living crawling families (Syllidae, Flabelligeridae, Paraonidae) were present in the Westwind Trough. Predators (Nephtyidae and Eusyllidae) clustered together between the glacier and Westwind trough.

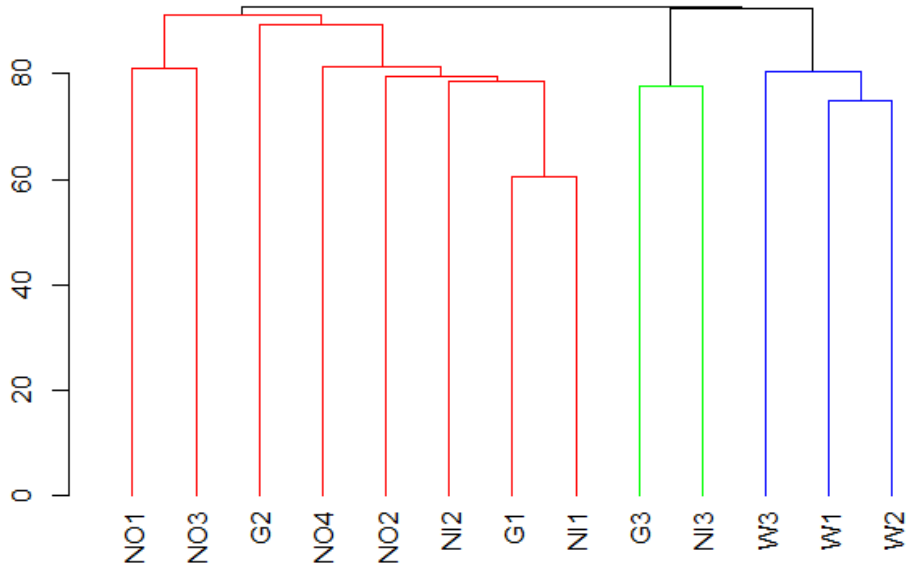

(A)

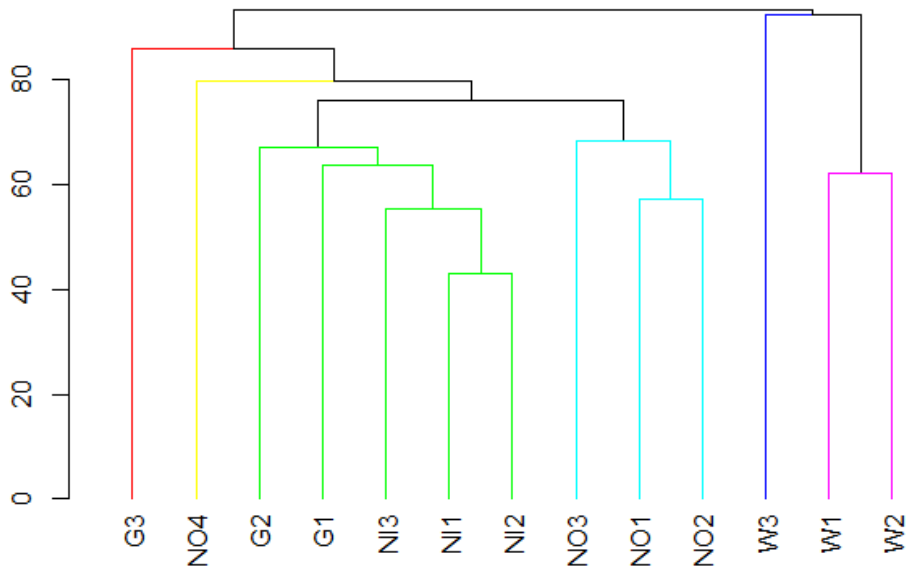

(B)

FIGURE 3.13: **Dendrogram representation of the results of Bray-Curtis distances-based SIMPROF analysis for non-transformed community density data.** Ex situ stations are excluded. Analyses were performed for (A) macrofauna and (B) macrofauna + foraminifera, respectively. The analysis identified 3 and 6 statistically distinct groups, respectively. Colours indicate clusters that are grouped together by the SIMPROF test.

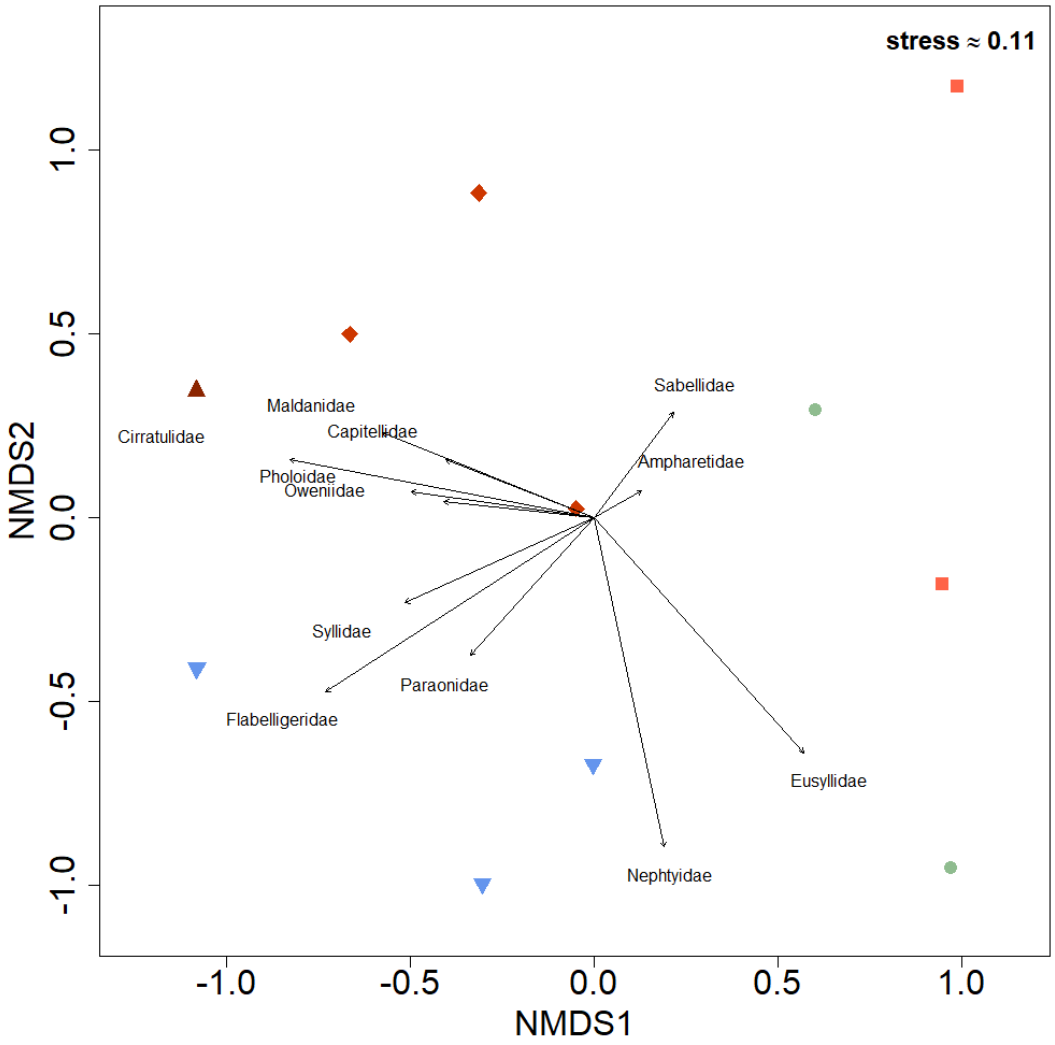

FIGURE 3.14: **non-metric multidimensional scaling (nMDS) plot on squareroot-transformed polychaeta with the twelve most abundant families fitted onto the ordination**. The projections of stations onto vectors have maximum correlation with corresponding families. Colored symbols represent stations. Blue downward triangles = Westwind Trough, green circles = 79N Glacier, lightred quadrangles = inner, darkred rhombi = outer Norske Trough. G3 and NI3 were excluded from the analysis because no polychaetes were recorded at these stations. Station NO4 was excluded.

In the correspondence analysis (CA) based on ex situ community density data (macrofauna + foraminfera), the eigenvalues of the first and second correspondence axes accounted for 17 and 13 % of the total variation, respectively (Table 3.5). Both axes explained 30 % of the overall variation. Variation was high between the 4 *a priori* distinguished sites when NO4 is excluded from the analysis (Fig. 3.15). The Westwind trough correlated negatively with the first axis, while the glacier stations correlated negatively and the Norske Trough stations positively with the second axis. The glacier stations were most similar to the inner Norske stations. Variation was lower between NO2 and NO3 and the inner Norske stations, while the variation of NO1 (the shallowest station) to all other stations was high along the second axis. When standardized and transformed environmental parameters are fitted on top of the ordination, it is visible that Chl *a* correlates best with the Westwind Trough stations along the first axis, and attenuation, grain size and temperature along the second axis. Current velocities and depth played a less important role in the representation with the first two CA axes and therefore for the community patterns.

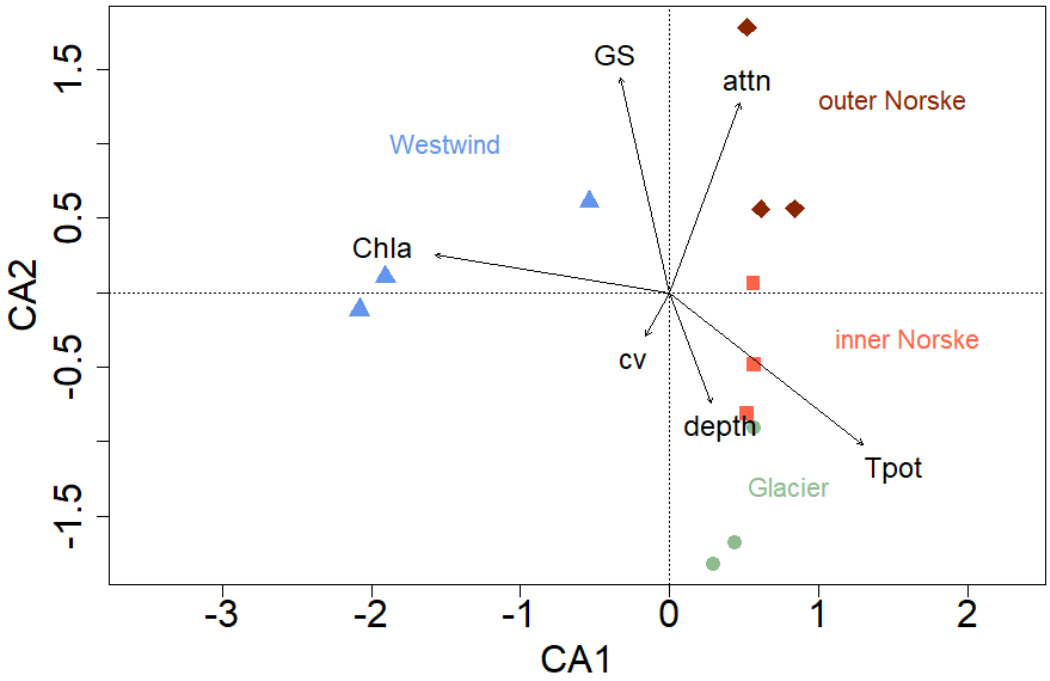

FIGURE 3.15: **Visualisation of the Correspondance analysis (CA) results on Hellinger-transformed ex situ community density (macrofauna+foraminifera) with standardised and transformed environmental parameters fitted onto their ordination.** Symbols represent stations. Station NO4 was excluded. The projections of points onto vectors have maximum correlation with corresponding environmental variables. Blue downward triangles = Westwind Trough, green circles = 79N Glacier, lightred quadrangles = inner, darkred rhombi = outer Norske Trough.

PERMANOVA revealed significant differences between sites in terms of each community abundance parameter (density and biomass; Table 3.6), though the strength of the factor "sites" differed depending on the parameter taken into account. Highest dissimilarity among groups was detected when foraminifera were taken into account ($R^2 = 0.491$ for untransformed and $R^2 = 0.493$ for transformed data). Differences among sites based on Polychaeta densities could be explained with an R^2 between 0.410 and 0.418. When macrofauna densities excluding foraminifera were taken into account, much more variance remained unexplained (R^2 between 0.30 and 0.37). However, the post-hoc pairwise comparisons showed that none of the tested locations showed differences between pairs in any of the tested community parameters (Table 3.7).

The best linear model based on Bray-Curtis dissimilarities explaining community density patterns (macrofauna + foraminifera) included Chl *a* and attenuation (turbidity), with significant (although not very high) R^2 values of 0.25 and 0.15, respectively. All other environmental variables did not contribute significantly to the model.

TABLE 3.5: **Results of the correspondence analysis (CA) on Hellinger-transformed ex situ community data (macrofauna+foraminifera) during PS109 on the NEG shelf.** Eigenvalues and the proportion explained by the 6 ordination axes and station scores are given. Station NO4 was excluded from the analysis.

	CA1	CA2	CA3	CA4	CA5	CA6
Eigenvalue	0.676	0.492	0.453	0.408	0.369	0.331
Proportion explained	0.172	0.126	0.116	0.104	0.094	0.085
Cumulative proportion	0.172	0.298	0.414	0.518	0.612	0.696
Station scores (weighted averages of species scores)						
19	-1.906	0.108	-1.577	1.933	-1.083	0.390
36	-2.080	-0.115	0.072	-1.876	0.871	-0.148
46	-0.538	0.610	2.701	1.462	0.623	0.106
76	0.572	-0.906	0.221	-0.181	-0.273	1.499
84	0.296	-1.819	0.528	-0.768	-1.242	-0.276
85	0.444	-1.677	0.028	0.373	-1.182	-0.729
93	0.518	-0.806	0.068	0.077	0.380	0.106
105	0.567	-0.481	-0.293	0.244	0.200	-0.850
115	0.560	0.068	-0.491	0.429	0.350	-1.683
122	0.520	1.780	0.129	-0.812	-1.450	0.000
125	0.842	0.564	-0.981	0.067	1.471	1.672
139	0.614	0.560	-0.736	0.220	1.390	-1.934

TABLE 3.6: **one-way PERMANOVA results of Bray-Curtis distance based community abundance matrices.** Analyses were performed with the factor "sites" with 4 levels (Westwind Trough, 79N Glacier, inner Norske Trough, outer Norske Trough) on untransformed and Hellinger-transformed community abundance data and applied on macrofauna density, macrofauna + foraminifera density, polychaeta density and macrofauna biomass, respectively. Station NO4 was excluded. R^2 and p-values are given for each analysis.

factor: "sites" with 4 levels

	DENSITY			BIOMASS
	Macrofauna	Macrofauna & Foraminifera	Polychaeta	Macrofauna
	untransformed data			
R^2	0.364	0.491	0.41	0.3
p	0.006**	0.001**	0.018*	0.049*
	Hellinger-transformed data			
R2	0.368	0.493	0.418	0.33
p	0.003**	0.001**	0.016*	0.014*

TABLE 3.7: **Results of multilevel pairwise comparisons among groups (locations) of Bray-Curtis distances based community data for untransformed and Hellinger-transformed abundances.** For each pairwise comparison, F, R^2, p and adjusted p-values are given. W= Westwind Trough, G = 79N Glacier, NI = inner Norske Trough, NO = outer Norske Trough.

	DENSITY												BIOMASS			
	Macrofauna				Macrofauna+Foraminifera				Polychaeta				Macrofauna			
	untransformed data															
pairs	F	R2	p	adj. P	F	R2	p	adj. P	F	R2	p	adj. P	F	R2	p	adj. P
W vs G	1.33	0.25	0.10	0.60	2.35	0.37	0.10	0.60	1.81	0.38	0.10	0.60	1.10	0.22	0.30	1.00
W vs NI	2.23	0.36	0.10	0.60	3.21	0.45	0.10	0.60	1.54	0.28	0.20	1.00	1.37	0.26	0.10	0.60
W vs NO	1.91	0.32	0.10	0.60	2.66	0.40	0.10	0.60	2.15	0.35	0.10	0.60	1.07	0.21	0.30	1.00
G vs NI	1.00	0.20	0.50	1.00	1.86	0.32	0.10	0.60	0.79	0.21	0.70	1.00	1.06	0.21	0.30	1.00
G vs NO	1.32	0.25	0.10	0.60	2.80	0.41	0.10	0.60	1.96	0.40	0.10	0.60	1.05	0.21	0.30	1.00
NI vs NO	1.55	0.28	0.20	1.00	2.42	0.38	0.10	0.60	1.63	0.29	0.10	0.60	1.11	0.22	0.20	1.00
	Hellinger-transformed data															
pairs	F	R2	p	adj. P	F	R2	p	adj. P	F	R2	p	adj. P	F	R2	p	adj. P
W vs G	1.30	0.25	0.10	0.60	2.49	0.38	0.10	0.60	1.90	0.39	0.10	0.60	1.11	0.22	0.30	1.00
W vs NI	2.31	0.37	0.10	0.60	3.61	0.47	0.10	0.60	1.49	0.27	0.20	1.00	1.79	0.31	0.10	0.60
W vs NO	2.03	0.34	0.10	0.60	2.53	0.39	0.10	0.60	2.19	0.35	0.10	0.60	1.36	0.25	0.20	1.00
G vs NI	1.02	0.20	0.60	1.00	2.19	0.35	0.10	0.60	0.78	0.21	0.70	1.00	1.05	0.21	0.60	1.00
G vs NO	1.32	0.25	0.10	0.60	2.38	0.37	0.10	0.60	2.24	0.43	0.10	0.60	1.20	0.23	0.10	0.60
NI vs NO	1.57	0.28	0.10	0.60	2.03	0.34	0.10	0.60	1.74	0.30	0.10	0.60	1.46	0.27	0.10	0.60

TABLE 3.8: **Bray-Curtis distance based linear model of community patterns (macrofauna + foraminifera densities) against environmental drivers in stepwise sequential tests on the NEG shelf during PS109.** Station NO4 was excluded. Df = Degrees of freedom, SS = sum of squares, R^2 = Proportion of variance in community patterns explained by environmental variables, p = significance level of proportion of variance explained. Asterisks indicate significance codes of p < 0.05 (*), 0.01 (**), 0.001 (***).

	Df	SS	F.Model	R^2	p
Chl *a*	1	0.85	3.85	0.25	**0.0001*****
attn	1	0.52	2.37	0.15	**0.019***
Tpot	1	0.17	0.75	0.05	0.711
cv	1	0.25	1.14	0.07	0.318
depth	1	0.23	1.03	0.07	0.399
GS	1	0.26	1.19	0.08	0.257
Residuals	5	1.10	0.33		
Total	11	3.37			

TABLE 3.9: **Results of two-way ANOVA and Tukey pairwise comparison test for differences in macrofauna total density and CPE concentrations among regions (Westwind (W), inner Norske Trough (NI), outer Norske Trough (NO)) and time (1992, 2017).** Data from 1992 were retrieved from Ambrose and Renaud (1995). Df = Degrees of freedom, SS = sum of squares, p = significance level of proportion of variance explained, p adj = adjusted p-value. Asterisks indicate significance codes of p < 0.05 (*), 0.01 (**), 0.001 (***).

	two-way ANOVA				
	factor	Df	SS	F	p
	factor	Df	SS	F	p
Macrofauna density	region	2	41268442	5.56	**0.013***
	time	1	16994159	4.58	**0.046***
CPE	region	2	460.16	2.68	0.094
	time	1	647.83	7.55	**0.013***

	TukeyHSD for factor "region"				
	pairs	diff	lower	upper	p adj
Macrofauna density	NO-NI	174.3643	-2547.9406	2896.67	0.986
	WW-NI	2792.77	265.9512	5319.59	**0.029***
	WW-NO	2618.4057	207.0284	5029.78	**0.032***
CPE	NO-NI	-6.769286	-19.858598	6.32	0.405
	WW-NI	3.786	-8.363381	15.94	0.713
	WW-NO	10.555286	-1.039033	22.15	0.078

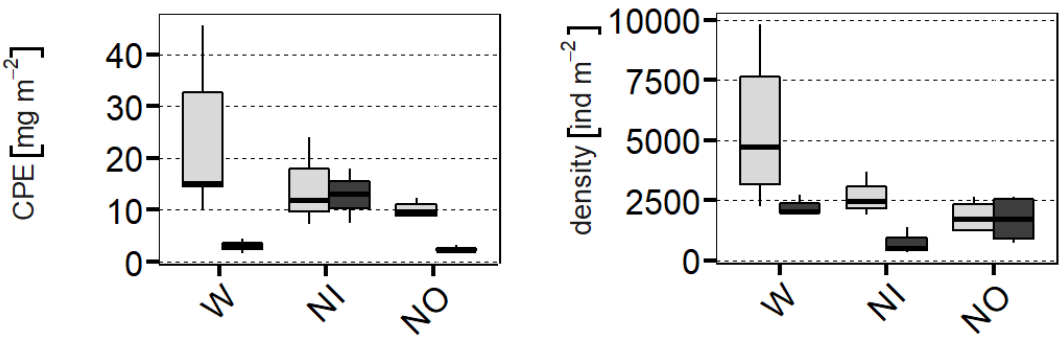

FIGURE 3.16: **CPE and total macrofauna density in 1992 (lightgrey) and 2017 (darkgrey) for Westwind (W), inner Norske Trough (NI) and outer Norske Trough (NO).** Data from 1992 were taken from Ambrose and Renaud (1995).

The results of the two-way ANOVA revealed that differences of macrofauna densities among regions (Westwind Trough, inner and outer Norske Trough) and time (1992 and 217) were significant (Table 3.9; Fig. 3.16). The pairwise comparison showed that based on the factor "region", the main differences were present between the Westwind Trough and the Norske Trough, while differences were not significant between the inner and outer Norske Trough. CPE concentrations differed significantly between 1992 and 2017, but not among regions.

4 Discussion

4.1 Environmental drivers

4.1.1 The role of water circulation on the NEG shelf

The water circulation on the NEG shelf is an important driver that is responsible for the environmental conditions in the Westwind Trough, at the 79N Glacier and in the Norske Trough. It interacts strongly with glacial runoff and, most probably, with sea ice dynamics on the NEG shelf. It influences vertical mixing and upwelling (Meire et al., 2016). Attenuation (for easier visualization hereafter referred to as turbidity), is a result of the interaction between the different water masses and current velocities with the glacier and the sediment properties. Temperature and salinity in the bottom water differed between the Norske Trough, the glacier and the Westwind Trough, in accordance with the circulation patterns on the NEG shelf that had been revealed by recent and past oceanographic investigations (Bourke et al., 1987; Budéus et al., 1997; Wilson and Straneo, 2015; Schaffer et al., 2017).

In the following I will discuss how the different water masses influence the study locations and their different environmental settings.

The East Greenland Current (EGC) flows southwards along the NEG Shelf and carries along Atlantic water which is recirculating at the shelf edge. The deepest station NO4 is located at 1177 *m* water depth on the shelf slope where old cold and saline Atlantic Deep Water is flowing along. These conditions lead to a distinct environment in contrast to the stations on the NEG shelf.

Warm and saline AIW originating from the recirculation in the EGC enters the NEG shelf via the Norske Trough and occupies depths below 250 m (Fig. 2.2; Schaffer et al., 2017). The benthic stations in the Norske Trough are located at around 300 m and are therefore under the influence of AIW. The clockwise circulation of the water masses leads to the advection of AIW towards the glacier margin. At the calving front of the glacier, AIW of temperatures warmer than 1.5 °C is present (Wilson and Straneo, 2015), which is reflected in the bottom water temperature of these stations. At the glacier tongue, glacial melting is induced by the high temperature differences between the calving front and AIW (Wilson and Straneo, 2015), and the water masses get mixed. Due to the more buoyant melt water plume (from now on glacially modified AIW; mAIW) very high turbidity is observed close to the glacier margin. mAIW leaves the glacier cavity through the calving front and the Djmphna Sund, following the clockwise circulation towards the Westwind Trough (Schaffer, 2017). The stations located in the Westwind Trough are colder and less saline than the stations in the Norske Trough because of the mAIW influence. Station W3 was located in the Djmphna Sund at a shallow site, therefore directly in the outflow of mAIW. This explains its much lower bottom water salinity compared to W1 and W2.

In contrast to the other stations in the Norske Trough, NO2 was under influence of Polar Water (PW) because it was located on the Belgica Bank above 200 *m* water depth. PW is circulating in an equally clockwise manner as smaller gyres across the

shallow banks that are located in the center of the study region (Bourke et al., 1987).

In the Norske Trough, the water column is highly stratified between PW, intermediate Knee Water (KW) and warm AIW (Fig. A.2). The more buoyant mAIW leads to a slight homogenisation of the water bodies in the Westwind Trough compared to the Norske Trough. It is likely that the mAIW induces an upwelling in the Westwind Trough which brings up nutrient-rich deep water, since Wallace et al. (1995) had observed that cold nutrient-rich water was rising from the southwest (i.e. where the 79NG is located) into the NEW Polynya which is located in the Westwind Trough. Particle flux was reported to be higher in the western compared to the eastern part of the polynya (Bauerfeind et al., 1997). Upwelling right in front of marine-terminating glaciers induced by the rising subsurface meltwater plume has been documented for other fjord ecosystems around Greenland (Meire et al., 2017) and in the well-studied Kongsfjorden system on Svalbard (van de Poll et al., 2018). Another indication for upwelling in the Westwind Trough induced by the 79NG is, that the turbidity in the Westwind Trough is higher than in the Norske Trough, but still lower than at the stations in the glacier vicinity.

At all stations, turbidity was highest in the upper 70 m of the water column. This observation is in accordance with the fluorescence signals (Fig. A.3) and I suspect this is likely caused by the presence of phytoplankton in the surface water. Additionally, turbidity was very high close to the sea floor (Fig 3.4) except for the outer Norske Trough. It is possible that the silty sediments are whirled up easily by currents. At the outer Norske Trough, silt content was lower and as a consequence, sediments might not be raised up that easily.

4.1.2 Grain size and current velocities

Similar to bottom water temperatures and salinities, the locations could be distinguished based on their sediment properties and the prevailing current velocities.

Except for the glacier station, larger grain sizes coincided with strong current velocities. The coarsest sediment with the lowest silt content was present at the shallow shelf station NO1 at Belgica Bank, revealing a distinct habitat in contrast to the other stations. Differences in the sediment surfaces on banks and in troughs might be attributed to higher current scouring on the banks in comparison to troughs (Ambrose and Renaud, 1995; Brandt, 1995) and troughs are naturally areas of deposition of fine material. This assumption is supported by the present study since current velocities at NO1 were indeed higher than at the other Norske Trough stations. From the banks towards the deep troughs the sediment became finer. Grain size might be low within the troughs due to sediment accumulation during repeated glacial advances or retreats (Arndt et al., 2015). This separation into two habitat types (shallow sites with coarse sediment vs deeper sites dominated by silt) was observed in the northwestern Barents Sea as well (Piepenburg et al., 1995).

In the inner Norske Trough, silt content was extremely high and current velocities were low, which indicates high sedimentation at this site.

Especially high silt content was detected in the vicinity of the glacier, which is most probably due to the high sedimentation rates and fine particles sinking close to the glacier. At first hand it seems surprising that the high content of fines is paired with high current velocities. Usually, strong currents propagate sediment pore space more easily and elutriate fine particles out of the sediment (Breitzke, 2006). It is

possible that the sedimentation induced by the glacier was extremely high so that the effect of the strong currents on the sediments was counter-acted. A sediment plume induced by outflowing mAIW would lead to higher turbidity and would support this hypothesis. At the glacier margin, AIW is flowing along the seabed with extremely high current velocities of almost 0.3 ms^{-1} and enters the glacier cavity, mixes with glacial melt water and leaves the cavity in a more buoyant state. It might "flush out" particles from underneath the glacier, and when mAIW is leaving the cavity, it might carry along these fine particles that settle down on the sea floor in front of the glacier margin, increasing sedimentation and leading to the extremely high turbidities.

4.1.3 Food availability

Arctic benthos is dependent on seasonal food input and is tightly coupled to pelagic processes (Grebmeier and Barry, 1991). OM from the water column, usually induced by a phytoplankton bloom in spring, is advected to the sea floor and constitutes the available food for the benthic environment (Jensen et al., 1990). Hence, when characterizing benthic communities and functioning in Arctic habitats it is important to take into account the food availability.

Benthic pigment concentrations were generally low on the NEG shelf. Highest Chl *a* concentrations were present in the Westwind Trough with values between 4.91 (W3) and 9.24 $mg\ m^{-2}$ (in 0-2 cm sediment depth; Table A.2). Chl *a* concentrations at all other sites were lower than 2.5 $mg\ m^{-2}$.

In two glacial fjords off West Spitsbergen in July, Górska and Włodarska-Kowalczuk (2017) recorded benthic Chl *a* concentrations between 1.8 (site with low food availability; depth = 121 m) and 42 $mg\ m^{-2}$ (at a site with high food availability, depth = 76) in 0-2 cm sediment depth. This suggests that the Norske Trough and the region close to the glacier are poor in food input. In the North Water Polynya (NOW) at Northwest Greenland, Chl *a* concentrations were about 10 times higher than on the NEG shelf (Mäkelä et al., 2017a).

The negative correlation of Chl *a*-CPE and Chl *a*-Phaeopigments ratios is not surprising, since it takes OM longer to settle down to deeper locations, hence less "fresh" food finally reaches the sea floor. The low Chl *a*-Phaeopigments ratios (except for W3) suggests that OM was in a rather degraded state. Fresh food might be a limiting factor for the benthos. Similarly low Chl *a*-CPE ratios (<0.5) at all stations indicate that the portion of fresh food of the pigments available was low, supporting the stated assumption.

The overall low concentrations of benthic pigments suggest that benthic communities experience low food input, and that the NEG shelf is a highly oligotrophic environment. Productivity in high latitude ecosystems depends on strong seasonal primary production (Sakshaug et al., 2009; Meire et al., 2016). With an approximate annual total primary production of $20 - 50\ g\ C\ m^{-2}\ yr^{-1}$ and a new production of $3 - 7\ g\ C\ m^{-2}\ yr^{-1}$, the NEG shelf is one of the less productive Arctic shelves (Sakshaug et al., 2009). The Barents Sea for example has an annual primary production of $< 20 - 200\ g\ C\ m^{-2}\ yr^{-1}$ and a new production of $8 - 100\ g\ C\ m^{-2}\ yr^{-1}$. The North Water Polynya, which is situated at the south-western side of Greenland, has an annual total primary production of 150 and a new production of $70\ g\ C\ m^{-2}\ yr^{-1}$. The annual primary production of Young Sound, a shallow fjord located at around 74°N on the NEG coast, was estimated to be lower with approx. $10\ g\ C\ m^{-2}\ yr^{-1}$.

In the correlation plot, benthic pigments appear to be negatively correlated with attenuation, which would indicate for high pigment concentrations at high turbidity and vice versa (Fig. 3.7). This is surprising, since a high turbidity would inhibit primary production due to the lower light conditions. The attenuation at the stations in the Westwind Trough is similar to those in the Norske trough, but the pigment concentrations are much higher which leads to Westwind Trough stations acting as outliers (Fig. A.7). An additional look into the PCA based on environmental variables shows that pigments and attenuation are not correlated (Fig. 3.8). Lateral advection of OM can lead to a mismatch between the primary production in the upper column and pigments on the seafloor at the same location (Reigstad and Wassmann, 1996), which might have happened in the Westwind Trough.

4.2 Benthic processes and communities

4.2.1 Mineralization patterns

Porewater nutrients

In the Westwind Trough, relatively high ammonia and DIC concentrations in the porewater point at higher OM mineralisation rates as compared to the other regions. This agrees with the higher silicate concentrations, in consistence with higher benthic pigment concentrations indicating a higher diatom input. Diatoms were reported to dominate the sedimented phytoplankton in the NEW Polynya (Bauerfeind et al., 1997). When oxygen is depleted, nitrate is used as the next suitable electron acceptor in microbial metabolism. Indeed, in Westwind Trough sediments, nitrate was depleted at depth, which could point at denitrification taking place in the deeper sediment layers. However, at W3 in the Djmphna Sund a peak of nitrite at around 10 cm sediment depth occurs, and ammonia concentrations are low until around 12 cm sediment depth, increasing from here downwards. This might be a sediment layer of oxic conditions where nitrification takes place (oxidation of ammonia to nitrite).

Phosphate is mainly released into the porewater either during microbial degradation of organic matter and/or concomitant with the reduction of ferric iron (Hensen et al., 2006). Phosphate concentrations slightly increased at two Westwind stations, while at all other stations the concentrations were mostly below 2.5 μM. The low phosphate concentrations indicate that none of these degradation processes are taking place on the NEG shelf.

At all other sites nitrate was not depleted with depth and ammonia, DIC and silicate concentrations were much lower. This indicates that oxygen is not limited and/or nitrate is not consumed, i.e. microbial metabolism is extremely low. One exception was NO3 where higher DIC and phosphate concentrations were observed.

The absence of sulfate and sulfide in the sampled cores shows that sulfate reduction does not take place on the NEG shelf. It indicates that at none of the sites the sediments are anoxic, i.e. oxygen is not completely depleted or limiting in the upper 20 cm of the sediments.

Ammonium, phosphate, nitrate and nitrite porewater concentrations were similar to concentrations in Arctic Kongsfjorden at very shallow depths of around 5 m, while silicate concentrations were much lower in Kongsfjorden with values between $2 - 15$ μM (Sevilgen et al., 2014). In Antarctic coastal sediments in Potter Cove ammonium concentrations of up to 800 μM in the upper 20 cm sediment depth were

observed, and sulfate concentrations were around 20 μM (Henkel et al., 2018). Phosphate concentrations were around 100 μM (Monien et al., 2014). These comparisons emphasize the heterogeneity among porewater nutrients in polar regions.

Oxygen fluxes

The overall low benthic TOU values across the NEG shelf were similar to TOU ranges found in the 1990s (between $0.3 - 3.6$ $mmol\ m^{-2}\ d^{-1}$ Piepenburg et al., 1997) which indicates extremely low benthic activity on the NEG shelf, and confirms previous reports about the region to be oligotrophic (Rowe et al., 1997).

At depths of around 50 m, in the Chukchi Sea rates of $5.58 - 16.82$ $mmol\ m^{-2}\ d^{-1}$, in the Northern Bering Sea $11.80 - 19.85$ $mmol\ m^{-2}\ d^{-1}$ were measured. Respiration was also lower on the NEG shelf than in an Arctic fjord during polar night (Morata et al., 2015), and was actually similar to TOU in deep-sea benthic communities in the Arctic Fram Strait (Hoffmann et al., 2018). In Young Sound at very shallow depths of about 35 m benthic oxygen uptake was around 5 $mmol\ m^{-2}\ d^{-1}$, while in summer rates increased up to 15 $mmol\ m^{-2}\ d^{-1}$ (Thamdrup et al., 2007). In Kongsfjorden at around 5 m depth, respiration was around 22.4 $mmol\ m^{-2}\ d^{-1}$ (Sevilgen et al., 2014).

4.2.2 General patterns in communities

Macrofauna

Overall abundance of macrofauna was generally low compared to other Arctic shelf regions in the Atlantic sector. Sites where densities were highest (Westwind Trough, NO1 and NO2) had similar densities compared to sites with low food availability recorded in Arctic fjords at Spitsbergen (Svalbard; shallow depths between 76 and 250 m; Włodarska-Kowalczuk and Pearson, 2004). In contrast, macroinfaunal density in the North Water Polynya (NOW) at Northwest Greenland was about 1000 times higher than on the NEG shelf (Mäkelä et al., 2017a). Abundances were similar to Young Sound, a shallow fjord on NE Greenland with a maximum depth of 150 m (Sejr et al., 2000).

Surprisingly, there were no clear dominance patterns, but all species were present in abundances lower than 4 individuals in a sample. This is also reflected in the high evenness across all sites (Fig. 3.12a). The same pattern was observed in the samples from the 1990s (Ambrose and Renaud, 1995). Maldanidae was a comparatively more abundant polychaete family which occurred in some samples with around 3 individuals, which was also the case in this study. Usually, benthic communities are dominated by a few species in high densities (e.g. Włodarska-Kowalczuk and Pearson, 2004; Blanchard et al., 2013), but this seems not to be the case for the infauna on the NEG shelf. It seems to harbour highly diverse communities with very low species numbers.

North Greenland is among the marine ecoregions of the Arctic with comparatively high species numbers (Piepenburg et al., 2011). The benthic fauna on the NEG shelf, especially in the area of the NEW polynya was previously described as "highly diverse" in terms of peracarida (Brandt, 1995), echinodermata (Piepenburg, 1988) and epifauna in general (Fredriksen, 2018).

The most abundant macrofauna phylum in this study was Annelida. This was expected, since most of the samples were taken within the troughs where endobenthic living forms dominate the communities due to the lower grain size (Piepenburg, 1988). From the troughs towards the shallower banks, the overall abundance and biomass

of benthic fauna increases, represented by mobile, epibenthic taxa such as peracarida (Brandt, 1995) and echinodermata (Piepenburg, 1988; Fredriksen, 2018). Different community compositions at shallow sites with coarse sediment versus deeper sites dominated by silt was also observed in an open shelf area (northwestern Barents Sea; Piepenburg et al., 1995) as well as in Young Soung on the NE Greenland coast (Sejr et al., 2000), and was reflected in benthic respiration patterns.

Piepenburg (1988) and Ambrose and Renaud (1995) described the large polychaete *Nothria conchylega* (Onuphidae) to be dominant on Belgica Bank. In consistence with this, we found this species in higher abundances only at the shallow station NO1 located on Belgica Bank. *N. conchylega* attaches coarse sediment grains by the excretion of mucus (personal observation), and thus the shallow banks with coarsest grain sizes seem to be a suitable habitat.

Due to the high diversity and low species numbers, communities could most likely not be adequatly covered with the sampling method. In the 1990s, where a higher sampling effort was carried out, more polychaete families were represented (Ambrose and Renaud, 1995). The polychaete families Chaetopteridae, Cossuridae, Hesionidae, Neridae, Orbinidae, Polynoidae, Scalibregmatidae and Sigalionidae which were found at that time were absent in this study.

In fact, it is assumed that macro- and megafauna species on North and East Greenland shelves are severely under-estimated, and the species found so far do not level off in species-based rarefaction curves (Piepenburg et al., 2011). This emphasizes that it is not straightforward - if possible at all - to achieve a statistically good sample size that is representative for the macrofauna community composition on the NEG shelf which appears to be characterized by low abundance in general.

Although the spatial scale in the region and distances between stations were very large, differences between benthic communities were low when foraminifera were excluded. A very well studied glacial fjord in terms of benthic communities is Kongsfjorden where differences between communities among a few kilometers were conspicuous (e.g. Włodarska-Kowalczuk et al., 2005; Bourgeois et al., 2016). However, it should be noted that the NEG shelf represents a "special case" since it is rather an open shelf system, but influenced by fjord-like glacial activity. Open shelf benthic systems have higher species diversity and higher numbers of rare species compared to fjord systems (Włodarska-Kowalczuk et al., 2012), and differences between sites emerge at much larger distances (Cochrane et al., 2012).

Moreover, although stations could be grouped into regions based on differences in environmental conditions, these differences were too small to cause a corresponding pattern in the benthic fauna. Most likely, stations were still similar to each other in terms of grain size and depth; two factors that affect benthic community composition strongly (Gray and Elliott, 2009). Additionally, the circulation of AIW might lead to quite similar hydrographic conditions among stations. When the slope station NO4 was included, the delineation of the stations based on the environmental variables was skewed, and the differences among shelf stations became neglectable when compared to NO4. In the end, this might have been reflected in the macrofauna communities which do not separate among regions on the NEG shelf.

On the other hand, in the 1990s Foraminifera, Nematoda, Polychaeta and Crustacea communities did separate between the Norske and the Westwind Trough (Piepenburg et al., 1997). This might be, again, a result of the higher sampling size in that study. When I took the foraminifera into account, differences between sites that were delineated by the environmental variables were finally reflected in the communities and species evenness decreased (Fig. 3.12b), because single foraminiferan

species generally occurred in very high densities (Fig. 3.3). The same was observed when polychaeta only were analysed (Fig. 3.14), which was the most abundant macrofauna taxon. The present study illustrates the importance of taking foraminifera into account for benthic studies since it contains important information about the distribution patterns of communities (Denoyelle et al., 2010), especially at small sample sizes.

Foraminifera

Differences between the Westwind Trough and the Norske Trough based on foraminifera assemblages on the NEG shelf have been reported previously (Piepenburg et al., 1997). Roberts et al. (2017) observed that foraminifera between the size range of 63 - 500 μm that were indicative of AW influence with relatively warm and saline conditions were present in the Norske Trough, usually represented through agglutinated species, while many calcareous species are indicative for cold water. The calcareous species *Elphidium excavatum* for example was present at stations NO1 and NO2 and is a species indicative of colder Arctic Water (Roberts et al., 2017). It was reported to be a dominating species further away from the glacier (Korsun, 2000).

In front of the glacier, Roberts et al. (2017) reported that communities were mixed showing evidence of Atlantic Water influence but also of colder Arctic Water. Foraminifera assemblageswere rich and calcareous species were dominating, including the species *Quinqueloculina sp.* (Roberts et al., 2017). This could also be observed in the present study for foraminifera >500 μm, where *Quinqueloculina sp.* was especially abundant at G2 and G3. A dominance of calcareous foraminifera near to the glacier was also observed by Włodarska-Kowalczuk et al. (2013). However, foraminifera are usually less abundant in glacier vicinities (Korsun, 2000; Włodarska-Kowalczuk et al., 2013). Korsun (2000) observed a higher taxonomic diversity and an increase in some foraminifera species in the glacier vicinity in winter, when the glacial meltwater discharge was weaker. This suggests a high negative effect of meltwater plume on foraminifera communities. The high abundance of live *Quinqueloculina sp.* in this study is contrasting to this result. However, *Quinqueloculina sp.* was most abundant at G3 where turbidity was very low and similar to the stations in the Westwind and Norske Trough. It was a very shallow station, located on an elevation right in front of the glacier margin (Fig. A.1). Maybe these conditions were favourable for this taxon. G1 and G2 had much lower foraminifera abundances.

In the 1990s, densities of live foraminifera populations sieved at 200 μm mesh size were reported to range from 10 $ind\ 10cm^{-2}$ (at fine mud sites) to 100 $ind\ 10cm^{-2}$ (Ambrose et al., 1994). This was much more than we had assessed in our study, but usually, foraminifera $> 500\mu m$ occur in much lower densities compared to smaller size fractions (e.g. Martins et al., 2016). Therefore they are often not taken into account in studies covering foraminifera assemblages, and comparisons regarding abundances between different mesh sizes should not be made. On the NEG shelf, higher fractions usually contain a large fraction of empty tests (Ambrose et al., 1994) which was also observed in this study.

Ambrose et al. (1994) reported fragile calcareous taxa such as *Buccella, Cassidulina, Islandiella, Elphidium and Melonis* to be more numerous than agglutinated species (e.g. *Rhabdammina, Hyperammina, Sacchoriza, Saccammina, Cribrostomoides*), the latter to be more common in the Norske Trough than in the Westwind Trough. Contrary, we found the calcareous taxa to be represented in rather low abundances (except for *Quinqueloculina sp.* which has a thick test), while the agglutinated species occurred in

high densities. The abundance of the fragile calcareous taxa may be underestimated in this study due to the large mesh size. Unfortunately, the agglutinated tubular foraminifera which were abundant at several sites, especially at NO4 and in the Westwind Trough, could not be taken into account in the analysis because single individuals could not be distinguished from broken tests. Especially the high abundance of the agglutinated species *Labrospira crassimargo* in the Djmphna Sund at W3, and the presence of *Cuneata arctica* at G1 is noteworthy. Komokioidea, a group of foraminifera of organic tests, were most abundant at W1 and W2, while other foraminifera were rare.

Nevertheless, it should be emphasized that only foraminifera larger than 500 μm were studied, and that it is important to take smaller mesh sizes into account to obtain a detailed picture of the community patterns in foraminifera on the NEG shelf. Possibly, other taxa that might occur in smaller size fractions cannot grow that large, and wrong conclusions about the overall communities can be drawn if they are disregarded.

4.2.3 Pelagic-benthic coupling

Pigments and attenuation were the most important drivers of benthic communities on the NEG shelf. Single cell abundances and total density and biomass of macrofauna + foraminifera, macrofauna only and polychaeta were highest in Westwind Trough compared to all other sites. Coupled with the benthic mineralization properties that followed the same patterns, it indicates an overall higher benthic metabolism in the Westwind Trough. This pattern correlates with the distribution of benthic pigments on the shelf, with highest concentrations in the Westwind Trough. Chl *a* concentrations were correlated with the macrofauna + foraminifera communities in the Westwind Trough (Fig. 3.15) and polychaeta communities followed this pattern (Fig. 3.14). The results suggest a strong pelagic-benthic coupling in this area.

The same patterns had been observed in the 1990s for benthic communities: Benthic pigments were correlated with total infaunal density and polychaete biomass (Ambrose and Renaud, 1995), and peracarid, nematode, polychaete and, to a lesser extent, foraminifera communities (Piepenburg et al., 1997). The latter was, contrary to the present study, highly associated with the influence of water depth, grain size and water bottom temperature (Piepenburg et al., 1997). These factors were not important in explaining benthic community patterns in this study.

The strong benthic-pelagic coupling on the NEG shelf has been reported for many locations in the Arctic, e.g. the southeastern Beaufort Sea (Link et al., 2013), the northern Bering and Chukchi Sea (Grebmeier and McRoy, 1989; McTigue et al., 2015) and in the marginal ice zone of the Barents Sea (Tamelander et al., 2006; Morata and Renaud, 2008). Even in the Arctic deep sea, pelagic particle flux is the key factor structuring benthic communities (Degen et al., 2015; Braeckman et al., 2018). The Arctic benthos is highly dependent on seasonal input from primary production in the upper water column. This relationship is tightly driven by sea ice dynamics (Renaud et al., 2007a). On the NEG shelf, benthic communities depend on distinct OM pulses around the seasonal cycle (Rowe et al., 1997).

An evident explanation for the lower abundance and biomass in the Norske Trough would be a lower primary production in the Norske Trough compared to the Westwind Trough (e.g. induced by the position of the marginal ice zone), which

would lead to less food input for the benthos in the Norske Trough through lateral advection. However, fluorescence measurements in the upper water column indicate that primary production was the same in both troughs (Fig. A.3). This is in consistence with the observations from the 1990s, where phytoplankton standing crops were reported to be the same as well (Ambrose and Renaud, 1995). Thus the possibility of different primary production in the two troughs needs to be be dismissed. However, in the 1990s benthic pigments were strongly correlated with water column pigments in the Westwind Trough, while this had not been the case for the Norske Trough.

Ambrose and Renaud (1995) suggested a "decoupling" of the benthic environment from the pelagic in the Norske Trough due to higher zooplankton grazing. Contrary to benthic patterns, lowest zooplankton biomass was present in the Westwind Trough while highest biomass was present in the Norske Trough (Ashjian et al., 1995), which indicates for higher pelagic grazing activity in the Norske Trough, finally leading to reduced food input for the benthos (Ambrose and Renaud, 1995). Ashjian et al. (1995) observed that grazing rates highly exceeded primary production in both, Westwind and Norske trough, but especially in the Norske Trough. It is possible that pelagic mineralization takes place before OM can settle down, and that a lower fraction of the surface production reaches the sea floor. Since in this study pigments in the water column did not differ between sites, but benthic pigment concentrations were much higher in the Westwind Trough, this "decoupling" could be still a driving force for the patterns in the benthos.

It should be noted that two stations in the outer Norkse Trough had biomasses and abundances similar to the Westwind Trough despite low pigment concentrations, namely NO1 and NO2.

Station NO1 is located on the Belgica Bank and differs from the troughs with respect to various environmental factors. The pathway of OM to the sea floor is "shortened" which leads to a higher and "fresher" input of OM for the benthos. This is reflected in the higher Chl *a*-Phaeopigments ratios. The ambient water is influenced by PW, therefore showing much lower temperature and salinity. Based on temperature, NO1 was more similar to the colder Westwind stations than to the other stations at the outer Norske Trough (Fig. 3.8).

In previous studies, especially high biodiversity and individual numbers had been observed on Belgica Bank as well (Piepenburg, 1988; Ambrose and Renaud, 1995; Fredriksen, 2018). Epibenthic species were most abundant due to the rather coarse grain sizes on the bank (Piepenburg, 1988; Brandt, 1995) and ice-associated fauna was found which was absent from the other stations (Fredriksen, 2018). Pigments might be faster consumed by the richer communities present, or they are advected through the high current velocities and coarse grain size which hinders the sedimentation of pigments. The surface circulation over the shallow banks follows a clockwise direction from the north to the south. This could further lead to the dispersion of OM in the water column across the banks, fuelling a rich mobile benthic community on the bank, additional to the more favourable conditions such as larger grain size, lower turbidity and shallower depth compared to the communities within the troughs. To prove this assumption, one single station on the bank is not sufficient, but it supports hypotheses stated before (Piepenburg, 1988; Brandt, 1995; Fredriksen, 2018).

For NO2, the reasons for the higher abundance and biomass compared to the other Norske Trough stations are not clear to me, because it was located deep within the trough. CPE concentrations were not very high; NO3 had even higher concentrations. One reason might be the higher Chl *a*-Phaeopigments and Chl *a*-CPE ratios

at NO2 compared to NO3 and NO4, which indicates fresher food available. Chl *a*-Phaeopigments ratios were highest at NO1 and NO2 compared to all other stations in the Norske Trough. At last, the patchiness of the distribution of benthic communities should not be dismissed.

4.2.4 Functional patterns in polychaeta

At first hand it seems surprising that tubiculous tentaculate species (Ampharetidae, Sabellidae) are especially present in the vicinity of the glacier (Fig. 3.14), because the high turbidity causes increased rates of suspension settling, sedimentary instability and mud deposition. Infaunal organisms may be buried, larval settlement may be hindered and/or filtering appendages of suspension feeders (e.g. Sabellidae) may become clogged (Görlich et al., 1987; Włodarska-Kowalczuk et al., 2005). This is why rather mobile fauna and polychaetes adapted to high unstable sediments were expected to occur here (Włodarska-Kowalczuk et al., 2005). Yet, in front of the glacier the large sea pen *Umbellula sp.* was found in high abundances (pers. comm. Ulrike Braeckman), and very high densities of zooplankton were observed (pers. comm. Holger Auel). Due to the mixing of water masses and the high current velocities right in front of the glacier OM might not be deposited on the seafloor but rather suspended in the water column, consequently leading to favourable conditions for suspension feeders. The input of warm and saline AIW might weaken the stress effect of low temperature and fresh water input on the benthic organisms. In Besselfjord, a fjord to the south of the Norske Trough, high taxon richness and a high abundance of suspension feeders were found in the vicinity of the glacier as well (Fredriksen, 2018). It is possible that a higher abundance of mobile epifauna is present in the glacier vicinity due to the high food availability and their ability to cope better with the environmental stress (Włodarska-Kowalczuk et al., 2005), which cannot be assessed with the sampling method for this study. Additionally, it should be noted that the sedentarian polychaetes found at this site were so small that the determination further than family level was not possible. Most likely they were juveniles. Fetzer et al. (2002) found an increase of juvenile suspension feeders from the fjord mouth towards the glacier margin in Kongsfjorden and suggested that they appear less disturbed by glacial discharge but more vulnerable to currents on the more exposed sites. In a Canadian fjord which is subject to high sediment loads and turbidity Farrow et al. (1983) found an increase of numbers of suspension feeders towards the upper inlet as well.

As expected, low biomass and abundance of polychaeta and overall macrofauna close to the glacier was observed in this study. In the vicinity of glaciers, individuals tend to be small-bodied, diversity and biomass tend to be low (Włodarska-Kowalczuk et al., 2005; Renaud et al., 2007b). Probably, not many macroinfaunal species can cope with the high physical stressors because of their higher fragility compared to epifaunal species.

The reason for the correlation of the Norske Trough with tube-dwelling and burrowing deposit-feeders in contrast to more mobile species in the Westwind Trough remains speculative. Grain sizes in the Westwind Trough and the Norske Trough (except for NO1) were roughly the same. A possible explanation could be the effect of current velocities, which were higher in the Westwind Trough compared to the Norske Trough (again, when NO1 was excluded). Less resuspension in the water column might prevail at sites with less current velocities, leading to a higher sedimentation of

OM and consequently to more favourable conditions for burrowing deposit-feeders. The deposit-feeding families which were present in the Norske Trough are rather slow movers, and therefore depend on OM that is advected on the sea floor right in their vicinity (Fauchald, 1979). Due to the higher overall macrofauna abundance in the Westwind Trough it might be easier to encounter prey compared to the Norske Trough, which makes the Westwind Trough more favourable for carnivorous families (Nephtyidae, Syllidae).

4.3 Indications for decreased food availability since the 1990s

It is especially noteworthy that abundances of macrofauna in this study were fivefold lower than they were recorded in the 1990s (Ambrose and Renaud, 1995). One could argue with the differing sampling sizes but in fact, the comparison between Lander and MUC sampling in this study demonstrated that macrofauna densities from MUC samples were rather overestimated. Lander samples had a higher surface area and abundance estimations were much lower compared to MUC samples (Fig. 3.10).

This change seems to go along with another difference to the patterns observed in the 1990s that needs to be mentioned: pigment concentrations found in this study were much lower across the whole NEG shelf compared to the findings before. Ambrose and Renaud (1995) reported CPE concentrations for the upper 2 cm between 7.22 and 45.62 $mg\ m^{-2}$ across the whole NEG shelf (between July-August), while in this study highest concentrations were found in the Westwind trough with values between 7.38 - 18.0 $mg\ m^{-2}$. At all other sites concentrations were close to 0 (September-October). While these detected differences are a further indication for the strong-pelagic coupling on the NEG shelf, possible reasons for the differences compared to the 1990s need to be discussed.

As observed everywhere in the Arctic, sea ice on the NEG shelf is declining (Stroeve et al., 2012). One scenario of shrinking sea ice in the Arctic is that the longer exposure to sunlight will result in a longer season for phytoplankton growth and higher production rates due to the longer exposure to sunlight (Arrigo et al., 2008), thus to a higher food input for the benthos. This study indicates that a different scenario might be happening on the NEG shelf.

Due to climate warming, sea ice melts earlier in the year, and the ice-free period is prolonged (Overland and Wang, 2013). As a consequence, primary production starts earlier in the year and nutrients are depleted faster. This makes food available for a longer period of time during the year, but at lower concentrations due to the fast nutrient consumption (Wassmann and Reigstad, 2011). Lower nutrient concentrations favour smaller phytoplankton with lower carbon export efficiency (Li et al., 2009). Arctic marine ecosystems are adapted to highly seasonal and short-term, thus intense "pulsed" food input (Grebmeier and Barry, 1991). Through this intense pulsing, a considerable amount of the biomass sinks ungrazed as high-quality food to the benthos (Atkinson and Wacasey, 1987; Wassmann, 1991). The described scenario would lead to a more evenly distributed primary production and food availability, i.e. a lower but steadier export of OM (Wassmann and Reigstad, 2011). The amount of OM reaching the sea floor depends strongly on the feeding intensity of zooplankton in the water column (Grebmeier and Barry, 1991; Wassmann, 1998), which had been previously discussed for the NEG shelf.

The wider the window of time for pelagic primary production is, the more time is available for heterotrophic pelagic primary consumers to exploit this resource by extended grazing periods and population growth (Olli et al., 2007). Accordingly, a smaller share of primary production may become available for the benthos. If the input of warmer AIW introduces more Atlantic zooplankton species onto the NEG shelf that could possibly survive under the extended period of food availability, enhanced zooplankton grazing on the overall NEG shelf could have lead to a "decoupling" of the benthic from the pelagic environment. A shifting away from pelagic-benthic coupling has been prophesied for Arctic ecosystems (Grebmeier and Barry, 1991) and was reported already for the Northern Bering Sea, with a northward shift of the pelagic-dominated ecosystem that was previously limited to the southeastern Bering Sea (Grebmeier et al., 2006).

Another possible explanation might be a stronger water column stratification on the NEG shelf.

AW warms by a mean temperature of 0.06 °C $year^{-1}$ (Beszczynska-Möller et al., 2012), leading to input of warmer water into the trough system of the NEG shelf through the EGC (Schaffer et al., 2017). AIW throughout the whole trough system has warmed in the period between 2000 - 2016 relative to 1979-1999, with a warming of 0.5 °C throughout the Norske Trough (Schaffer, 2017). Differences in bottom water temperature and salinity between the 1990s and 2017 indicate an increase of the influence of warm AIW on the shelf (Fig. A.4). The enhanced melting of the 79N Glacier, not only induced subglacially but also at the surface (Fig. A.2), results in a higher cold fresh water input in the upper water column.

Vertical water column stratification due to high freshwater accumulation prevents vertical mixing and upward nutrient supply for phytoplankton when wind stress is not acting (Ardyna et al., 2014). A stratification effect had been induced by glacial meltwater in Kongsfjorden further away from the glacier (van de Poll et al., 2018). Spring blooms are not initiated in the stratified part of a fjord system (Meire et al., 2016). Similarly, the enhanced melting of the 79NG might have led to a pronounced gradient between the AIW and the glacial melt water since the 1990s, resulting in higher upper water stratification on the NEG shelf. Subsequently, depleted nutrients in the upper water column would not become replenished, preventing primary production.

An "upwelling" or stratification effect resulting from glacial runoff depends strongly on other physical processes, especially wind circulation and sea-ice dynamics (Meire et al., 2016; van de Poll et al., 2018). To support this hypothesis of a higher stratification, the densities of the water masses and wind dynamics on the NE shelf need to be investigated and compared to the conditions from the 1990s with further detail.

A change in phytoplankton community composition may offer a further explanation for the lower amount of benthic pigments.

An earlier onset of glacial melting, e.g. induced by higher intrusions of warm AW, can limit biomass build-up and facilitates a smaller-sized phytoplankton community in blooms near the glacier vicinity (Piquet et al., 2013). It is possible that the enhanced glacier melt of the 79NG resulted in such an effect. Similarly, increasing sea surface temperature, sea ice retreat and the freshening of the upper ocean in the Arctic might trigger shifts in phytoplankton communities (Li et al., 2009; Braeckman et al., 2018).

Moreover, the primary production in the Arctic is dependent on both, ice algae and pelagic phytoplankton (Horner and Schrader, 1982). If sea ice shrinks further, the

primary production could shift towards phytoplankton, which would alter quality and quantity of food reaching the sea floor and finally change the composition of benthic communities. The preference of the higher quality ice algae over phytoplankton by benthic species is under debate and seems to differ region-wise (e.g. Mäkelä et al., 2017a). The ice alga *Melosira arctica* was reported to occur in massive patches underneath sea ice (Gutt, 1995) and was an important component of particle flux in the NEW Polynya (Bauerfeind et al., 1997).

Another important feature that should be noted is the decline of the polynya in the Westwind Trough (ISSI, 2008). During the PS109 sampling campaign, the inner parts of the Westwind and Norske Trough were covered by sea ice (Fig. A.5). Nevertheless, the overall region showed a much lower ice coverage than in the 1990s. In the NEW polynya, benthic communities were described to be richer compared to the Norske Trough, which is still observed today. It is possible that the shrinking sea ice counter-acted against the effect of the decline of the polynya, since it is a seasonal feature that provided an open water area. However, if the decline of the polynya would be the only reason for the lower benthic pigment concentrations, the concentrations and subsequently abundance of benthic macrofauna should be lower in the Westwind Trough only, while concentrations in the Norske Trough should stay in the same range compared to the 1990s. To fully understand the role of the polynya and the sea ice in the phytoplankton dynamics on the NEG shelf and its effect on benthic communities, it is important to look at the change in sea ice concentration since the 1990s, but this is beyond the scope of this master thesis.

At last, the difference in seasons or simply intra-annual variability should not be disregarded, especially with regard to sea ice cover. Samples were taken during different months in both studies (March-July in 1992/1993 vs September/October in 2017).

Upon reaching the sea floor, phytoplankton can be consumed rapidly by the benthos (Morata et al., 2015) and the signal from a spring bloom is faded out with time. A spring bloom might have occurred earlier in the year due to the earlier shrinking of sea ice, and nutrients might have been rapidly consumed by the phytoplankton, inhibiting further blooms during the year. This would result in an equally earlier shift of benthic response to food consumption, which would in turn lead to a lower detection of pigment concentrations late in the year than it did before. Sejr et al. (2000) for example showed an increase in macrofauna abundance in Young Sound from mid-July to mid-August, coupled to changes in primary production.

However, the overall low abundance and biomass of macrofauna on the NEG shelf and the extremely low respiration rates compared to other Arctic fjord systems (e.g. Morata et al., 2015) would speak against an efficient food consumption of the benthos. Sedimentation in the NEW Polynya was reported to increase from March onwards, with maximum sedimentation rates between August and October (Bauerfeind et al., 1997), in consistence with the prevailing ice cover conditions. Thus, the sampling campaign for this study would fall into the peak season, and benthic pigments and community abundances should be even higher than during the sampling campaigns in the 1990s. Moreover, it was suggested that carbon was stored in the benthos during open water conditions in summer and used up during the ice-covered winter, suggesting a time lag in the increase of biomass and respiration. Respiration rates and community biomass measured in 1992 and 1993 did not differ between each other (Rowe et al., 1997). Similarly, in Kongsfjord it was shown that seasonal variations

were not reflected in the structure of the benthic food web and that benthic fauna is resilient to changing seasonal conditions (Kędra et al., 2012).

To exclude the possibility of intra-annual or seasonal variation, the collection of time-series data is important. In the end, just as it was the case in the 1990s, this study provides only a one-time measurement of pigment concentrations and benthic community parameters, therefore comparisons between two snapshots should be interpreted with caution.

5 Conclusion

- The present study presents a first assessment of possible climate change effects on benthic infauna communities and their functions on the NEG shelf as compared to patterns that had been observed 25 years ago.
- Based on environmental parameters, the NEG shelf is delineated into 4 regions, namely Westwind Trough, inner and outer Norske Trough and 79N Glacier.
- Macrofauna community patterns do not resemble this regional structure, in contrast to studies from the 1990s and as it was expected for this study as well. However, the most abundant faunal groups, polychaetes and foraminiferans reflected the regional pattern. These findings either point towards an overall insufficient sampling effort and/or indicate that the differences between the environmental parameters on which the regionalisation was based upon were too small to cause a corresponding pattern in the benthic fauna. The present study illustrates the importance of taking foraminifera into account for benthic studies, especially at small sample sizes, since it can contain important information about the distribution patterns of communities.
- The differences in communities were distinctly related to benthic pigment concentrations, which confirms previous findings that benthic communities on the NEG shelf are driven by pelagic-benthic coupling. Other environmental parameters were less important.
- Community bulk parameters and functions in terms of total abundance, biomass, single cell abundances, total oxygen uptake and sediment profiles of DIC and ammonium were higher in the Westwind Trough compared to all other regions, in accordance with highest concentrations of benthic pigments. This indicates a higher pelagic-benthic coupling in the Westwind Trough. The "strength" of this coupling might probably be regulated by zooplankton grazing in the water column which determines the amount of sedimented food on the sea floor as it had been proposed before (Ambrose and Renaud, 1995), and grazing might be higher in the Norske Trough than in the Westwind Trough.
- As expected, abundance, biomass and diversity of macrofauna were lowest in the vicinity of the 79N Glacier. However, the presence of sedentarian polychaetes at this location was unanticipated due to the high sedimentation rates, turbidity and sedimentary instability which infaunal organisms are vulnerable to. The occurrence of other filter-feeding organisms indicates that there must be a high amount of suspended matter present and that some animals can cope with the environmental stress.
- It is especially noteworthy that, compared to the 1990s, pigment concentrations were three- to sevenfold lower, accompanied by a fivefold lower total abundance of macrofauna. The reasons for these differences remain speculative. Here I present the 2 most important hypotheses:

- A pelagic-benthic "decoupling" due to higher pelagic grazing by zooplankton of Atlantic origin. The shrinking of sea ice leads to a prolonged period of light availability, which in turn fuels a more evenly distributed primary production in the upper water column. This leads to a steadier, but lower export of organic matter. These conditions may foster zooplankton species that are adapted to longer periods of food availability and induce higher grazing activity, countervailing the "pulse" sinking of organic matter to the sea floor which is typical for Arctic marine ecosystems.
- A higher stratification of water masses on the overall NEG shelf, which inhibits vertical mixing and nutrient supply to primary producers in the upper water column. This stratification might be induced by the higher freshwater input from glacial and sea ice melt, and a higher input of warm Atlantic Water which results in an enhanced thermal gradient.

In the end, conclusions about trends from the comparison between two snapshots 25 years apart should be drawn with caution. However, the decline of the NEW polynya, higher glacial melt activity, shrinking sea ice and the enhanced input of warm Atlantic Water suggest that environmental conditions on the NEG shelf must have changed since the 1990s. Time series data on benthic ecosystems in the Arctic are scarce and their collection is costly, so this study provides a further stepping stone for the understanding of climate change effects on benthic communities and their functions.

Acknowledgements

Ulrike Braeckman ... for a giant amount of absolute trust, answering 245 e-mails since January 2018 "right away", challenging me and at the same time saving me from "overanalyzing" words and numbers... and incidentally sending me here and there to present a poster, meet great scientists and literally grow with this thesis. I felt like stepping out of being a student into getting a self-critical researcher.

Thomas Brey ... for dedicating the time to read the present work and for providing all the valuable input and the keen eye for scientific clarity.

Janine Felden ... for DOU data, explaining porewater profiles and flux calculations and the unofficial supervision.

The MarBiol group in Gent, Belgium ... especially **Guy de Smet** and **Annick Van Kenhove** for helping me out in the lab or with bureaucratic obstacles, **Bart Beuselinck** and **Bruno Vlaeminck** for the processing of pigment and grain size samples, **Nene Lefaible** and **Ee Zin Ong** for sharing the fume hood and exchanging taxonomic know-how.

The Deep-Sea Habitat group in Bremen, Germany ... especially **Frank Wenzhöfer** and **Verena Carvalho** for a proper office place (saving me from seeking for a place in the library every day) and a HiWi contract; **Jakob Barz, Martina Alisch** and **Wiebke Stiens** for taking and processing samples, and for teaching me the AODC method.

The IOPAN group in Sopot, Poland ... especially **Maria Włodarska-Kowalczuk, Jan Marcin Węsławski, Joanna Legeżyńska, Monika Kędra, Joanna Pawlowska, Marta Ronowicz, Kajetan Deja, Barbara Górska** and **Piotr Kukliński** ... for hosting me in their lab, dedicating the time to look over my samples, for valuable scientific input and the most cordial hospitality I could have expected. Thank you **Joanna Legeżyńska** additionally for taking care of the samples and sending them back!

The LifeWatch observatory ... as part of the Flemish contribution to the LifeWatch ESFRI by Flanders Marine Institute for the use of the ZooScanner, especially **Jonas Mortelmans**.

Janin Schaffer ... for data sharing and all the oceanographic counsel.

Christiane Hassenrück and **Pier Buttigieg** ... for important statistical input.

Paul Renaud and **Dieter Piepenburg** ... for providing the baseline for this thesis with their previous work on the NEG shelf, and for sharing literature and data.

Jutta Wollenburg ... for solving the "Komokioidea" mystery :)

Gritta Veit-Köhler ... my former Bachelor supervisor who introduced me into benthic ecology, moved on supporting me beyond my studies and opened up amazing possibilities to me. Otherwise I might have ended up writing stories for the local newspaper.

Tom and **Hannes** ... for coping with the ups and downs of overwhelming fascination or total capitulation during the species identification.

Kjetl, Andrew and **Mat** ... for the motivation boost to go for the last month.

Lena and **Benjamin** ... for always standing ready for a beer, a tea or a good meal.

Sonja and **Arif Bodur** ... for filtering bad moods and impatience, and for the fact that I'm sometimes wondering who's the one actually fascinated by muddy critters on the sea floor.

Melisa Bodur ... for being a safe harbour and a non-resident, but stable home.

Bibliography

Ambrose, W. G., Ahrens, M. J., Brandt, A., Dimmler, G. G., Gutt, J., Hermann, R., Jensen, P., Piepenburg, D., Queisser, P., Renaud, P. R., Ritzau, W., Scheltz, A., and Thomsen, L. (1994). Benthos. In: The 1993 Northeast Water Expedition. Scientific cruise report of RV Polarstern, Arctic cruises ARK IX/2 and 3, USC Polar Sea cruise NEWP and the NEWLand expedition. Technical report.

Ambrose, W. G. and Renaud, P. E. (1995). Benthic response to water column productivity patterns: Evidence for benthic-pelagic coupling in the Northeast Water Polynya. *Journal of Geophysical Research: Oceans*, 100(C3):4411–4421.

Arbizu, P. M. (2018). pairwiseAdonis: Pairwise multilevel comparison using adonis. https://github.com/pmartinezarbizu/pairwiseAdonis.

Ardyna, M., Babin, M., Gosselin, M., Devred, E., Rainville, L., and Tremblay, J.-E. (2014). Recent Arctic Ocean sea ice loss triggers novel fall phytoplankton blooms. *Geophysical Research Letters*, 41(17):6207–6212.

Arndt, J. E., Jokat, W., Dorschel, B., Myklebust, R., Dowdeswell, J. A., and Evans, J. (2015). A new bathymetry of the Northeast Greenland continental shelf: Constraints on glacial and other processes. *Geochemistry, Geophysics, Geosystems*, 16(10):3733–3753.

Arndt, J. E., Schenke, H. W., Jakobsson, M., Nitsche, F. O., Buys, G., Goleby, B., Rebesco, M., Bohoyo, F., Hong, J., Black, J., Greku, R., Udintsev, G., Barrios, F., Reynoso-Peralta, W., Taisei, M., and Wigley, R. (2013). The International Bathymetric Chart of the Southern Ocean (IBCSO) Version 1.0-A new bathymetric compilation covering circum-Antarctic waters: IBCSO VERSION 1.0. *Geophysical Research Letters*, 40(12):3111–3117.

Arrigo, K. R., van Dijken, G., and Pabi, S. (2008). Impact of a shrinking Arctic ice cover on marine primary production. *Geophysical Research Letters*, 35(19).

Ashjian, C. J., Smith, S. L., and Lane, P. V. Z. (1995). The Northeast Water Polynya during summer 1992: Distribution and aspects of secondary production of copepods. *Journal of Geophysical Research: Oceans*, 100(C3):4371–4388.

Atkinson, E. G. and Wacasey, J. W. (1987). Sedimentation in arctic Canada: Particulate organic carbon flux to a shallow marine benthic community in Frobisher bay. *Polar Biology*, 8(1):3–7.

Bauerfeind, E., Garrity, C., Krumbholz, M., Ramseier, R. O., and Voβ, M. (1997). Seasonal variability of sediment trap collections in the Northeast Water Polynya. Part 2. Biochemical and microscopic composition of sedimenting matter. *Journal of Marine Systems*, 10(1):371–389.

Bernhard, J. M. (1992). Benthic foraminiferal distribution and biomass related to pore-water oxygen content: Central California continental slope and rise. *Deep Sea Research Part A. Oceanographic Research Papers*, 39(3-4):585–605.

Bernhard, J. M. (2000). Distinguishing live from dead foraminifera: Methods review and proper applications. *Micropaleontology*, 46:38–46.

Beszczynska-Möller, A., Fahrbach, E., Schauer, U., and Hansen, E. (2012). Variability in Atlantic water temperature and transport at the entrance to the Arctic Ocean, 1997–2010. *ICES Journal of Marine Science*, 69(5):852–863.

Blanchard, A. L., Parris, C. L., Knowlton, A. L., and Wade, N. R. (2013). Benthic ecology of the northeastern Chukchi Sea. Part I. Environmental characteristics and macrofaunal community structure, 2008–2010. *Continental Shelf Research*, 67:52–66.

Bourgeois, S., Philippe, K., Calleja, M., Many, G., and Morata, N. (2016). Glacier inputs influence organic matter composition and prokaryotic distribution in a high Arctic fjord (Kongsfjorden, Svalbard). *Journal of Marine Systems*, 164.

Bourke, R. H., Newton, J. L., Paquette, R. G., and Tunnicliffe, M. D. (1987). Circulation and water masses of the East Greenland shelf. *Journal of Geophysical Research: Oceans*, 92(C7):6729–6740.

Braeckman, U., Janssen, F., Lavik, G., Elvert, M., Marchant, H., Buckner, C., Bienhold, C., and Wenzhöfer, F. (2018). Carbon and nitrogen turnover in the Arctic deep sea: In situ benthic community response to diatom and coccolithophorid phytodetritus. *Biogeosciences Discussions*, pages 1–32.

Brandt, A. (1995). Peracarid fauna (Crustacea, Malacostraca) of the Northeast Water Polynya off Greenland: Documenting close benthic-pelagic coupling in the Westwind Trough. *Marine Ecology Progress Series*, pages 39–51.

Breitzke, M. (2006). Physical properties of marine sediments. In *Marine Geochemistry*, pages 27–71. Springer.

Budéus, G. and Schneider, W. (1995). On the hydrography of the Northeast Water Polynya. *Journal of Geophysical Research*, 100:4287–4300.

Budéus, G. and Schneider, W. (2010a). Physical oceanography during POLARSTERN cruise ARK-IX/2.

Budéus, G. and Schneider, W. (2010b). Physical oceanography during POLARSTERN cruise ARK-IX/3.

Budéus, G., Schneider, W., and Kattner, G. (1997). Distribution and exchange of water masses in the Northeast Water polynya (Greenland Sea). *Journal of Marine Systems*, 10(1):123–138.

Buttigieg, P. L. and Ramette, A. (2014). A guide to statistical analysis in microbial ecology: A community-focused, living review of multivariate data analyses. *FEMS Microbiology Ecology*, 90(3):543–550.

Callard, L., Roberts, D. D., Cofaigh, C. O., Lloyd, J., and Smith, J. (2018). Reconstructing Late Quaternary retreat of the NE Greenland Ice Stream. *Geophysical Research Abstracts*, 20:1.

Christman, D. W. a. M. (2014). Clustsig: Significant Cluster Analysis.

Clarke, K. R. (1993). Non-parametric multivariate analyses of changes in community structure. *Australian Journal of Ecology*, 18(1):117–143.

Cline, J. D. (1969). Spectrophotometric Determination of Hydrogen Sulfide in Natural Waters. *Limnology and Oceanography*, 14(3):454–458.

Clough, L. M., Ambrose, W. G., Kirk Cochran, J., Barnes, C., Renaud, P. E., and Aller, R. C. (1997). Infaunal density, biomass and bioturbation in the sediments of the Arctic Ocean. *Deep Sea Research Part II: Topical Studies in Oceanography*, 44(8):1683–1704.

Cochrane, S. K., Denisenko, S. G., Renaud, P. E., Emblow, C. S., Ambrose Jr, W. G., Ellingsen, I. H., and Skarḥhamar, J. (2009). Benthic macrofauna and productivity regimes in the Barents Sea—ecological implications in a changing Arctic. *Journal of Sea Research*, 61(4):222–233.

Cochrane, S. K. J., Pearson, T. H., Greenacre, M., Costelloe, J., Ellingsen, I. H., Dahle, S., and Gulliksen, B. (2012). Benthic fauna and functional traits along a Polar Front transect in the Barents Sea – Advancing tools for ecosystem-scale assessments. *Journal of Marine Systems*, 94:204–217.

Corliss, B. H. and Emerson, S. (1990). Distribution of rose bengal stained deep-sea benthic foraminifera from the Nova Scotian continental margin and Gulf of Maine. *Deep Sea Research Part A. Oceanographic Research Papers*, 37(3):381–400.

Dalsgaard, T., Nielsen, L. P., Brotas, V., Viaroli, P., Underwood, G., Nedwell, D., Sundbäck, K., Rysgaard, S., Miles, A., Bartoli, M., Dong, L., Thornton, D., Ottosen, L., Castaldelli, G., and Risgaard-Petersen, N. (2000). Protocol handbook for NICE-Nitrogen cycling in estuaries: A project under the EU research programme. *Marine Science and Technology (MAST III)*.

Degen, R., Vedenin, A., Gusky, M., Boetius, A., and Brey, T. (2015). Patterns and trends of macrobenthic abundance, biomass and production in the deep Arctic Ocean. *Polar Research*, 34(1):24008.

Denoyelle, M., Jorissen, F. J., Martin, D., Galgani, F., and Miné, J. (2010). Comparison of benthic foraminifera and macrofaunal indicators of the impact of oil-based drill mud disposal. *Marine Pollution Bulletin*, 60(11):2007–2021.

Dickson, A. (1981). An exact definition of total alkalinity and a procedure for the estimation of alkalinity and total inorganic carbon from titration data. *Deep Sea Research Part A. Oceanographic Research Papers*, 28(6):609–623.

Dierssen, H. M., Smith, R. C., and Vernet, M. (2002). Glacial meltwater dynamics in coastal waters west of the Antarctic peninsula. *Proceedings of the National Academy of Sciences of the United States of America*, 99(4):1790–1795.

Drinkwater, K. F. (2006). The regime shift of the 1920s and 1930s in the North Atlantic. *Progress in Oceanography*, 68(2):134–151.

ENVEO (2017). ENVEO, Greenland Calving Front Dataset, 1990 - 2016, v2.0, Greenland Ice Sheet CCI. http://cryoportal.enveo.at/data/.

Falk-Petersen, S., Sargent, J. R., Henderson, J., Hegseth, E. N., Hop, H., and Okolodkov, Y. B. (1998). Lipids and fatty acids in ice algae and phytoplankton from the Marginal Ice Zone in the Barents Sea. *Polar Biology*, 20(1):41–47.

Farrow, G. E., Syvitski, J. P. M., and Tunnicliffe, V. (1983). Suspended Particulate Loading on the Macrobenthos in a Highly Turbid Fjord: Knight Inlet, British Columbia. *Canadian Journal of Fisheries and Aquatic Sciences*, 40(S1):s273–s288.

Fauchald, K. (1979). The diet of worms: A study of polychaete feeding guilds. *Oceanography and Marine Biology - An Annual Review*, 17:193–284.

Fetzer, I., Lønne, O. J., and Pearson, T. (2002). The distribution of juvenile benthic invertebrates in an arctic glacial fjord. *Polar Biology*, 25:303–315.

Fleischer, D., Schaber, M., and Piepenburg, D. (2007). Atlantic snake pipefish (Entelurus aequoreus) extends its northward distribution range to Svalbard (Arctic Ocean). *Polar Biology*, 30(10):1359–1362.

Fredriksen, R. (2018). *Epibenthic Community Structure in Northeast Greenland and the Kitikmeot Sea in the Canadian Arctic Archipelago*. PhD thesis, University of Tromso.

Gasparini, S. and Antajan, E. (2007). *PLANKTON IDENTIFIER: A Software for Automatic Recognition of Planktonic Organisms*.

Gooday, A. J., Levin, L. A., Linke, P., and Heeger, T. (1992). The Role of Benthic Foraminifera in Deep-Sea Food Webs and Carbon Cycling. In *Deep-Sea Food Chains and the Global Carbon Cycle*, NATO ASI Series, pages 63–91. Springer, Dordrecht.

Görlich, K., Węsławski, J. M., and Zajaczkowski, M. (1987). Suspension settling effect on macrobenthos biomass distribution in the Hornsund fjord, Spitsbergen. *Polar Research*, 5(2):175–192.

Górska, B. and Włodarska-Kowalczuk, M. (2017). Food and disturbance effects on Arctic benthic biomass and production size spectra. *Progress in Oceanography*, 152:50–61.

Gotelli, N. J. and Colwell, R. K. (2011). Estimating species richness. *Biological diversity: frontiers in measurement and assessment*, 12:39–54.

Graf, G. (1989). Benthic-pelagic coupling in a deep-sea benthic community. *Nature*, 341(6241):437–439.

Gray, J. S. and Elliott, M. (2009). *The Ecology of Marine Sediments: From Science to Management*. Oxford University Press, Oxford ; New York, 2nd ed edition.

Grebmeier, J., Overland, J., E Moore, S., V Farley, E., Carmack, E., Cooper, L., Frey, K., H Helle, J., Mclaughlin, F., and Mcnutt, L. (2006). A Major Ecosystem Shift in the Northern Bering Sea. *Science (New York, N.Y.)*, 311:1461–4.

Grebmeier, J. M. and Barry, J. P. (1991). The influence of oceanographic processes on pelagic-benthic coupling in polar regions: A benthic perspective. *Journal of Marine Systems*, 2(3-4):495–518.

Grebmeier, J. M. and McRoy, C. P. (1989). Pelagic-benthic coupling on the shelf of the northern Bering and Chukchi Seas. III. Benthic food supply and carbon cycling. page 13.

Gregory, B., Christophe, L., and Martin, E. (2009). Rapid biogeographical plankton shifts in the North Atlantic Ocean. *Global Change Biology*, 15(7):1790–1803.

Gutt, J. (1995). The occurrence of sub-ice algal aggregations off northeast Greenland. *Polar Biology*, 15(4).

Gutt, J. (2001). On the direct impact of ice on marine benthic communities, a review. *Polar Biology*, 24(8):553–564.

Hartmann-Schröder, G. (1996). *Annelida, Borstenwürmer, Polychaeta*, volume 58. Gustav Fischer.

Hegseth, E. N. and Sundfjord, A. (2008). Intrusion and blooming of Atlantic phytoplankton species in the high Arctic. *Journal of Marine Systems*, 74(1):108–119.

Henkel, S., Kasten, S., Hartmann, J. F., Silva-Busso, A., and Staubwasser, M. (2018). Iron cycling and stable Fe isotope fractionation in Antarctic shelf sediments, King George Island. *Geochimica et Cosmochimica Acta*, 237:320–338.

Hensen, C., Zabel, M., and Schulz, H. N. (2006). Benthic cycling of oxygen, nitrogen and phosphorus. In *Marine Geochemistry*, pages 207–240. Springer.

Hobbie, J. E., Daley, R. J., and Jasper, S. (1977). Use of nuclepore filters for counting bacteria by fluorescence microscopy. *Applied and Environmental Microbiology*, 33(5):1225–1228.

Hobson, K. A., Ambrose, W. G., and Renaud, P. R. (1996). Sources of primary production, benthicpelagic coupling, and trophic relationships within the northeast Water Polynya: Insights from 13C and 15N analysis. *Oceanographic Literature Review*, 7(43):689.

Hoffmann, R., Braeckman, U., Hasemann, C., and Wenzhöfer, F. (2018). Deep-sea benthic communities and oxygen fluxes in the Arctic Fram Strait controlled by sea-ice cover and water depth. *Biogeosciences Discussions*, pages 1–40.

Hopwood, M. J., Carroll, D., Browning, T. J., Meire, L., Mortensen, J., Krisch, S., and Achterberg, E. P. (2018). Non-linear response of summertime marine productivity to increased meltwater discharge around Greenland. *Nature Communications*, 9(1):3256.

Horner, R. and Schrader, G. C. (1982). Relative Contributions of Ice Algae, Phytoplankton, and Benthic Microalgae to Primary Production in Nearshore Regions of the Beaufort Sea. *ARCTIC*, 35(4):485–503.

Hughes, N. E., Wilkinson, J. P., and Wadhams, P. (2011). Multi-satellite sensor analysis of fast-ice development in the Norske Øer Ice Barrier, northeast Greenland. *Annals of Glaciology*, 52(57):151–160.

IPCC (2013). *Summary for Policymakers. In: Climate Change 2013: The Physical Science Basis. Contribution of Working Group I to the Fifth Assessment Report of the Intergovernmental Panel on Climate Change [Stocker, T.F., D. Qin, G.-K. Plattner, M. Tignor, S.K. Allen, J. Boschung, A. Nauels, Y. Xia, V. Bex and P.M. Midgley (Eds.)].* Cambridge University Press, Cambridge.

ISSI (2008). Arctic change and Polynyas: Focus on the Northeast Water Polynya and North Water Polynya/Nares Strait system team. http://www.issibern.ch/teams/Polynya/.

Jakobsson, M., Mayer, L., Coakley, B., Dowdeswell, J. A., Forbes, S., Fridman, B., Hodnesdal, H., Noormets, R., Pedersen, R., Rebesco, M., Schenke, H. W., Zarayskaya, Y., Accettella, D., Armstrong, A., Anderson, R. M., Bienhoff, P., Camerlenghi, A., Church, I., Edwards, M., Gardner, J. V., Hall, J. K., Hell, B., Hestvik, O., Kristoffersen, Y., Marcussen, C., Mohammad, R., Mosher, D., Nghiem, S. V., Pedrosa, M. T., Travaglini, P. G., and Weatherall, P. (2012). The International Bathymetric Chart of the Arctic Ocean (IBCAO) Version 3.0: IBCAO VERSION 3.0. *Geophysical Research Letters*, 39(12):n/a–n/a.

Jensen, M., Lomstein, E., and Sørensen, J. (1990). Benthic NH4 and NO3 flux following sedimentation of a spring phytoplankton bloom in Aarhus Bight, Denmark. *Marine Ecology Progress Series*, 61:87–96.

Jorissen, F. J., de Stigter, H. C., and Widmark, J. G. (1995). A conceptual model explaining benthic foraminiferal microhabitats. *Marine Micropaleontology*, 26(1-4):3–15.

Kanzow, T., von Appen, W.-J., Schaffer, J., Köhn, E., Tsubouchi, T., Wilson, N., and Wisotzki, A. (2017). Physical oceanography measured with CTD/Large volume Watersampler-system during POLARSTERN cruise PS100 (ARK-XXX/2).

Kattner, G. and Budéus, G. (1997). Nutrient status of the northeast water polynya. *Journal of marine systems*, 10(1-4):185–197.

Khan, S. A., Kjær, K. H., Bevis, M., Bamber, J. L., Wahr, J., Kjeldsen, K. K., Bjørk, A. A., Korsgaard, N. J., Stearns, L. A., van den Broeke, M. R., Liu, L., Larsen, N. K., and Muresan, I. S. (2014). Sustained mass loss of the northeast Greenland ice sheet triggered by regional warming. *Nature Climate Change*, 4(4):292–299.

Kędra, M., Kuliński, K., Walkusz, W., and Legeżyńska, J. (2012). The shallow benthic food web structure in the high Arctic does not follow seasonal changes in the surrounding environment. *Estuarine, Coastal and Shelf Science*, 114:183–191.

Korsun, S. (2000). Seasonal dynamics of benthic Foraminifera in a glacially fed fjord of Svalbard, European Arctic. *Journal of Foraminiferal Research - J FORAMIN RES*, 30:251–271.

Kortsch, S., Primicerio, R., Beuchel, F., Renaud, P. E., Rodrigues, J. a., Lønne, O. J., and Gulliksen, B. (2012). Climate-driven regime shifts in Arctic marine benthos. *Proceedings of the National Academy of Sciences of the United States of America*, 109(35):14052–14057.

Lara, R. J., Kattner, G., Tillmann, U., and Hirche, H.-J. (1994). The North East Water polynya (Greenland Sea). II. Mechanisms of nutrient supply and influene on phytoplankton distribution. *Polar Biology*, 14(7):483–490.

Legendre, P. and Gallagher, E. D. (2001). Ecologically meaningful transformations for ordination of species data. *Oecologia*, 129(2):271–280.

Leu, E., Mundy, C. J., Assmy, P., Campbell, K., Gabrielsen, T. M., Gosselin, M., Juul-Pedersen, T., and Gradinger, R. (2015). Arctic spring awakening – Steering principles behind the phenology of vernal ice algal blooms. *Progress in Oceanography*, 139:151–170.

Li, W. K. W., McLaughlin, F. A., Lovejoy, C., and Carmack, E. C. (2009). Smallest Algae Thrive As the Arctic Ocean Freshens. *Science*, 326(5952):539–539.

Licari, L. (2004). *Ecological Preferences of Benthic Foraminifera in the Eastern South Atlantic: Distribution Patterns, Stable Carbon Isotopic Composition, and Paleoceanographic Implications*. PhD thesis, University of Bremen.

Link, H., Chaillou, G., Forest, A., Piepenburg, D., and Archambault, P. (2013). Multivariate benthic ecosystem functioning in the Arctic - benthic fluxes explained by environmental parameters in the southeastern Beaufort Sea. *Biogeosciences*, 10(9):5911–5929.

Lutze, G. F. and Altenbach, A. (1991). Technik und Signifikanz der Lebendfärbung benthischer Foraminiferen in Bengalrot. *Geologisches Jahrbuch, Reihe A*, 128(251):165.

Mäkelä, A., Witte, U., and Archambault, P. (2017a). Benthic macroinfaunal community structure, resource utilisation and trophic relationships in two Canadian Arctic Archipelago polynyas. *PLOS ONE*, 12(8):e0183034.

Mäkelä, A., Witte, U., and Archambault, P. (2017b). Ice algae vs. phytoplankton: Resource utilization by Arctic deep sea macroinfauna revealed through isotope labelling experiments. *Marine Ecology Progress Series*, 572:1–18.

Martins, M. V. A., Laut, L. L. M., Frontalini, F., Sequeira, C., Rodrigues, R., Fonseca, M. C. M., Bergamashi, S., Pereira, E., Delavy, F. P., Figueiredo Jr., A. G., Miranda, P., Terroso, D., Pena, A. L., Laut, V. M., Figueira, R., and Rocha, F. (2016). Controlling factors on the abundance, diversity and size of living benthic foraminifera in the NE sector of Guanabara Bay (Brazil). *Journal of Sedimentary Environments*, 1(4).

Mayer, C., Reeh, N., Jung-Rothenhäusler, F., Huybrechts, P., and Oerter, H. (2000). The subglacial cavity and implied dynamics under Nioghalvfjerdsfjorden Glacier, NE-Greenland. *Geophysical Research Letters*, 27(15):2289–2292.

McMahon, K., Ambrose WG, J., Johnson, B., Sun, M., Lopez, G., Clough, L., and Carroll, M. (2006). Benthic community response to ice algae and phytoplankton in Ny Ålesund, Svalbard. *Marine Ecology Progress Series*, 310:1–14.

McTigue, N. D., Bucolo, P., Liu, Z., and Dunton, K. H. (2015). Pelagic-benthic coupling, food webs, and organic matter degradation in the Chukchi Sea: Insights from sedimentary pigments and stable carbon isotopes. *Limnology and Oceanography*, 60(2):429–445.

Meire, L., Mortensen, J., Meire, P., Juul-Pedersen, T., Sejr, M. K., Rysgaard, S., Nygaard, R., Huybrechts, P., and Meysman, F. J. R. (2017). Marine-terminating glaciers sustain high productivity in Greenland fjords. *Global Change Biology*, 23(12):5344–5357.

Meire, L., Mortensen, J., Rysgaard, S., Bendtsen, J., Boone, W., Meire, P., and Meysman, F. J. R. (2016). Spring bloom dynamics in a subarctic fjord influenced by tidewater outlet glaciers (Godthåbsfjord, SW Greenland): Spring in a Subarctic Fjord. *Journal of Geophysical Research: Biogeosciences*, 121(6):1581–1592.

Mojtahid, M., Jorissen, F., and Pearson, T. H. (2008). Comparison of benthic foraminiferal and macrofaunal responses to organic pollution in the Firth of Clyde (Scotland). *Marine Pollution Bulletin*, 56(1):42–76.

Monien, P., Lettmann, K. A., Monien, D., Asendorf, S., Wölfl, A.-C., Lim, C. H., Thal, J., Schnetger, B., and Brumsack, H.-J. (2014). Redox conditions and trace metal cycling in coastal sediments from the maritime Antarctic. *Geochimica et Cosmochimica Acta*, 141:26–44.

Moon, T. and Joughin, I. (2008). Changes in ice front position on Greenland's outlet glaciers from 1992 to 2007. *Journal of Geophysical Research*, 113(F2).

Morata, N., Michaud, E., and Włodarska-Kowalczuk, M. (2015). Impact of early food input on the Arctic benthos activities during the polar night. *Polar Biology*, 38(1):99–114.

Morata, N. and Renaud, P. (2008). Sedimentary pigments in the western Barents Sea: A reflection of pelagic–benthic coupling? *Deep Sea Research Part II: Topical Studies in Oceanography*, 55:2381–2389.

Mouginot, J., Rignot, E., Scheuchl, B., Fenty, I., Khazendar, A., Morlighem, M., Buzzi, A., and Paden, J. (2015). Fast retreat of Zachariae Isstrom, northeast Greenland. *Science*, 350(6266):1357–1361.

Murray, J. W. and Alve, E. (2000). Major aspects of foraminiferal variability (standing crop and biomass) on a monthly scale in an intertidal zone. *The Journal of Foraminiferal Research*, 30(3):177–191.

Nick, F. M., Luckman, A., Vieli, A., Veen, C. J. V. D., As, D. V., Wal, R. S. W. V. D., Pattyn, F., Hubbard, A. L., and Floricioiu, D. (2012). The response of Petermann Glacier, Greenland, to large calving events, and its future stability in the context of atmospheric and oceanic warming. *Journal of Glaciology*, 58(208):229–239.

Nick, F. M., Vieli, A., Andersen, M. L., Joughin, I., Payne, A., Edwards, T. L., Pattyn, F., and van de Wal, R. S. W. (2013). Future sea-level rise from Greenland's main outlet glaciers in a warming climate. *Nature*, 497(7448):235–238.

Nothold, H. (1998). Die Auswirkungen der" NorthEastWater"-Polynya auf die Sedimentation vor NO-Grönland und Untersuchungen zur Paläo-Ozeanographie seit dem Mittelweichsel. *Berichte zur Polarforschung (Reports on Polar Research)*, 275.

Oksanen, J., Blanchet, F. G., Friendly, M., Kindt, R., Legendre, P., McGlinn, D., Minchin, P. R., O'Hara, R. B., Simpson, G. L., Solymos, P., Stevens, M. H. H., Szoecs, E., and Wagner, H. (2018). Vegan: Community Ecology Package.

Olli, K., Wassmann, P., Reigstad, M., N. Ratkova, T., Arashkevich, E., Pasternak, A., Matrai, P., Knulst, J., Tranvik, L., Klais, R., and Jacobsen, A. (2007). The fate of production in the central Arctic Ocean - Top-down regulation by zooplankton expatriates? *Progress In Oceanography*, 72:84–113.

Overland, J. E. and Wang, M. (2013). When will the summer Arctic be nearly sea ice free? *Geophysical Research Letters*, 40(10):2097–2101.

Paliy, O. and Shankar, V. (2016). Application of multivariate statistical techniques in microbial ecology. *Molecular Ecology*, 25(5):1032–1057.

Pasotti, F., Manini, E., Giovannelli, D., Wölfl, A.-C., Monien, D., Verleyen, E., Braeckman, U., Abele, D., and Vanreusel, A. (2015). Antarctic shallow water benthos in an area of recent rapid glacier retreat. *Marine Ecology*, 36(3):716–733.

Piepenburg, D. (1988). *Zur Zusammensetzung der Bodenfauna in der westlichen Fram-Strasse*. PhD thesis, University of Kiel.

Piepenburg, D., Ambrose, W. G., Brandt, A., Renaud, P. E., Ahrens, M. J., and Jensen, P. (1997). Benthic community patterns reflect water column processes in the Northeast Water polynya (Greenland). *Journal of Marine Systems*, 10(1-4):467–482.

Piepenburg, D., Archambault, P., Ambrose, W. G., Blanchard, A. L., Bluhm, B. A., Carroll, M. L., Conlan, K. E., Cusson, M., Feder, H. M., Grebmeier, J. M., Jewett, S. C., Lévesque, M., Petryashev, V. V., Sejr, M. K., Sirenko, B. I., and Włodarska-Kowalczuk, M. (2011). Towards a pan-Arctic inventory of the species diversity of the macro- and megabenthic fauna of the Arctic shelf seas. *Marine Biodiversity*, 41(1):51–70.

Piepenburg, D., Blackburn, T., von Dorrien, C., Gutt, J., Hall, P., Hulth, S., Kendall, M., Opalinski, K., Rachor, E., and Schmid, M. (1995). Partitioning of benthic community respiration in the Arctic (northwestern Barents Sea). *Marine Ecology Progress Series*, 118:199–213.

Piquet, A., van de Poll, W., J. W. Visser, R., Wiencke, C., Bolhuis, H., and Buma, A. (2013). Springtime phytoplankton dynamics in Arctic Krossfjorden and Kongsfjorden (Spitsbergen) as a function of glacier proximity. *Biogeosciences Discussions*, 10:15519–15557.

R Core Team (2018). *R: A Language and Environment for Statistical Computing*. R Foundation for Statistical Computing, Vienna, Austria.

Reigstad, M. and Wassmann, P. (1996). Importance of advection for pelagic-benthic coupling in north Norwegian fjords. *Sarsia*, 80(4):245–257.

Renaud, P. E., Riedel, A., Michel, C., Morata, N., Gosselin, M., Juul-Pedersen, T., and Chiuchiolo, A. (2007a). Seasonal variation in benthic community oxygen demand: A response to an ice algal bloom in the Beaufort Sea, Canadian Arctic? *Journal of Marine Systems*, 67(1-2):1–12.

Renaud, P. E., Włodarska-Kowalczuk, M., Trannum, H., Holte, B., Węsławski, J. M., Cochrane, S., Dahle, S., and Gulliksen, B. (2007b). Multidecadal stability of benthic community structure in a high-Arctic glacial fjord (van Mijenfjord, Spitsbergen). *Polar Biology*, 30(3):295–305.

Revsbech, N. P. (1989). An oxygen microsensor with a guard cathode. *Limnology and Oceanography*, 34(2):474–478.

Rignot, E. and Kanagaratnam, P. (2006). Changes in the Velocity Structure of the Greenland Ice Sheet. *Science*, 311(5763):986–990.

Roberts, D., Lloyd, J., Cofaigh, C. O., Callard, L., Grob, H., and Kappelsberger, M. (2017). NEGIS: Understanding the mechanisms controlling the long-term stability of the Northeast Greenland Ice Stream. In: The Expedition PS100 of the Research Vessel POLARSTERN to the Fram Strait in 2016 (Ed. T. Kanzow). Technical report.

Rowe, G. T., Boland, G. S., Escobar Briones, E. G., Cruz-Kaegi, M. E., Newton, A., Piepenburg, D., Walsh, I., and Deming, J. (1997). Sediment community biomass and respiration in the Northeast water polynya, Greenland: A numerical simulation of benthic lander and spade core data. *Journal of Marine Systems*, 10(1-4):497–515.

Sakshaug, E., Johnsen, G., Kristiansen, S., von Quillfeldt, C. H., Rey, F., Slagstad, D., and Thingstad, F. (2009). Phytoplankton and Primary Production. In Sakshaug, E., Johnsen, G., and Kovacs, K. M., editors, *Ecosystem Barents Sea*, pages 147–. Tapir Academic Press, Tronheim.

Schaffer, J. (2017). *Ocean impact on the 79 North Glacier, Northeast Greenland*. phd, University of Bremen.

Schaffer, J., von Appen, W.-J., Dodd, P. A., Hofstede, C., Mayer, C., de Steur, L., and Kanzow, T. (2017). Warm water pathways toward Nioghalvfjerdsfjorden Glacier, Northeast Greenland. *Journal of Geophysical Research: Oceans*, 122(5):4004–4020.

Schlüter, M., Sauter, E. J., Schäfer, A., and Ritzrau, W. (2000). Spatial budget of organic carbon flux to the seafloor of the northern North Atlantic (60°N–80°N). *Global Biogeochemical Cycles*, 14(1):329–340.

Schneider, W. (1997). The Northeast Water Polynya: Origin and hydrography.

Schneider, W. and Budéus, G. (1994). The north east water polynya (Greenland Sea). I. A physical concept of its generation. *Polar Biology*, 14(1):1–9.

Schneider, W. and Budéus, G. (1995). On the generation of the Northeast Water Polynya. *Journal of Geophysical Research*, 100(C3):4269.

Schneider, W. and Budéus, G. (1997). Summary of the Northeast Water Polynya formation and development (Greenland sea). *Journal of Marine Systems*, 10(1):107–122.

Sejr, M. K., Jensen, K. T., and Rysgaard, S. (2000). Macrozoobenthic community structure in a high-arctic East Greenland fjord. *Polar Biology*, 23(11):792–801.

Sevilgen, D., de Beer, D., Al-Handal, A., Brey, T., and Polerecky, L. (2014). Oxygen budgets in subtidal arctic (Kongsfjorden, Svalbard) and temperate (Helgoland, North Sea) microphytobenthic communities. *Marine Ecology Progress Series*, 504:27–42.

Shepherd, A., Ivins, E. R., A, G., Barletta, V. R., Bentley, M. J., Bettadpur, S., Briggs, K. H., Bromwich, D. H., Forsberg, R., Galin, N., Horwath, M., Jacobs, S., Joughin, I., King, M. A., Lenaerts, J. T. M., Li, J., Ligtenberg, S. R. M., Luckman, A., Luthcke, S. B., McMillan, M., Meister, R., Milne, G., Mouginot, J., Muir, A., Nicolas, J. P., Paden, J., Payne, A. J., Pritchard, H., Rignot, E., Rott, H., Sørensen, L. S., Scambos, T. A., Scheuchl, B., Schrama, E. J. O., Smith, B., Sundal, A. V., van Angelen, J. H., van de Berg, W. J., van den Broeke, M. R., Vaughan, D. G., Velicogna, I., Wahr, J., Whitehouse, P. L., Wingham, D. J., Yi, D., Young, D., and Zwally, H. J. (2012). A Reconciled Estimate of Ice-Sheet Mass Balance. *Science*, 338(6111):1183–1189.

Ślubowska, M. A., Koç, N., Rasmussen, T. L., and Klitgaard-Kristensen, D. (2005). Changes in the flow of Atlantic water into the Arctic Ocean since the last deglaciation: Evidence from the northern Svalbard continental margin, 80°N. *Paleoceanography*, 20(4).

Smith, K. L., Ruhl, H. A., Kahru, M., Huffard, C. L., and Sherman, A. D. (2013). Deep ocean communities impacted by changing climate over 24 y in the abyssal northeast Pacific Ocean. *Proceedings of the National Academy of Sciences*, 110(49):19838–19841.

Smith, S. D., Muench, R. D., and Pease, C. H. (1990). Polynyas and leads: An overview of physical processes and environment. *Journal of Geophysical Research*, 95(C6):9461.

Smith, W., Gosselin, M., Legendre, L., Wallace, D., Daly, K., and Kattner, G. (1997). New production in the Northeast Water Polynya: 1993. *Journal of Marine Systems*, 10(1):199–209.

Straneo, F., Sutherland, D. A., Holland, D., Gladish, C., Hamilton, G. S., Johnson, H. L., Rignot, E., Xu, Y., and Koppes, M. (2012). Characteristics of ocean waters reaching Greenland's glaciers. *Annals of Glaciology*, 53(60):202–210.

Stroeve, J. C., Serreze, M. C., Holland, M. M., Kay, J. E., Malanik, J., and Barrett, A. P. (2012). The Arctic's rapidly shrinking sea ice cover: A research synthesis. *Climatic Change*, 110(3-4):1005–1027.

Tamelander, T., Renaud, P. E., Hop, H., Carroll, M. L., Jr, W. G. A., and Hobson, K. A. (2006). Trophic relationships and pelagic–benthic coupling during summer in the Barents Sea Marginal Ice Zone, revealed by stable carbon and nitrogen isotope measurements. *Marine Ecology Progress Series*, 310:33–46.

Thamdrup, B., Glud, R., and Hansen, J. (2007). Benthic carbon cycling in Young Sound, Northeast Greenland. *Meddelelser om Grønland, Bioscience*, 58:138–157.

Thomsen, H. H., Reeh, N., Olesen, O. B., Boggild, C. E., Starzer, W., Weidick, A., and Higgins, A. K. (1997). The Nioghalvfjerdsfjorden glacier project, North-East Greenland: A study of ice sheet response to climatic change. *Geology of Greenland Survey Bulletin*, 176:95–103.

Topp, R. and Johnson, M. (1997). Winter intensification and water mass evolution from yearlong current meters in the Northeast Water Polynya. *Journal of Marine Systems*, 10(1):157–173.

Turner, J. and Marshall, G. (2011). *Climate Change in the Polar Regions*. Cambridge University Press, Cambridge.

van de Poll, W. H., Kulk, G., Rozema, P. D., Brussaard, C. P. D., Visser, R. J. W., and Buma, A. G. J. (2018). Contrasting glacial meltwater effects on post-bloom phytoplankton on temporal and spatial scales in Kongsfjorden, Spitsbergen. *Elem Sci Anth*, 6(1).

Wadhams, P. (1981). The ice cover in the Greenland and Norwegian seas. *Reviews of Geophysics*, 19(3):345.

Wallace, D. W. R., Minnett, P. J., and Hopkins, T. S. (1995). Nutrients, oxygen, and inferred new production in the Northeast Water Polynya, 1992. *Journal of Geophysical Research*, 100(C3):4323.

Walton, W. R. (1952). *Techniques for Recognition of Living Foraminifera*. Scripps Institution of Oceanography.

Wassmann, P. (1991). Dynamics of primary production and sedimentation in shallow fjords and polls of western Norway. *Oceanography and marine biology: an annual review. Vol. 29*, 29:87–154.

Wassmann, P. (1998). Retention versus export food chains: Processes controlling sinking loss from marine pelagic systems. In Tamminen, T. and Kuosa, H., editors, *Eutrophication in Planktonic Ecosystems: Food Web Dynamics and Elemental Cycling*, pages 29–57. Springer Netherlands, Dordrecht.

Wassmann, P. and Reigstad, M. (2011). Future Arctic Ocean Seasonal Ice Zones and Implications for Pelagic-Benthic Coupling. *Oceanography*, 24(3):220–231.

Wei, T., Simko, V., Levy, M., Xie, Y., Jin, Y., and Zemla, J. (2017). Corrplot: Visualization of a Correlation Matrix.

Wessel, P. and Smith, W. H. F. (1996). A global, self-consistent, hierarchical, high-resolution shoreline database. *Journal of Geophysical Research: Solid Earth*, 101(B4):8741–8743.

Wilson, N. J. and Straneo, F. (2015). Water exchange between the continental shelf and the cavity beneath Nioghalvfjerdsbræ (79 North Glacier). *Geophysical Research Letters*, 42(18):2015GL064944.

Włodarska-Kowalczuk, M. and Kedra, M. (2007). Surrogacy in natural patterns of benthic distribution and diversity: Selected taxa versus lower taxonomic resolution. *Marine Ecology Progress Series*, 351:53–63.

Włodarska-Kowalczuk, M., Pawłowska, J., and Zajączkowski, M. (2013). Do foraminifera mirror diversity and distribution patterns of macrobenthic fauna in an Arctic glacial fjord? *Marine Micropaleontology*, 103:30–39.

Włodarska-Kowalczuk, M. and Pearson, T. H. (2004). Soft-bottom macrobenthic faunal associations and factors affecting species distributions in an Arctic glacial fjord (Kongsfjord, Spitsbergen). *Polar Biology*, 27(3):155–167.

Włodarska-Kowalczuk, M., Pearson, T. H., and Kendall, M. A. (2005). Benthic response to chronic natural physical disturbance by glacial sedimentation in an Arctic fjord. *Marine Ecology Progress Series*, 303:31–41.

Włodarska-Kowalczuk, M., Renaud, P. E., Węsławski, J. M., Cochrane, S. K., and Denisenko, S. G. (2012). Species diversity, functional complexity and rarity in Arctic fjordic versus open shelf benthic systems. *Marine Ecology Progress Series*, 463:73–87.

Wolff, G. (2008). D. J. Burdige 2006. Geochemistry of Marine Sediments. xix + 609 pp. Princeton, Woodstock: Princeton University Press. Price £55.00, US $85.00 (hard covers). ISBN 0 691 09506 X. *Geological Magazine*, 145(1):153–153.

Wright, S. W., Jeffrey, S. W., and Mantoura, R. F. C. (2005). *High-Resolution HPLC System for Chlorophylls and Carotenoids of Marine Phytoplankton. In: Jeffrey SW, Mantoura RFC, Wright SW, Editors. Phytoplankton Pigments in Oceanography: Guidelines to Modern Methods*. Unesco Pub.

A Appendix

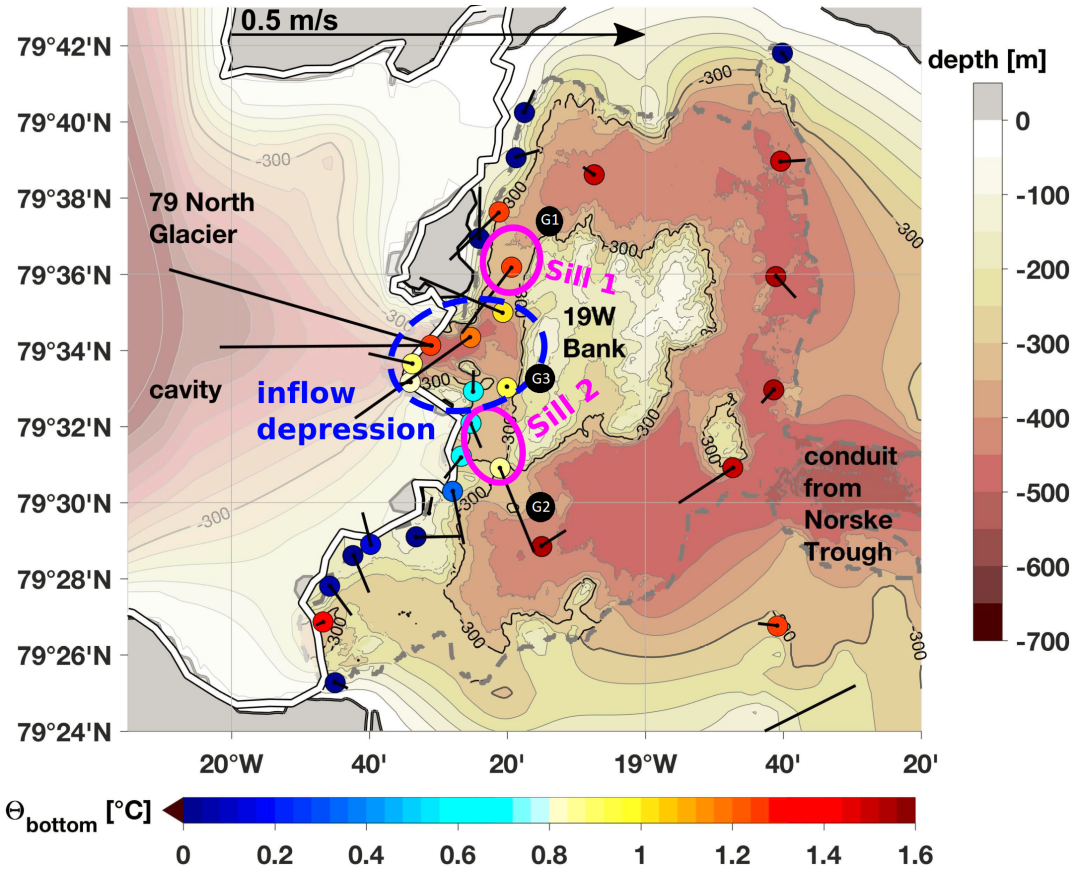

FIGURE A.1: **Locations of the stations at the glacier front (black dots) with detailed bathymetry.** Coloured dots indicate bottom temperatures, thick black lines indicate bottom velocities at the CTD/LADCP stations. The bathymetry based on RTopo-2.0.2 is covered by the bathymetry from the multibeam echo sounder data within the region surrounded by the grey dashed line. Bottom variables are means between the deepest depth of the CTD/LADCP cast and 20 m above. The length of the velocity vectors are scaled by 1°-longitude equivalent to 0.5 $m\ s^{-1}$. (Figure adapted from and changed after Schaffer, 2017).

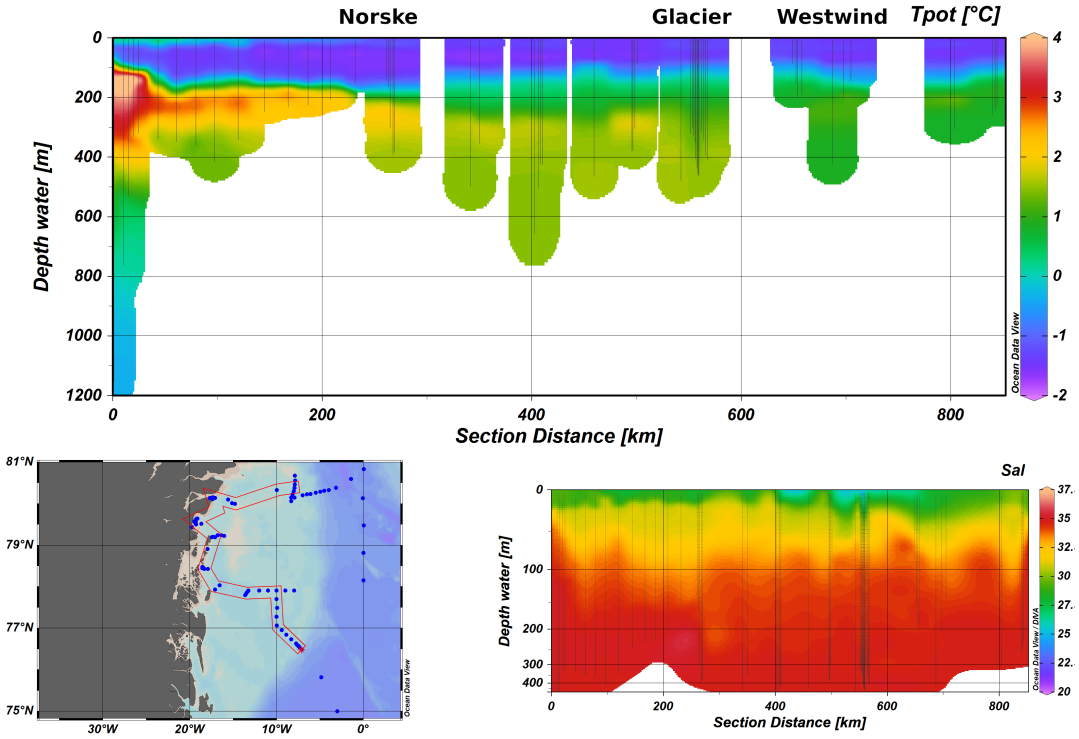

FIGURE A.2: **Temperature (upper) and salinity (lower right) profiles along a section within the trough system on the NEG shelf (lower left).**

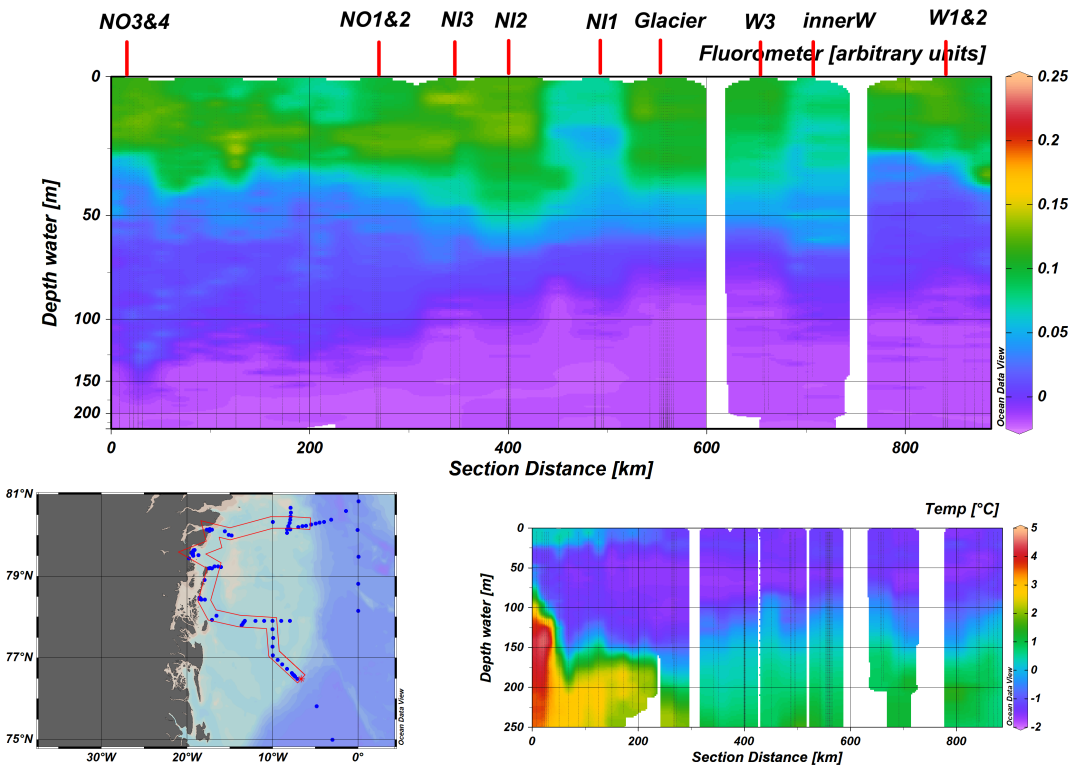

FIGURE A.3: **Uncalibrated raw fluoromenter values from the CTD during PS109 in the upper 200 meters.**

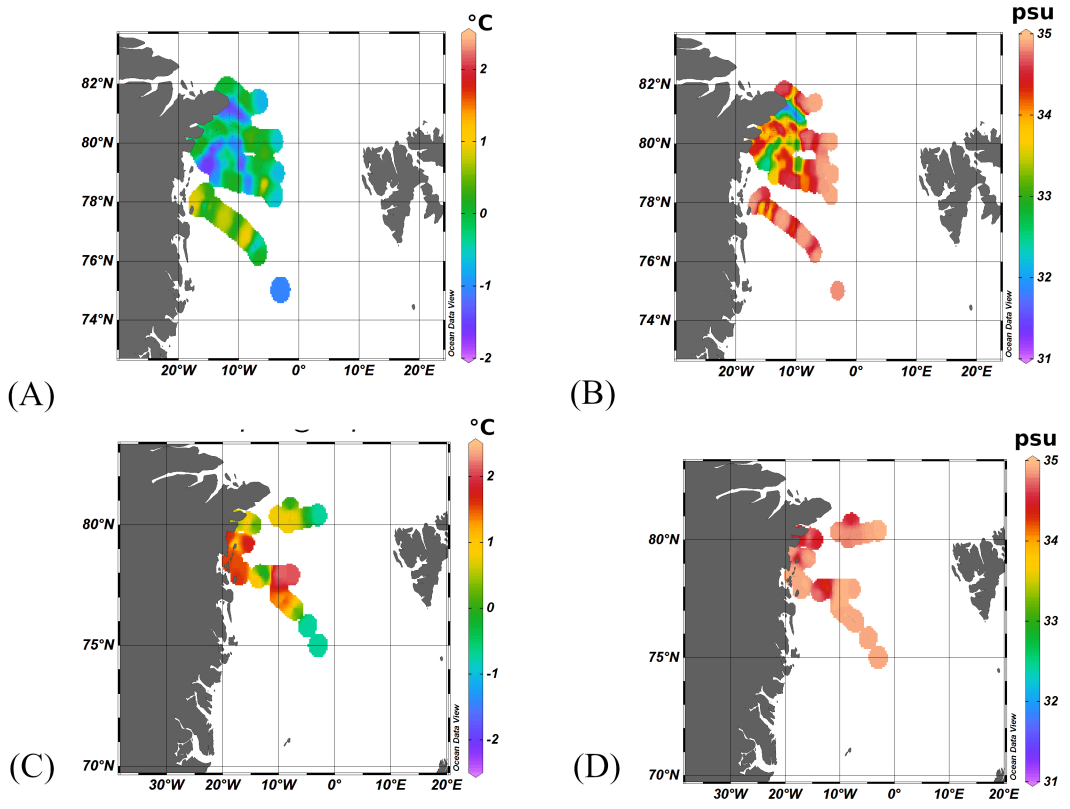

FIGURE A.4: **Bottom water temperature (A, C) and salinity (B,D) from PS25 (1993; A,B) and PS109 (217; C,D).**

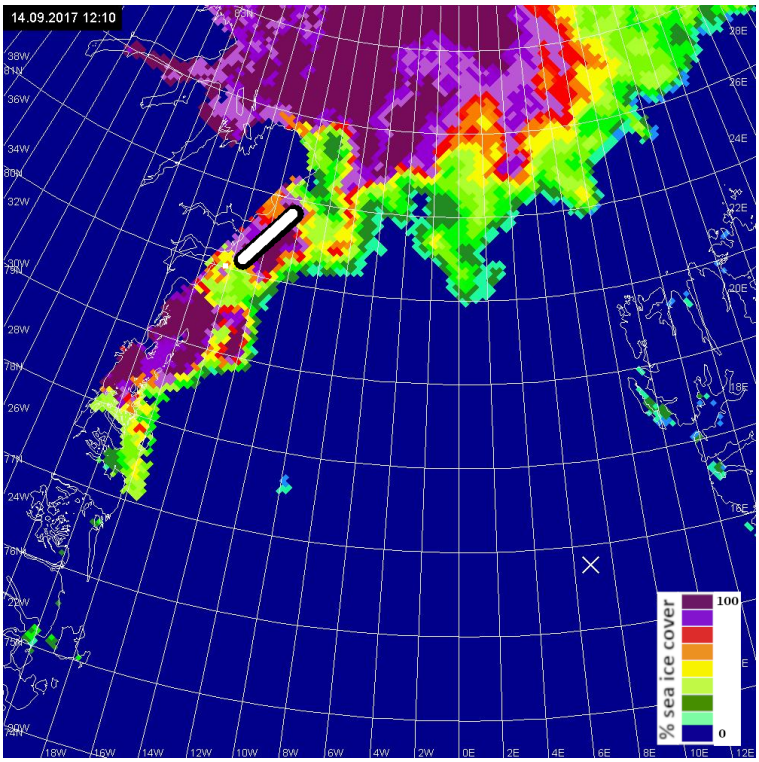

FIGURE A.5: **Sea ice conditions on 14th of September, 2017 during PS109.** Black-and-white area indicates roughly the region of the NEW polynya.

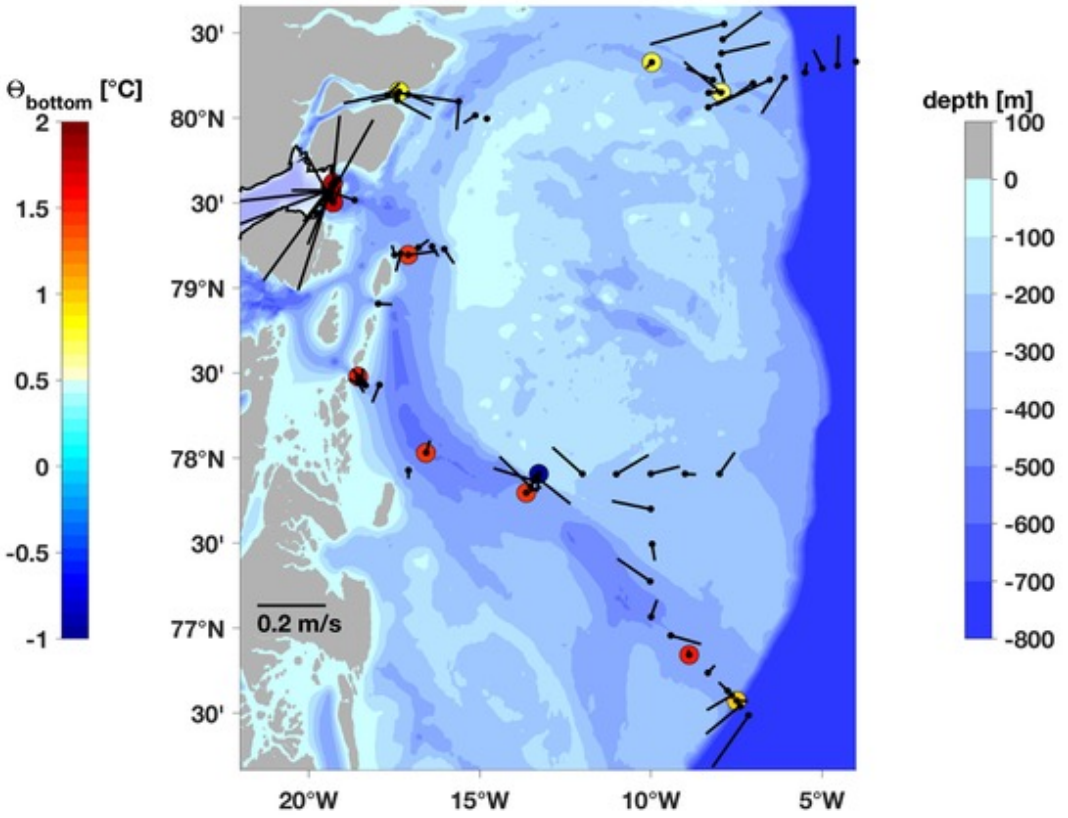

FIGURE A.6: **Bottom water current velocities and temperatures on the NEG shelf during PS109**. Colours represent temperature, lines the strength and direction of current velocities. By courtesy of J. Schaffer.

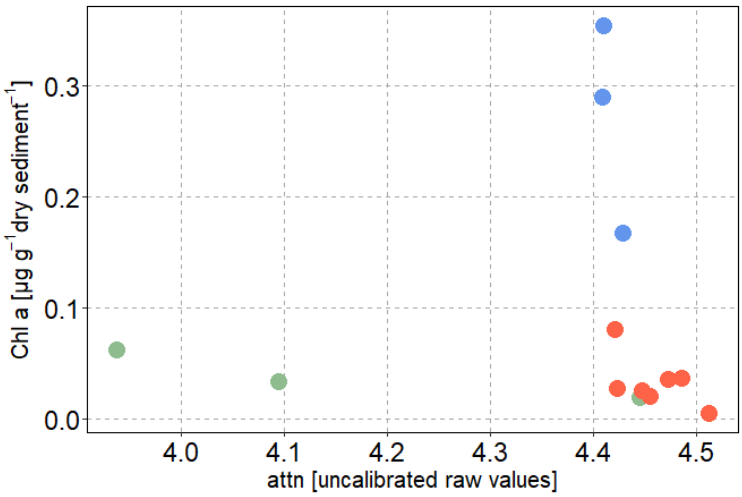

FIGURE A.7: **Attenuation and chlorophyll a concentrations.**. Blue = Westwind Trough, green = Glacier, red = Norske Trough.

TABLE A.1: **Mean values and standard deviations (if available) for environmental parameters and TOU for each station.** Phaeopigments = sum of Phaeophytin and Phaeophorbid, CPE = Chloroplastic pigment equivalents, DIC = Dissolved inorganic carbon, TOU = total oxygen uptake.

		W1	**W2**	**W3**	**G1**	**G2**	**G3**	**NI1**	**NI2**	**NI3**	**NO1**	**NO2**	**NO3**	**NO4**
Water column properties	Depth	315	310	206	367	309	156	386	440	502	140	391	354	1177
	Tpot	0.67	0.79	0.86	1.70	1.74	1.67	1.44	1.51	1.46	-1.08	1.47	1.54	-0.33
	Salinity	34.85	34.86	34.64	34.91	34.88	34.85	34.92	34.92	34.94	33.96	34.93	34.93	34.91
	Current velocity	0.15	0.02	0.19	0.13	0.07	0.28	0.09	0.01	0.04	0.08	0.04	0.02	0.17
	Attenuation	4.41	4.41	4.43	4.44	4.09	3.94	4.45	4.45	4.42	4.49	4.47	4.42	4.51
Sediment properties	Grain size	77.1±0.58	79.19±0.46	87.38±0.04	89.63±0.93	90.49±0.34	90.97±0.03	87.57±0.14	89.31±0.18	87.96±0.74	51.17±0.05	84.58±0.22	79.53±0.29	73.26±0.16
	Silt fraction	82.72±0.16	82.96±0.86	96.18±0.75	91.02±0.54	97.51±0.6	97±0.08	94.92±0.95	95.74±0.35	95.02±0.27	56.19±0.81	84.43±0.46	83.46±0.63	73.01±0.86
Biogenic compounds	Phaeophorbid	0.09±0.02	0.11±0.03	0.03±0.04	0.01±0.02	0.02±0.02	0.02±0.02	0.01±0.02	0.01±0.02	0.02±0.02	0.01±0.01	0.01±0.01	0.01±0.01	0
	Phaeophytin	0.28±0.02	0.39±0.03	0.07±0.06	0.03±0.03	0.04±0.04	0.06±0.02	0.04±0.03	0.04±0.04	0.08±0.06	0.02±0.02	0.04±0.03	0.05±0.03	0.01±0.01
	Phaeopigments	0.37±0.03	0.51±0.05	0.1±0.09	0.05±0.05	0.06±0.06	0.08±0.04	0.05±0.05	0.05±0.05	0.09±0.08	0.03±0.03	0.04±0.04	0.06±0.04	0.02±0.02
	Fucoxanthin	0.11±0.06	0.12±0.09	0.05±0.1	0.01±0.01	0.01±0.02	0.02±0.03	0.01±0.02	0.01±0.02	0.03±0.05	0.01±0.02	0.01±0.02	0.01±0.01	0
	Chla	0.29±0.11	0.35±0.22	0.17±0.24	0.02±0.04	0.03±0.05	0.06±0.08	0.03±0.05	0.02±0.04	0.08±0.14	0.04±0.05	0.04±0.05	0.03±0.03	0±0.01
	CPE	0.66±0.11	0.86±0.26	0.27±0.33	0.07±0.09	0.09±0.11	0.14±0.11	0.08±0.09	0.07±0.09	0.17±0.22	0.06±0.08	0.08±0.09	0.09±0.07	0.02±0.02
	Chla/Phaeo	0.79±0.28	0.68±0.39	1.15±0.71	0.2±0.24	0.53±0.26	0.6±0.46	0.27±0.31	0.23±0.21	0.49±0.62	0.84±0.73	0.54±0.43	0.32±0.25	0.21±0.12
	Chla/CPE	0.43±0.09	0.38±0.12	0.5±0.14	0.14±0.15	0.33±0.11	0.34±0.17	0.18±0.16	0.17±0.12	0.26±0.2	0.38±0.26	0.31±0.18	0.22±0.14	0.17±0.08
Porewater compounds	Ammonia	0.00	1.93	1.41	1.16	0.71	0.00	0.38	0.13	0.00	0.04	0.00	0.00	0.84
	Nitrate	7.42	10.33	8.61	5.88	2.12	12.80	13.46	12.03	14.40	4.59	15.34	13.74	13.47
	Nitrite	0.20	0.04	0.06	0.00	0.44	0.00	0.00	0.00	0.00	0.00	0.00	0.00	0.00
	Phosphate	0.92	0.74	0.93	0.60	1.03	0.86	0.82	0.79	0.96	0.61	1.00	0.75	1.02
	Silicate	5.29	8.94	7.50	6.01	8.25	8.82	9.02	12.38	11.76	7.16	10.48	7.09	10.49
	Alkalinity	2.51	2.07	2.28	1.77	2.21	2.13	2.22	0.98	2.46	1.71	2.47	2.00	2.23
	DIC	2.26	2.10	2.17	1.80	2.20	2.16	2.28	1.57	2.33	2.14	2.24	2.00	2.13
	Chloride	510.59	514.47	539.40	469.56	530.61	543.98	547.50	550.50	539.92	466.37	542.25	540.19	527.60
Sediment fluxes	TOU	-1.26±0.25	-1.56±0.04	-2.17±0.16	-1.34±0.16	-1.23±0.27	-1.29±0.18	-1.23±0.27	-1.4±0.44	-1.67±0.23	-1.62±0.28	-1.18±0.34	-2.4±0.6	-0.69

TABLE A.2: **Modelled mean porosity per sediment depth from silt fraction (fraction of grain size <63 μm) and benthic pigment concentrations in $\mu g\ g^{-1}\ dry\ sediment^{-1}$ (measured values) and $mg\ ml^{-1}$ (calculated from modelled porosity) for each station on the NEG shelf during PS109.**

			Chl a		Phaeo		CPE		Fuco	
St	sed depth [cm]	modelled porosity	$\mu g\ g^{-1}$	$mg\ m^{-2}$	$\mu g\ g^{-1}$	$mg\ m^{-2}$	$\mu g\ g^{-1}$	$mg\ m^{-2}$	$\mu g\ g^{-1}$	$mg\ m^{-2}$
19	1	0.668	0.462	3.914	0.393	3.332	0.855	7.246	0.203	1.718
19	2	0.647	0.322	2.892	0.325	2.919	0.646	5.810	0.107	0.959
19	3	0.665	0.226	1.930	0.360	3.075	0.586	5.006	0.095	0.811
19	4	0.685	0.203	1.629	0.412	3.305	0.615	4.934	0.062	0.495
19	5	0.688	0.237	1.886	0.362	2.879	0.600	4.765	0.073	0.583
36	1	0.664	0.740	6.344	0.551	4.726	1.291	11.069	0.281	2.410
36	2	0.667	0.341	2.898	0.479	4.071	0.820	6.969	0.109	0.926
36	3	0.666	0.249	2.115	0.484	4.114	0.732	6.229	0.083	0.706
36	4	0.678	0.279	2.294	0.571	4.697	0.850	6.990	0.096	0.786
36	5	0.685	0.163	1.309	0.449	3.604	0.612	4.914	0.035	0.284
46	1	0.734	0.597	4.049	0.258	1.747	0.855	5.796	0.228	1.543
46	2	0.730	0.126	0.870	0.103	0.711	0.230	1.581	0.030	0.209
46	3	0.735	0.061	0.410	0.062	0.422	0.123	0.832	0.011	0.077
46	4	0.739	0.035	0.233	0.048	0.320	0.083	0.553	0.004	0.029
46	5	0.739	0.018	0.122	0.038	0.251	0.056	0.373	0.000	0.000
76	1	0.707	0.082	0.611	0.135	1.008	0.216	1.619	0.026	0.195
76	2	0.722	0.012	0.085	0.050	0.353	0.062	0.438	0.002	0.017
76	3	0.714	0.002	0.012	0.023	0.165	0.024	0.177	0.000	0.000
76	4	0.700	0.001	0.005	0.014	0.105	0.014	0.110	0.000	0.000
76	5	0.563	0.000	0.004	0.013	0.141	0.013	0.145	0.000	0.000
84	1	0.742	0.116	0.760	0.164	1.075	0.279	1.835	0.039	0.258
84	2	0.737	0.014	0.092	0.036	0.244	0.050	0.335	0.004	0.025
84	3	0.741	0.010	0.068	0.039	0.256	0.049	0.324	0.001	0.009
84	4	0.743	0.020	0.133	0.023	0.151	0.043	0.284	0.005	0.035
84	5	0.745	0.006	0.041	0.015	0.098	0.021	0.139	0.001	0.007
85	1	0.732	0.196	1.339	0.148	1.012	0.344	2.351	0.065	0.442
85	2	0.741	0.053	0.352	0.076	0.499	0.129	0.851	0.014	0.090
85	3	0.742	0.032	0.213	0.058	0.384	0.091	0.597	0.003	0.020
85	4	0.737	0.016	0.107	0.066	0.445	0.082	0.553	0.000	0.000
85	5	0.744	0.010	0.067	0.059	0.385	0.069	0.453	0.000	0.000
93	1	0.691	0.106	0.834	0.133	1.050	0.239	1.884	0.039	0.308
93	2	0.711	0.014	0.106	0.051	0.378	0.066	0.484	0.003	0.025
93	3	0.770	0.004	0.022	0.035	0.205	0.039	0.227	0.000	0.000
93	4	0.628	0.001	0.013	0.022	0.206	0.023	0.218	0.000	0.000
105	1	0.795	0.083	0.432	0.139	0.728	0.222	1.161	0.040	0.211
105	2	0.683	0.013	0.102	0.051	0.409	0.063	0.511	0.002	0.013
105	3	0.825	0.005	0.024	0.033	0.147	0.038	0.171	0.001	0.003
105	4	0.660	0.001	0.012	0.023	0.197	0.024	0.208	0.000	0.000
105	5	0.693	0.001	0.005	0.007	0.052	0.007	0.058	0.000	0.000
115	1	0.757	0.337	2.092	0.212	1.317	0.550	3.409	0.120	0.742
115	2	0.758	0.042	0.260	0.110	0.678	0.152	0.938	0.016	0.101
115	3	0.850	0.011	0.041	0.068	0.259	0.078	0.300	0.001	0.005
115	4	0.763	0.007	0.040	0.036	0.218	0.043	0.258	0.001	0.008
115	5	0.778	0.004	0.025	0.028	0.157	0.032	0.182	0.001	0.004
122	1	0.531	0.127	1.514	0.067	0.801	0.194	2.315	0.045	0.542
122	2	0.618	0.039	0.380	0.038	0.374	0.077	0.754	0.014	0.133
122	3	0.553	0.015	0.171	0.015	0.175	0.030	0.346	0.004	0.046
122	4	0.530	0.002	0.024	0.006	0.076	0.008	0.100	0.000	0.000
122	5	0.478	0.000	0.000	0.002	0.027	0.002	0.027	0.000	0.000
125	1	0.767	0.126	0.750	0.107	0.637	0.233	1.387	0.043	0.258
125	2	0.715	0.026	0.187	0.048	0.351	0.074	0.538	0.003	0.019
125	3	0.648	0.005	0.048	0.030	0.267	0.035	0.315	0.001	0.006
125	4	0.668	0.018	0.155	0.026	0.220	0.044	0.376	0.004	0.034
125	5	0.680	0.001	0.011	0.011	0.087	0.012	0.098	0.000	0.000
139	1	0.763	0.080	0.484	0.118	0.716	0.198	1.199	0.018	0.109
139	2	0.825	0.040	0.179	0.083	0.369	0.123	0.547	0.007	0.031
139	3	0.733	0.010	0.068	0.044	0.300	0.054	0.368	0.001	0.009
139	4	0.715	0.005	0.036	0.044	0.317	0.049	0.354	0.001	0.007
139	5	0.663	0.002	0.017	0.021	0.184	0.023	0.201	0.000	0.000
154	1	0.516	0.018	0.218	0.042	0.519	0.060	0.737	0.004	0.049
154	2	0.617	0.001	0.013	0.013	0.127	0.014	0.140	0.000	0.000
154	3	0.610	0.001	0.010	0.006	0.060	0.007	0.070	0.000	0.000
154	4	0.460	0.001	0.018	0.006	0.087	0.008	0.106	0.000	0.000
154	5	0.575	0.002	0.018	0.010	0.105	0.011	0.123	0.001	0.007

TABLE A.3: **List of macrofauna taxa on the NEG shelf sampled during PS109.** Count (upper number) and weight (lower number) are given with their standard deviation for each taxon from 3 replicates at each station.

Phylum	Taxon	19-4	36-2	45-4	76-2	69-1	84-1	68-1	85-1	93-2	105-1	115-2	107-1	122-1 129-1	125-2	139-3	139-2	154-1
Annelida	*Aglaophamus malmgreni*	0±0 0±0	0±0 0±0	0±0 0±0	0±0 0±0	0±0 0±0	0±0 0±0	0±0 0±0	0±0 0±0	0±0 0±0	0±0 0±0	0±0 0±0	0.33±0.58 70.18±121.56	0±0 0±0	0±0 0±0	0±0 0±0	0±0 0±0	0±0 0±0
Annelida	*Amage auricula*	0±0 0±0	0±0 0±0	0±0 0±0	0±0 0±0	0±0 0±0	0.33±0.58 2.02±3.49	0±0 0±0	0±0 0±0	0±0 0±0	0±0 0±0	0±0 0±0	0±0 0±0	0±0 0±0	0±0 0±0	0±0 0±0	0±0 0±0	0±0 0±0
Annelida	*Melinnopsis sp.*	0±0 0±0	0±0 0±0	0±0 0±0	1.67±1.53 1.79±1.7	0±0 0±0	0±0 0±0	0±0 0±0	0±0 0±0	1.67±1.53 2.86±3.16	0±0 0±0	0±0 0±0	0±0 0±0	0±0 0±0	0.33±0.58 2.4±4.16	0.33±0.58 0.29±0.5	0±0 0±0	0±0 0±0
Annelida	Ampharetidae II	0±0 0±0	0±0 0±0	0±0 0±0	0.33±0.58 0.94±1.63	0±0 0±0	0±0 0±0	0±0 0±0	0±0 0±0	0±0 0±0	0±0 0±0	0±0 0±0	0±0 0±0	0±0 0±0	0.67±1.15 2.49±4.32	0.33±0.58 1.35±2.33	0±0 0±0	0±0 0±0
Annelida	Ampharetidae III	0±0 0±0	0.33±0.58 0.86±1.48	0±0 0±0	0.33±0.58 0.38±0.67	0±0 0±0	0±0 0±0	0±0 0±0	0±0 0±0	0.33±0.58 3.55±6.16	0±0 0±0	0±0 0±0	0±0 0±0	0±0 0±0	0±0 0±0	0±0 0±0	0±0 0±0	0±0 0±0
Annelida	Ampharetidae IV	0±0 0±0	0±0 0±0	0±0 0±0	0±0 0±0	0±0 0±0	0±0 0±0	0.33±0.58 0.38±0.66	0±0 0±0	0.33±0.58 0.04±0.08	0±0 0±0	0±0 0±0	0±0 0±0	0±0 0±0	0±0 0±0	0±0 0±0	0±0 0±0	0±0 0±0
Annelida	Ampharetidae V	0±0 0±0	0±0 0±0	0±0 0±0	0.67±1.15 0.02±0.03	0±0 0±0	0±0 0±0	0±0 0±0	0±0 0±0	0±0 0±0	0±0 0±0	0±0 0±0	0±0 0±0	0.33±0.82 0.44±1.08	0±0 0±0	0±0 0±0	0.67±1.15 0.1±0.17	0±0 0±0
Annelida	Ampharetidae VI	0±0 0±0	0±0 0±0	0±0 0±0	0±0 0±0	0±0 0±0	0±0 0±0	0.67±1.15 2.25±3.89	0±0 0±0	0±0 0±0	0.33±0.58 1.16±2.01	0±0 0±0	0±0 0±0	0±0 0±0	0±0 0±0	0±0 0±0	0±0 0±0	0±0 0±0
Annelida	Ampharetidae VII	0±0 0±0	1±1 0.25±0.26	0±0 0±0	2.67±3.06 0.57±0.8	0±0 0±0	0.67±1.15 0.14±0.25	0±0 0±0	0±0 0±0	0.67±0.58 1.22±1.29	0±0 0±0	0±0 0±0	0±0 0±0	0±0 0±0	0±0 0±0	0±0 0±0	0±0 0±0	0.33±0.58 0.03±0.05
Annelida	Ampharetidae?	0±0 0±0	0±0 0±0	0.25±0.5 1.34±2.68	0±0 0±0	0±0 0±0	0±0 0±0	0±0 0±0	0±0 0±0	0±0 0±0	0±0 0±0	0±0 0±0	0±0 0±0	0±0 0±0	0±0 0±0	0±0 0±0	0±0 0±0	0±0 0±0
Annelida	*Amphicteis gunneri*	0.33±0.58 14.23±24.65	0±0 0±0	0±0 0±0	0±0 0±0	0±0 0±0	0±0 0±0	0±0 0±0	0±0 0±0	0±0 0±0	0±0 0±0	0±0 0±0	0±0 0±0	0±0 0±0	0±0 0±0	0±0 0±0	0±0 0±0	0±0 0±0
Annelida	*Aricidea sp.*	0±0 0±0	0.33±0.58 0.31±0.53	0.25±0.5 0.1±0.2	0±0 0±0	0.33±0.58 0.69±1.2	0±0 0±0	0±0 0±0	0±0 0±0	0±0 0±0	0±0 0±0	0±0 0±0	0±0 0±0	0.17±0.41 0.18±0.44	0±0 0±0	0±0 0±0	0±0 0±0	0±0 0±0
Annelida	*Brada villosa*	0±0 0±0	0.33±0.58 0.38±0.65	0.25±0.5 0.08±0.15	0±0 0±0	0±0 0±0	0±0 0±0	0±0 0±0	0±0 0±0	0±0 0±0	0±0 0±0	0±0 0±0	0±0 0±0	0±0 0±0	0±0 0±0	0±0 0±0	0±0 0±0	0±0 0±0
Annelida	*Capitella sp.*	0±0 0±0	0±0 0±0	0±0 0±0	0±0 0±0	0±0 0±0	0±0 0±0	0±0 0±0	0±0 0±0	0±0 0±0	0±0 0±0	0±0 0±0	0.67±0.58 2.39±2.25	0±0 0±0	0±0 0±0	0±0 0±0	0±0 0±0	0±0 0±0
Annelida	*Chaetozone jubata*	0±0 0±0	0±0 0±0	0.5±0.58 0.2±0.23	0±0 0±0	0±0 0±0	0±0 0±0	0±0 0±0	0±0 0±0	0±0 0±0	0±0 0±0	0±0 0±0	0±0 0±0	0.17±0.41 0.08±0.2	0±0 0±0	0±0 0±0	0.33±0.58 0.18±0.32	0±0 0±0
Annelida	*Chaetozone setosa*	0±0 0±0	0±0 0±0	0±0 0±0	0±0 0±0	0±0 0±0	0±0 0±0	0±0 0±0	0±0 0±0	0±0 0±0	0±0 0±0	0±0 0±0	0±0 0±0	0.17±0.41 4.92±12.04	0±0 0±0	0±0 0±0	0±0 0±0	0±0 0±0
Annelida	Chrysopetalidae?	0±0 0±0	0±0 0±0	0±0 0±0	0±0 0±0	0±0 0±0	0±0 0±0	0±0 0±0	0±0 0±0	0±0 0±0	0±0 0±0	0±0 0±0	0±0 0±0	0±0 0±0	0±0 0±0	0.33±0.58 4.36±7.55	0±0 0±0	0±0 0±0
Annelida	Cirratulidae I	0±0 0±0	0±0 0±0	0±0 0±0	0±0 0±0	0±0 0±0	0±0 0±0	0±0 0±0	0±0 0±0	0±0 0±0	0±0 0±0	0±0 0±0	0±0 0±0	0.17±0.41 0.35±0.87	0±0 0±0	0±0 0±0	0±0 0±0	0±0 0±0
Annelida	*Diplocirrus glaucus*	0±0 0±0	0±0 0±0	0±0 0±0	0±0 0±0	0±0 0±0	0±0 0±0	0±0 0±0	0±0 0±0	0±0 0±0	0±0 0±0	0±0 0±0	0±0 0±0	0±0 0±0	0±0 0±0	0±0 0±0	0.67±1.15 12.28±21.27	0±0 0±0
Annelida	Dorvilleidae I	0±0 0±0	0±0 0±0	0±0 0±0	0±0 0±0	0.67±1.15 0.77±1.33	0±0 0±0	0±0 0±0	0±0 0±0	0±0 0±0	0±0 0±0	0±0 0±0	0±0 0±0	0.17±0.41 0±0.01	0±0 0±0	0±0 0±0	0±0 0±0	0±0 0±0
Annelida	*Echiurus echiurus* juv.	0±0 0±0	3.33±5.77 0.24±0.41	0±0 0±0	0±0 0±0	0±0 0±0	0±0 0±0	0±0 0±0	0±0 0±0	0±0 0±0	0±0 0±0	0±0 0±0	0±0 0±0	0±0 0±0	0±0 0±0	0±0 0±0	0±0 0±0	0±0 0±0
Annelida	Eusyllidae? I	0±0 0±0	0.33±0.58 0.04±0.07	0±0 0±0	0±0 0±0	0±0 0±0	0.67±0.58 0.06±0.07	0±0 0±0	0±0 0±0	0.33±0.58 0.11±0.19	0±0 0±0	0±0 0±0	0±0 0±0	0±0 0±0	0±0 0±0	0±0 0±0	0±0 0±0	0±0 0±0
Annelida	Flabelligeridae I	0.33±0.58 0±0	0.33±0.58 0.11±0.19	0±0 0±0	0±0 0±0	0±0 0±0	0±0 0±0	0±0 0±0	0±0 0±0	0±0 0±0	0±0 0±0	0±0 0±0	0±0 0±0	0±0 0±0	0±0 0±0	0.33±0.58 0.4±0.69	0±0 0±0	0±0 0±0
Annelida	*Galathoweina cf. oculata*	0±0 0±0	0±0 0±0	0±0 0±0	0±0 0±0	0±0 0±0	0±0 0±0	0±0 0±0	0±0 0±0	0±0 0±0	0±0 0±0	0±0 0±0	0±0 0±0	0±0 0±0	0±0 0±0	1.33±1.15 16.82±15.58	0±0 0±0	0±0 0±0
Annelida	*Galathowenia fragilis*	0±0 0±0	0.33±0.58 0.64±1.12	0.25±0.5 0.06±0.11	0±0 0±0	0±0 0±0	0±0 0±0	0±0 0±0	0±0 0±0	0±0 0±0	0±0 0±0	0±0 0±0	0±0 0±0	0.5±0.84 0.07±0.15	0.67±0.58 0.79±0.72	0±0 0±0	0±0 0±0	0±0 0±0
Annelida	*Galathowenia oculata*	0±0 0±0	0±0 0±0	0±0 0±0	0.33±0.58 1.23±2.13	0±0 0±0	0±0 0±0	0.67±1.15 1.09±1.89	0±0 0±0	0±0 0±0	0.33±0.58 0.09±0.16	0±0 0±0	0.33±0.58 0.19±0.32	0.17±0.41 0.01±0.02	0±0 0±0	0±0 0±0	0±0 0±0	1.33±1.15 0.03±0.03
Annelida	*Galathowenia sp.*	0±0 0±0	0±0 0±0	0±0 0±0	0±0 0±0	0±0 0±0	0±0 0±0	0±0 0±0	0±0 0±0	0±0 0±0	0±0 0±0	0±0 0±0	0±0 0±0	0.17±0.41 0.03±0.07	0±0 0±0	0±0 0±0	0±0 0±0	0±0 0±0
Annelida	*Glyphanostosum pallescens*	0±0 0±0	0±0 0±0	0±0 0±0	0±0 0±0	0±0 0±0	0±0 0±0	0±0 0±0	0±0 0±0	0±0 0±0	0±0 0±0	0±0 0±0	0±0 0±0	0±0 0±0	0.67±1.15 0.84±1.46	0±0 0±0	0±0 0±0	0±0 0±0
Annelida	Lumbrineridae I	0±0 0±0	0±0 0±0	0±0 0±0	0±0 0±0	0±0 0±0	0±0 0±0	0±0 0±0	0±0 0±0	0±0 0±0	0±0 0±0	0±0 0±0	0±0 0±0	0±0 0±0	0±0 0±0	0.67±0.58 2.22±2.44	0±0 0±0	0±0 0±0

Table A.3 – continued

Phylum	Taxon	19-4	36-2	45-4	76-2	69-1	84-1	68-1	85-1	93-2	105-1	115-2	107-1	122-1 129-1	125-2	139-3	139-2	154-1
Annelida	Lumbrineris sp.?	0±0 0±0	0±0 0±0	0±0 0±0	0±0 0±0	0±0 0±0	0±0 0±0	0±0 0±0	0±0 0±0	0±0 0±0	0±0 0±0	0±0 0±0	0±0 0±0	0±0 0±0	0.33±0.58 0.98±1.7	0±0 0±0	0±0 0±0	0±0 0±0
Annelida	*Lysippe fragilis*	0±0 0±0	0±0 0±0	0.25±0.5 1.01±2.03	0±0 0±0	0±0 0±0	0±0 0±0	0±0 0±0	0±0 0±0	0±0 0±0	0±0 0±0	0±0 0±0	0±0 0±0	0±0 0±0	0±0 0±0	0±0 0±0	0±0 0±0	0±0 0±0
Annelida	*Lysippe cf. sexcirrata*	0±0 0±0	0±0 0±0	0±0 0±0	0±0 0±0	0±0 0±0	0±0 0±0	0±0 0±0	0±0 0±0	0±0 0±0	0±0 0±0	0±0 0±0	0±0 0±0	0.17±0.41 2.65±6.5	0.33±0.58 0±0	0±0 0±0	0±0 0±0	0±0 0±0
Annelida	*Lysippe sp.*	0±0 0±0	0±0 0±0	0.25±0.5 0.09±0.18	0±0 0±0	0±0 0±0	0±0 0±0	0±0 0±0	0±0 0±0	0±0 0±0	0±0 0±0	0±0 0±0	0±0 0±0	0±0 0±0	0±0 0±0	0±0 0±0	0.33±0.58 0±0	0±0 0±0
Annelida	*Maldane sarsi*	0.67±1.15 2.6±4.5	1±1 57.45±93.22	0±0 0±0	0±0 0±0	0±0 0±0	0±0 0±0	0±0 0±0	0±0 0±0	0±0 0±0	0±0 0±0	0±0 0±0	0±0 0±0	0±0 0±0	0±0 0±0	0±0 0±0	0±0 0±0	0±0 0±0
Annelida	*Maldane sp.*	0.67±1.15 4±6.93	0.33±0.58 2.15±3.72	0±0 0±0	0±0 0±0	0±0 0±0	0±0 0±0	0±0 0±0	0±0 0±0	0±0 0±0	0±0 0±0	0±0 0±0	0±0 0±0	0±0 0±0	0±0 0±0	0±0 0±0	0±0 0±0	0±0 0±0
Annelida	Maldanidae	0.33±0.58 2.94±5.09	0±0 0.27±0.47	0±0 0±0	0±0 0±0	0±0 0±0	0±0 0±0	0±0 0±0	0±0 0±0	0±0 0±0	0±0 0±0	0±0 0±0	0±0 0±0	0.83±1.6 0.1±0.2	4.67±1.15 6.72±4.88	0.33±0.58 1.55±2.68	0.33±0.58 0.26±0.44	0±0 0±0
Annelida	Maldanidae I	0.33±0.58 1.57±2.71	0±0 0±0	0±0 0±0	0±0 0±0	0±0 0±0	0±0 0±0	0±0 0±0	0±0 0±0	0±0 0±0	0±0 0±0	0±0 0±0	0±0 0±0	0±0 0±0	0±0 0±0	0±0 0±0	0±0 0±0	0±0 0±0
Annelida	*Mediomastus sp.*	0±0 0±0	0±0 0±0	0±0 0±0	0±0 0±0	0±0 0±0	0±0 0±0	0±0 0±0	0±0 0±0	0±0 0±0	0±0 0±0	0±0 0±0	0±0 0±0	0.17±0.41 0.47±1.15	0±0 0±0	0±0 0±0	0.33±0.58 1.36±2.35	0±0 0±0
Annelida	*Myriochele heeri*	0±0 0±0	0±0 0±0	0±0 0±0	0±0 0±0	0±0 0±0	0±0 0±0	0±0 0±0	0±0 0±0	0±0 0±0	0±0 0±0	0±0 0±0	0.33±0.58 0.22±0.39	0±0 0±0	0.33±0.58 0.1±0.17	0±0 0±0	0±0 0±0	0±0 0±0
Annelida	*Nephtys sp.*	0.67±0.58 23.35±34.73	0.67±0.58 0.6±0.73	0±0 0±0	0±0 0±0	0±0 0±0	0.33±0.58 0.29±0.51	0±0 0±0	0±0 0±0	0±0 0±0	0±0 0±0	0±0 0±0	0±0 0±0	0±0 0±0	0±0 0±0	0.33±0.58 0.02±0.04	0±0 0±0	0±0 0±0
Annelida	*Nicomache personata*	0±0 0±0	0±0 0±0	0±0 0±0	0±0 0±0	0±0 0±0	0±0 0±0	0±0 0±0	0±0 0±0	0±0 0±0	0±0 0±0	0±0 0±0	0±0 0±0	0±0 0±0	0±0 0±0	0.33±0.58 1.22±2.12	0±0 0±0	0±0 0±0
Annelida	*Nothria conchylega*	0±0 0±0	0±0 0±0	0±0 0±0	0±0 0±0	0±0 0±0	0±0 0±0	0±0 0±0	0±0 0±0	0±0 0±0	0±0 0±0	0±0 0±0	0±0 0±0	4±3.29 125.83±154.4	0±0 0±0	0±0 0±0	0±0 0±0	0±0 0±0
Annelida	*Owenia fusiformis*	0±0 0±0	0±0 0±0	0±0 0±0	0±0 0±0	0±0 0±0	0±0 0±0	0±0 0±0	0±0 0±0	0±0 0±0	0±0 0±0	0±0 0±0	0±0 0±0	0±0 0±0	0±0 0±0	0±0 0±0	0±0 0±0	1.33±1.53 0.24±0.31
Annelida	Oweniidae	0±0 0±0	0±0 0±0	0±0 0±0	0±0 0±0	0±0 0±0	0±0 0±0	0±0 0±0	0±0 0±0	0±0 0±0	0±0 0±0	0±0 0±0	0±0 0±0	0±0 0±0	0.33±0.58 0.3±0.51	0±0 0±0	0±0 0±0	0±0 0±0
Annelida	Oweniidae I	0.67±1.15 0.33±0.58	0±0 0±0	1±2 0.11±0.23	0±0 0±0	0±0 0±0	0±0 0±0	0±0 0±0	0±0 0±0	0±0 0±0	0±0 0±0	0±0 0±0	0±0 0±0	0±0 0±0	0±0 0±0	0±0 0±0	0±0 0±0	0±0 0±0
Annelida	*Parougia sp.*	0±0 0±0	0±0 0±0	0±0 0±0	0±0 0±0	0±0 0±0	0±0 0±0	0±0 0±0	0±0 0±0	0±0 0±0	0±0 0±0	0±0 0±0	0±0 0±0	0±0 0±0	0.33±0.58 2.52±4.36	0±0 0±0	0±0 0±0	0±0 0±0
Annelida	*Pholoe sp.*	0±0 0±0	0±0 0±0	0.25±0.5 0.07±0.13	0±0 0±0	0±0 0±0	0±0 0±0	0±0 0±0	0±0 0±0	0±0 0±0	0±0 0±0	0±0 0±0	0±0 0±0	1.5±1.05 0.49±0.36	0±0 0±0	0±0 0±0	0±0 0±0	0±0 0±0
Annelida	*Praxillura longissima*	0±0 0±0	0.33±0.58 10.3±17.84	0±0 0±0	0±0 0±0	0±0 0±0	0±0 0±0	0±0 0±0	0±0 0±0	0±0 0±0	0±0 0±0	0±0 0±0	0±0 0±0	0±0 0±0	0±0 0±0	0±0 0±0	0±0 0±0	0±0 0±0
Annelida	Sabellidae I	0±0 0±0	0±0 0±0	0±0 0±0	0±0 0±0	0±0 0±0	0±0 0±0	0±0 0±0	0±0 0±0	0±0 0±0	0±0 0±0	0±0 0±0	0±0 0±0	0±0 0±0	0.33±0.58 0.03±0.06	0±0 0±0	0±0 0±0	0±0 0±0
Annelida	Sabellidae II	0±0 0±0	0±0 0±0	0±0 0±0	0±0 0±0	0±0 0±0	0±0 0±0	0±0 0±0	0±0 0±0	0.33±0.58 3.52±6.1	0±0 0±0	0±0 0±0	0±0 0±0	0±0 0±0	0±0 0±0	0±0 0±0	0±0 0±0	0±0 0±0
Annelida	Serpulidae	0±0 0±0	0±0 0±0	0±0 0±0	0.33±0.58 0±0	0±0 0±0	0±0 0±0	0±0 0±0	0±0 0±0	0.33±0.58 0.4±0.7	0±0 0±0	0±0 0±0	0±0 0±0	0.17±0.41 0.13±0.31	0±0 0±0	0±0 0±0	0±0 0±0	0±0 0±0
Annelida	Serpulidae II	0±0 0±0	0±0 0±0	0±0 0±0	0±0 0±0	0±0 0±0	0±0 0±0	0±0 0±0	0±0 0±0	0±0 0±0	0±0 0±0	0±0 0±0	0±0 0±0	0.17±0.41 0.3±0.74	0±0 0±0	0±0 0±0	0±0 0±0	0±0 0±0
Annelida	Serpulidae? I	0±0 0±0	0±0 0±0	0±0 0±0	0±0 0±0	0±0 0±0	0±0 0±0	0±0 0±0	0±0 0±0	0±0 0±0	0±0 0±0	0±0 0±0	0.33±0.58 0.11±0.19	0±0 0±0	0±0 0±0	0±0 0±0	0±0 0±0	0±0 0±0
Annelida	*Sphaerodinium spp.*	0±0 0±0	0.33±0.58 0.19±0.33	0±0 0±0	0±0 0±0	0±0 0±0	0±0 0±0	0±0 0±0	0±0 0±0	0±0 0±0	0±0 0±0	0±0 0±0	0±0 0±0	0±0 0±0	0±0 0±0	0±0 0±0	0±0 0±0	0±0 0±0
Annelida	*Sphaerodoropsis phillipi*	0±0 0±0	0±0 0±0	0.25±0.5 0.1±0.19	0±0 0±0	0±0 0±0	0±0 0±0	0±0 0±0	0±0 0±0	0±0 0±0	0±0 0±0	0±0 0±0	0±0 0±0	0±0 0±0	0±0 0±0	0±0 0±0	0±0 0±0	0±0 0±0
Annelida	Syllidae I	0±0 0±0	0±0 0±0	0.25±0.5 0.13±0.26	0±0 0±0	0±0 0±0	0±0 0±0	0±0 0±0	0±0 0±0	0±0 0±0	0±0 0±0	0±0 0±0	0±0 0±0	0±0 0±0	0±0 0±0	0±0 0±0	0±0 0±0	0±0 0±0
Annelida	*Syllis gracilis*	0±0 0±0	0±0 0±0	0.75±0.96 0.14±0.19	0±0 0±0	0±0 0±0	0±0 0±0	0±0 0±0	0±0 0±0	0±0 0±0	0±0 0±0	0±0 0±0	0±0 0±0	0±0 0±0	0±0 0±0	0±0 0±0	0±0 0±0	0±0 0±0
Annelida	Polychaeta bodies	0±0 0±0	0±0 1.25±2.01	0±0 1.01±1.19	0±0 0±0	0±0 0.15±0.27	0±0 0.05±0.09	0±0 0±0	0±0 0±0	0±0 0±0	0±0 0±0	0±0 0±0	0±0 0±0	0±0 0.49±0.97	0±0 2.24±1.86	0±0 1.97±3.42	0±0 0.82±1.41	0±0 0±0
Annelida	Polychaeta indef II	0±0 0±0	0±0 0±0	0±0 0±0	0±0 0±0	0±0 0±0	0±0 0±0	0±0 0±0	0±0 0±0	0±0 0±0	0±0 0±0	0±0 0±0	0±0 0±0	0±0 0±0	0.33±0.58 0±0	0±0 0±0	0±0 0±0	0±0 0±0

Table A.3 – continued

Phylum	Taxon	19-4	36-2	45-4	76-2	69-1	84-1	68-1	85-1	93-2	105-1	115-2	107-1	122-1	125-2	139-3	139-2	154-1
														129-1				
Annelida	Polychaeta indef III	0±0	0±0	0±0	0±0	0±0	0±0	0.33±0.58	0±0	0±0	0±0	0±0	0±0	0±0	0±0	0±0	0±0	0±0
		0±0	0±0	0±0	0±0	0±0	0±0	6.39±11.07	0±0	0±0	0±0	0±0	0±0	0±0	0±0	0±0	0±0	0±0
Annelida	Polychaeta indef IV	0±0	0±0	0.25±0.5	0±0	0±0	0±0	0±0	0±0	0±0	0±0	0±0	0±0	0±0	0±0	0±0	0±0	0±0
		0±0	0±0	0.02±0.03	0±0	0±0	0±0	0±0	0±0	0±0	0±0	0±0	0±0	0±0	0±0	0±0	0±0	0±0
Annelida	Polychaeta indef V	0±0	0±0	0±0	0±0	0±0	0.33±0.58	0±0	0±0	0±0	0±0	0±0	0±0	0±0	0±0	0±0	0±0	0±0
		0±0	0±0	0±0	0±0	0±0	0.64±1.1	0±0	0±0	0±0	0±0	0±0	0±0	0±0	0±0	0±0	0±0	0±0
Annelida	Polychaeta indef VI	0±0	0±0	0.25±0.5	0±0	0±0	0±0	0±0	0±0	0±0	0±0	0±0	0±0	0±0	0±0	0±0	0±0	0±0
		0±0	0±0	1.11±2.21	0±0	0±0	0±0	0±0	0±0	0±0	0±0	0±0	0±0	0±0	0±0	0±0	0±0	0±0
Annelida	Polychaeta indef VII	0±0	0.33±0.58	0±0	0±0	0±0	0±0	0±0	0±0	0±0	0±0	0±0	0±0	0.17±0.41	0±0	0±0	0±0	0±0
		0±0	0.12±0.2	0±0	0±0	0±0	0±0	0±0	0±0	0±0	0±0	0±0	0±0	0.05±0.13	0±0	0±0	0±0	0±0
Bryozoa	Bryozoa I	0±0	0±0	0±0	0±0	0±0	0±0	0±0	0±0	0±0	0±0	0±0	0±0	0±0	0±0	0±0	0±0	0±0
		0±0	0±0	0±0	0±0	0±0	0±0	0±0	0±0	1.17±2.02	0±0	0±0	0±0	0±0	0±0	0±0	0±0	0±0
Bryozoa	*Crisia sp.*	0±0	0±0	0±0	0±0	0±0	0±0	0±0	0±0	0±0	0±0	0±0	0±0	0±0	0±NA	0±0	0±0	0±0
		0±0	0±0	0.92±1.84	0±0	0±0	0±0	0±0	0±0	0±0	0±0	0±0	18.03±31.23	0±0	0.98±1.7	5.34±9.25	0±0	0±0
Bryozoa	*Escharella sp.*	0±0	0±0	0±0	0±0	0±0	0±0	0±0	0±0	0±0	0±0	0±0	0±0	0±0	0±0	0±0	0±0	0±0
		0±0	0±0	0±0	0±0	0±0	0±0	0±0	0±0	0±0	0±0	0±0	0±0	0±0	0±0	0±0	0±0	0±0
Bryozoa	*Hornera sp.*	0±0	0±0	0±0	0±0	0±0	0±0	0±0	0±0	0±0	0±0	0±0	0±0	0±0	0±0	0±0	0±0	0±0
		0±0	0±0	0±0	0±0	0±0	0±0	0±0	0±0	0±0	0±0	0±0	0±0	0.83±2.04	0±0	0±0	0±0	0±0
Bryozoa	*Membranipora sp.*	0±0	0±0	0±0	0±0	0±0	0±0	0±0	0±0	0±0	0±0	0±0	0±0	0±0	0±0	0±0	0±0	0±0
		0±0	0±0	0±0	0±0	0±0	0±0	0±0	0±0	2.34±4.05	0±0	0±0	0±0	0±0	0±0	0±0	0±0	0±0
Bryozoa	*Pseudoflustra sinuosa*	0±0	0±0	0±0	0±0	0±0	0±0	0±0	0±0	0±0	0±0	0±0	0±0	0±0	0±0	0±0	0±0	0±0
		0±0	0±0	0±0	0±0	0±0	0±0	0±0	0±0	0±0	0±0	0±0	0±0	0±0	0±0	55.23±95.67	0±0	0±0
Bryozoa	*Sarsiflustra abissycola*	0±0	0±0	0±0	0±0	0±0	0±0	0±0	0±0	0±0	0±0	0±0	0±0	0±0	0±0	0±0	0±0	0±0
		0±0	0±0	70.46±89.93	0±0	0±0	0±0	0±0	0±0	0±0	0±0	0±0	0±0	0±0	5.82±10.08	0±0	0±0	0±0
Bryozoa	*Tricellaria cf. gracilis*	0±0	0±0	0±0	0±0	0±0	0±0	0±0	0.33±0.58	0±0	0±0	0±0	0±0	0±0	0±0	0±0	0±0	0±0
		0±0	0±0	0±0	0±0	0±0	0±0	0±0	0.38±0.65	0±0	0±0	0±0	0±0	0±0	0±0	0±0	0±0	0±0
Cephalorhyncha	Priapulida	0±0	0±0	0±0	0±0	0±0	0±0	0±0	0±0	0±0	0±0	0±0	0±0	0±0	0±0	0±0	0±0	0±0
		0±0	0±0	0±0	0±0	0±0	0±0	0±0	0±0	0±0	0±0	0±0	0±0	0±0	0±0	0±0	0±0	0±0
Cephalorhyncha	*Priapulus bicaudatus*	0±0	0.33±0.58	0±0	0±0	0±0	0±0	0±0	0±0	0±0	0±0	0±0	0±0	0±0	0±0	0±0	0±0	0±0
		0±0	948.7±1643.2	0±0	0±0	0±0	0±0	0±0	0±0	0±0	0±0	0±0	0±0	0±0	0±0	0±0	0±0	0±0
Cephalorhyncha	*Priapulus caudatus*	0.67±1.15	0±0	0±0	0±0	0±0	0±0	0±0	0±0	0±0	0±0	0±0	0±0	0±0	0±0	0±0	0±0	0±0
		0±0	0±0	0±0	0±0	0±0	0±0	0±0	0±0	0±0	0±0	0±0	0±0	0±0	0±0	0±0	0±0	0±0
Chordata	*Ascidia sp.*	0±0	0±0	0±0	0±0	0±0	0±0	0±0	0±0	0±0	0±0	0±0	0±0	0±0	0±0	0±0	0±0	0.33±0.58
		0±0	0±0	0±0	0±0	0±0	0±0	0±0	0±0	0±0	0±0	0±0	0±0	0±0	0±0	0±0	0±0	5.66±9.81
Chordata	Ascidiacea juv.	0±0	0±0	0±0	0±0	0±0	0±0	0±0	0±0	0±0	0±0	0±0	0±0	0.17±0.41	0±0	0±0	0±0	0±0
		0±0	0±0	0±0	0±0	0±0	0±0	0±0	0±0	0±0	0±0	0±0	0±0	0.02±0.05	0±0	0±0	0±0	0±0
Chordata	Ascidiacea juv. II	0±0	0.33±0.58	0±0	0±0	0±0	0±0	0±0	0±0	0±0	0±0	0±0	0±0	0±0	0±0	0±0	0±0	0±0
		0±0	0.38±0.65	0±0	0±0	0±0	0±0	0±0	0±0	0±0	0±0	0±0	0±0	0±0	0±0	0±0	0±0	0±0
Chordata	*Boltenia ovifera?*	0±0	0±0	0±0	0±0	0±0	0±0	0±0	0±0	2.67±0.58	1±1.73	0.67±0.58	0.67±1.15	0±0	5.33±2.52	1±0	0.33±0.58	0±0
		0±0	0±0	0±0	0±0	0±0	0±0	0±0	0±0	3.89±2.27	1.32±2.29	0.6±0.97	1.09±1.88	0±0	3.3±4.08	3.02±3.77	0.92±1.6	0±0
Chordata	*Kukenthalia borealis?*	0±0	0±0	0.25±0.5	0±0	0±0	0±0	0±0	0±0	0±0	0±0	0±0	0±0	0±0	0±0	0±0	0±0	0±0
		0±0	0±0	0.05±0.1	0±0	0±0	0±0	0±0	0±0	0±0	0±0	0±0	0±0	0±0	0±0	0±0	0±0	0±0
Chordata	*Molgula occulata*	0±0	0±0	0.5±0.58	0±0	0±0	0±0	0±0	0±0	0±0	0±0	0±0	0±0	0.33±0.52	0±0	0±0	0±0	0±0
		0±0	0±0	16.84±30.38	0±0	0±0	0±0	0±0	0±0	0±0	0±0	0±0	0±0	1.28±3	0±0	0±0	0±0	0±0
Chordata		0±0	0.33±0.58	0±0	0±0	0±0	0±0	0±0	0±0	0±0	0±0	0±0	0±0	0±0	0±0	0±0	0±0	0±0
		0±0	0.11±0.19	0±0	0±0	0±0	0±0	0±0	0±0	0±0	0±0	0±0	0±0	0±0	0±0	0±0	0±0	0±0
Cnidaria	Actiniaria	0±0	0±0	0±0	0±0	0±0	0±0	0±0	0±0	0±0	0±0	0±0	0±0	0±0	0±0	0.33±0.58	0±0	0±0
		0±0	0±0	0±0	0±0	0±0	0±0	0±0	0±0	0±0	0±0	0±0	0±0	0±0	0±0	68.7±118.99	0±0	0±0
Cnidaria	Actiniaria II	0±0	0±0	0±0	0±0	0±0	0.33±0.58	0±0	0±0	0±0	0±0	0±0	0±0	0±0	0±0	0±0	0±0	0±0
		0±0	0±0	0±0	0±0	0±0	0.09±0.15	0±0	0±0	0±0	0±0	0±0	0±0	0±0	0±0	0±0	0±0	0±0
Cnidaria	*Allantactis parasitica*	0±0	0±0	0±0	0±0	0±0	0±0	0±0	0±0	0±0	0±0	0±0	0±0	0±0	0±0	0.33±0.58	0±0	0±0
		0±0	0±0	0±0	0±0	0±0	0±0	0±0	0±0	0±0	0±0	0±0	0±0	0±0	0±0	1006.13±1742.67	0±0	0±0
Cnidaria	Campanulariidae	0±0	0±0	0±0	0±0	0±0	0±0	0±0	0±0	0±0	0±0	0±0	0±0	0±0	0±0	0±0	0±0	0±0
		0±0	0±0	0±0	0±0	0±0	0±0	0±0	0±0	0±0	0±0	0±0	0±0	0±0	0±0	13.67±23.67	0±0	0±0
Cnidaria	Cnidaria	0±0	0±0	0±0	0±0	0±0	0±0	0±0	0±0	0±0	0±0	0±0	0.33±0.58	0±0	0±0	0±0	0±0	0±0
		0±0	0±0	0±0	0±0	0±0	0±0	0±0	0±0	0±0	0±0	0±0	46.23±80.07	0±0	0±0	0±0	0±0	0±0
Cnidaria	Cnidaria II	0±0	0±0	0±0	0.33±0.58	0±0	0±0	0±0	0±0	0±0	0±0	0±0	0±0	0±0	0±0	0±0	0±0	0±0
		0±0	0±0	0±0	1.35±2.33	0±0	0±0	0±0	0±0	0±0	0±0	0±0	0±0	0±0	0±0	0±0	0±0	0±0
Cnidaria	*Desmophyllum sp.?*	0±0	0±0	0±0	0±0	0±0	0±0	0±0	0±0	0±0	0±0	0±0	0±0	0±0	0±0	0±0	0±0	0±0
		0±0	0±0	0±0	0±0	0±0	0±0	0±0	0±0	0±0	0±0	0±0	0±0	0±0	0±0	0±0	0±0	491.7±851.65
Cnidaria	*Funicula quadrangularis*	0±0	0±0	0±0	0±0	0±0	0±0	0±0	0±0	0±0	0±0	0±0	0±0	0±0	0±0	0.33±0.58	0±0	0±0
		0±0	0±0	0±0	0±0	0±0	0±0	0±0	0±0	0±0	0±0	0±0	0±0	0±0	0±0	55.9±96.82	0±0	0±0

Table A.3 – continued

Phylum	Taxon	19-4	36-2	45-4	76-2	69-1	84-1	68-1	85-1	93-2	105-1	115-2	107-1	122-1 129-1	125-2	139-3	139-2	154-1
Cnidaria	Hydrozoa	0±0 0±0	0±0 0±0	0±0 0±0	0±0 0±0	0±0 0±0	0±0 0±0	0±0 0±0	0±0 0±0	0±0 0±0	0±0 0±0	0±0 0±0	0±0 0±0	0±0 27.77±68.01	0±0 0±0	0±0 0±0	0±0 0±0	0±0 0±0
Cnidaria	*Sertularella polyzonias*	0±0 0±0	0±0 0±0	0±0 0±0	0±0 0±0	0±0 0±0	0±0 0±0	0±0 0±0	0±0 0±0	0±0 0±0	0±0 0±0	0±0 0±0	0±0 0±0	0±0 0±0	0±0 0±0	0±0 0±0	0±0 0±0	0±0 0.54±0.94
Cnidaria	*Umbellula sp.*	0±0 0±0	0±0 0±0	0±0 0±0	0±0 0±0	0.33±0.58 150.53±260.73	0±0 0±0	0±0 0±0	0±0 0±0	0±0 0±0	0±0 0±0	0±0 0±0	0±0 0±0	0±0 0±0	0±0 0±0	0±0 0±0	0±0 0±0	0±0 0±0
Crustacea	*Akanthophoreus gracilis*	0±0 0±0	0±0 0±0	0±0 0±0	0±0 0±0	0±0 0±0	0±0 0±0	0±0 0±0	0±0 0±0	0±0 0±0	0±0 0±0	0±0 0±0	0±0 0±0	0±0 0±0	0.33±0.58 0.03±0.05	0±0 0±0	0±0 0±0	0±0 0±0
Crustacea	Amphipoda	0±0 0±0	0±0 0±0	0±0 0±0	0±0 0±0	0±0 0±0	0±0 0±0	0±0 0±0	0±0 0±0	0±0 0±0	0±0 0±0	0±0 0±0	0±0 0±0	0.17±0.41 0±0.01	0±0 0±0	0±0 0±0	0±0 0±0	0±0 0±0
Crustacea	*Apseudes talpa*	0±0 0±0	0±0 0±0	0±0 0±0	0±0 0±0	0±0 0±0	0±0 0±0	0±0 0±0	0±0 0±0	0±0 0±0	0±0 0±0	0±0 0±0	0±0 0±0	0±0 0±0	0±0 0±0	0.33±0.58 0.12±0.2	0±0 0±0	0±0 0±0
Crustacea	*Brachydiastylis resima*	1.67±0.58 0.49±0.11	0.67±1.15 0.1±0.17	0.25±0.5 0.05±0.1	0±0 0±0	0±0 0±0	0±0 0±0	0±0 0±0	0±0 0±0	0±0 0±0	0±0 0±0	0±0 0±0	0±0 0±0	0±0 0±0	0±0 0±0	0.33±0.58 0.09±0.15	0±0 0±0	0±0 0±0
Crustacea	*Caecognathia elongata*	0±0 0±0	0±0 0±0	0±0 0±0	0±0 0±0	0±0 0±0	0±0 0±0	0±0 0±0	0±0 0±0	0±0 0±0	0±0 0±0	0±0 0±0	0±0 0±0	0.17±0.41 0.21±0.51	0±0 0±0	0±0 0±0	0±0 0±0	0±0 0±0
Crustacea	*Caecognathia stygia*	0±0 0±0	0±0 0±0	0±0 0±0	0±0 0±0	0±0 0±0	0±0 0±0	0±0 0±0	0±0 0±0	0±0 0±0	0±0 0±0	0±0 0±0	0±0 0±0	0±0 0±0	0.33±0.58 1.89±3.28	0±0 0±0	0±0 0±0	0±0 0±0
Crustacea	*Calathura brachiata*	0.33±0.58 0.35±0.61	1±1 0.93±1.57	0±0 0±0	0±0 0±0	0±0 0±0	0±0 0±0	0.33±0.58 0.84±1.45	0±0 0±0	0±0 0±0	0±0 0±0	0±0 0±0	0±0 0±0	0±0 0±0	0±0 0±0	0.33±0.58 0.01±0.01	0±0 0±0	0±0 0±0
Crustacea	*Campylaspis sp.*	0±0 0±0	0±0 0±0	0.25±0.5 0.05±0.11	0±0 0±0	0±0 0±0	0±0 0±0	0±0 0±0	0±0 0±0	0±0 0±0	0±0 0±0	0±0 0±0	0±0 0±0	0±0 0±0	0±0 0±0	0±0 0±0	0±0 0±0	0±0 0±0
Crustacea	*Cryptocope sp.?*	0±0 0±0	0±0 0±0	0±0 0±0	0±0 0±0	0±0 0±0	0±0 0±0	0±0 0±0	0±0 0±0	0±0 0±0	0±0 0±0	0±0 0±0	0±0 0±0	0±0 0±0	0±0 0±0	0±0 0±0	0±0 0±0	0.33±0.58 0.01±0.02
Crustacea	Desmosomatidae	0±0 0±0	0±0 0±0	0±0 0±0	0±0 0±0	0±0 0±0	0±0 0±0	0.33±0.58 0.17±0.29	0±0 0±0	0±0 0±0	0±0 0±0	0±0 0±0	0±0 0±0	0±0 0±0	0±0 0±0	0±0 0±0	0±0 0±0	0±0 0±0
Crustacea	Desmosomatidae?	0±0 0±0	0±0 0±0	0±0 0±0	0±0 0±0	0±0 0±0	0±0 0±0	0±0 0±0	0±0 0±0	0±0 0±0	0.33±0.58 0.02±0.03	0±0 0±0	0±0 0±0	0±0 0±0	0±0 0±0	0±0 0±0	0±0 0±0	0±0 0±0
Crustacea	*Diastylis lucifera*	0±0 0±0	0±0 0±0	0±0 0±0	0±0 0±0	0±0 0±0	0±0 0±0	0±0 0±0	0±0 0±0	0±0 0±0	0±0 0±0	0±0 0±0	0±0 0±0	0.33±0.52 0.29±0.45	0±0 0±0	0.33±0.58 0.07±0.13	0±0 0±0	0±0 0±0
Crustacea	*Diastylis rathkei*	0±0 0±0	0.33±0.58 2.58±4.47	0±0 0±0	0±0 0±0	0±0 0±0	0±0 0±0	0±0 0±0	0±0 0±0	0±0 0±0	0±0 0±0	0±0 0±0	0±0 0±0	0±0 0±0	0±0 0±0	0.33±0.58 1.01±1.76	0±0 0±0	0±0 0±0
Crustacea	*Diastylis spinulosa*	0±0 0±0	0±0 0±0	0±0 0±0	0±0 0±0	0±0 0±0	0±0 0±0	0±0 0±0	0±0 0±0	0±0 0±0	0±0 0±0	0±0 0±0	0±0 0±0	0.17±0.41 0.19±0.45	0±0 0±0	0±0 0±0	0±0 0±0	0±0 0±0
Crustacea	*Gnathia arctica*	0±0 0±0	0±0 0±0	0.5±1 0.66±1.32	0±0 0±0	0±0 0±0	0±0 0±0	0±0 0±0	0±0 0±0	0±0 0±0	0±0 0±0	0±0 0±0	0±0 0±0	0±0 0±0	0±0 0±0	0±0 0±0	0±0 0±0	0±0 0±0
Crustacea	Gnathia Praniza I	0±0 0±0	0±0 0±0	0.25±0.5 0.17±0.34	0±0 0±0	0±0 0±0	0±0 0±0	0±0 0±0	0±0 0±0	0±0 0±0	0±0 0±0	0±0 0±0	0±0 0±0	0.17±0.41 0.02±0.04	0±0 0±0	0.33±0.58 0.17±0.29	0±0 0±0	0±0 0±0
Crustacea	Gnathia Praniza II	0±0 0±0	0±0 0±0	0±0 0±0	0±0 0±0	0±0 0±0	0±0 0±0	0±0 0±0	0±0 0±0	0±0 0±0	0±0 0±0	0±0 0±0	0±0 0±0	0.17±0.41 0.04±0.09	0±0 0±0	0±0 0±0	0±0 0±0	0±0 0±0
Crustacea	*Haploniscus bicuspis*	0±0 0±0	0±0 0±0	0±0 0±0	0±0 0±0	0±0 0±0	0±0 0±0	0±0 0±0	0±0 0±0	0.33±0.58 0.17±0.29	0±0 0±0	0±0 0±0	0±0 0±0	0±0 0±0	0±0 0±0	0±0 0±0	0±0 0±0	0±0 0±0
Crustacea	*Harpinia mucronata*	0±0 0±0	0±0 0±0	0±0 0±0	0±0 0±0	0±0 0±0	0±0 0±0	0±0 0±0	0±0 0±0	0±0 0±0	0±0 0±0	0±0 0±0	0±0 0±0	0±0 0±0	0±0 0±0	0±0 0±0	0.67±0.58 0.92±1.43	0±0 0±0
Crustacea	*Harpinia propinqua*	0±0 0±0	0±0 0±0	0.25±0.5 0.49±0.99	0±0 0±0	0±0 0±0	0±0 0±0	0±0 0±0	0±0 0±0	0±0 0±0	0±0 0±0	0±0 0±0	0±0 0±0	0±0 0±0	0±0 0±0	0±0 0±0	0±0 0±0	0±0 0±0
Crustacea	*Harpinia sp.*	0±0 0±0	0±0 0±0	0±0 0±0	0±0 0±0	0±0 0±0	0±0 0±0	0±0 0±0	0±0 0±0	0±0 0±0	0±0 0±0	0±0 0±0	0±0 0±0	0±0 0±0	0±0 0±0	0.33±0.58 0.03±0.06	0±0 0±0	0±0 0±0
Crustacea	*Ilyarachna sp.*	1.67±2.08 1.2±1.88	0±0 0±0	0±0 0±0	0.33±0.58 0.08±0.14	0±0 0±0	0±0 0±0	0±0 0±0	0±0 0±0	0±0 0±0	0±0 0±0	0±0 0±0	0±0 0±0	0±0 0±0	0±0 0±0	0±0 0±0	0±0 0±0	0±0 0±0
Crustacea	*Ilyarachna sp. I*	0±0 0±0	0±0 0±0	0.25±0.5 0.49±0.98	0.33±0.58 1.08±1.87	0±0 0±0	0±0 0±0	0.33±0.58 0.22±0.39	0±0 0±0	0±0 0±0	0±0 0±0	0±0 0±0	0±0 0±0	0±0 0±0	0±0 0±0	0±0 0±0	0±0 0±0	0±0 0±0
Crustacea	*Ilyarachna sp. II*	0±0 0±0	0±0 0±0	0±0 0±0	0±0 0±0	0±0 0±0	0±0 0±0	0±0 0±0	0±0 0±0	0.33±0.58 0.81±1.41	0±0 0±0	0±0 0±0	0±0 0±0	0±0 0±0	0±0 0±0	0±0 0±0	0±0 0±0	0±0 0±0
Crustacea	Isopoda indef.	0±0 0±0	0±0 0±0	0±0 0±0	0±0 0±0	0±0 0±0	0±0 0±0	0±0 0±0	0±0 0±0	0±0 0±0	0±0 0±0	0±0 0±0	0±0 0±0	0.17±0.41 0.02±0.05	0±0 0±0	0±0 0±0	0±0 0±0	0±0 0±0
Crustacea	*Leptostylis sp.*	0±0 0±0	0±0 0±0	0.5±0.58 0.19±0.23	0±0 0±0	0±0 0±0	0±0 0±0	0±0 0±0	0±0 0±0	0±0 0±0	0±0 0±0	0±0 0±0	0±0 0±0	0±0 0±0	0±0 0±0	0±0 0±0	0±0 0±0	0±0 0±0
Crustacea	*Macrostylis sp.*	0±0 0±0	0±0 0±0	0±0 0±0	0±0 0±0	0±0 0±0	0±0 0±0	0±0 0±0	0±0 0±0	0.33±0.58 0.04±0.06	0±0 0±0	0±0 0±0	0±0 0±0	0±0 0±0	0±0 0±0	0±0 0±0	0±0 0±0	0±0 0±0

Table A.3 – continued

Phylum	Taxon	19-4	36-2	45-4	76-2	69-1	84-1	68-1	85-1	93-2	105-1	115-2	107-1	122-1 129-1	125-2	139-3	139-2	154-1
Crustacea	*Macrostylis spinifera*	0±0	0±0	0±0	0.33±0.58	0±0	0±0	0±0	0±0	0±0	0±0	0±0	0±0	0±0	0±0	0±0	0±0	0±0
		0±0	0±0	0±0	0.08±0.13	0±0	0±0	0±0	0±0	0±0	0±0	0±0	0±0	0±0	0±0	0±0	0±0	0±0
Crustacea	Melitidae	0±0	0±0	0±0	0±0	0±0	0±0	0±0	0±0	0±0	0±0	0±0	0±0	0±0	0±0	0.33±0.58	0±0	0±0
		0±0	0±0	0±0	0±0	0±0	0±0	0±0	0±0	0±0	0±0	0±0	0±0	0±0	0±0	0.37±0.64	0±0	0±0
Crustacea	*Microjaera anisopoda*	0±0	0±0	0±0	0±0	0.33±0.58	0±0	0±0	0±0	0±0	0±0	0±0	0±0	0±0	0±0	0±0	0±0	0±0
		0±0	0±0	0±0	0±0	0.13±0.22	0±0	0±0	0±0	0±0	0±0	0±0	0±0	0±0	0±0	0±0	0±0	0±0
Crustacea	*Munna acanthifera*	0±0	0±0	0±0	0±0	0±0	0±0	0±0	0±0	0±0	0±0	0±0	0±0	0±0	0±0	0±0	0±0	0.33±0.58
		0±0	0±0	0±0	0±0	0±0	0±0	0±0	0±0	0±0	0±0	0±0	0±0	0±0	0±0	0±0	0±0	0.19±0.33
Crustacea	*Munna sp. I*	0±0	0±0	0±0	0±0	0±0	0±0	0±0	0±0	0±0	0±0	0±0	0±0	0±0	0±0	0±0	0±0	0.33±0.58
		0±0	0±0	0±0	0±0	0±0	0±0	0±0	0±0	0±0	0±0	0±0	0±0	0±0	0±0	0±0	0±0	0.13±0.23
Crustacea	Nannastacidae indet	0±0	0±0	0±0	0±0	0±0	0±0	0±0	0±0	0±0	0±0	0±0	0±0	0.17±0.41	0±0	0±0	0±0	0±0
		0±0	0±0	0±0	0±0	0±0	0±0	0±0	0±0	0±0	0±0	0±0	0±0	0.03±0.07	0±0	0±0	0±0	0±0
Crustacea	*Nannastacus sp.*	0±0	0.33±0.58	0±0	0±0	0±0	0±0	0.33±0.58	0±0	0±0	0±0	0±0	0±0	0±0	0±0	0±0	0±0	0±0
		0±0	0.5±0.87	0±0	0±0	0±0	0±0	0.01±0.02	0±0	0±0	0±0	0±0	0±0	0±0	0±0	0±0	0±0	0±0
Crustacea	*Ornatoscalpellum stroemi*	0±0	0±0	0±0	0±0	0±0	0±0	0±0	0±0	0±0	0±0	0±0	0±0	0±0	0±0	0.33±0.58	0±0	0±0
		0±0	0±0	0±0	0±0	0±0	0±0	0±0	0±0	0±0	0±0	0±0	0±0	0±0	0±0	2.37±4.1	0±0	0±0
Crustacea	Ostracoda	0.33±0.58	0±0	0±0	0±0	0±0	0±0	0±0	0±0	0±0	0±0	0±0	0±0	0±0	0±0	0±0	0±0	0±0
		0.06±0.1	0±0	0±0	0±0	0±0	0±0	0±0	0±0	0±0	0±0	0±0	0±0	0±0	0±0	0±0	0±0	0±0
Crustacea	Ostracoda I	0±0	0±0	0±0	0±0	0±0	0±0	0±0	0±0	0±0	0±0	0±0	0±0	0.17±0.41	0±0	0±0	0±0	0±0
		0±0	0±0	0±0	0±0	0±0	0±0	0±0	0±0	0±0	0±0	0±0	0±0	0.04±0.1	0±0	0±0	0±0	0±0
Crustacea	Ostracoda II	0±0	0±0	0±0	0±0	0±0	0±0	0±0	0±0	0±0	0±0	0±0	0±0	0.17±0.41	0±0	0±0	0±0	0±0
		0±0	0±0	0±0	0±0	0±0	0±0	0±0	0±0	0±0	0±0	0±0	0±0	0.19±0.48	0±0	0±0	0±0	0±0
Crustacea	Ostracoda III	0±0	1±1	0±0	0±0	0±0	0±0	0±0	0±0	0±0	0±0	0±0	0±0	0±0	0±0	0±0	0±0	0±0
		0±0	0.06±0.05	0±0	0±0	0±0	0±0	0±0	0±0	0±0	0±0	0±0	0±0	0±0	0±0	0±0	0±0	0±0
Crustacea	Ostracoda IV	0±0	0±0	0.25±0.5	0±0	0±0	0±0	0±0	0±0	0±0	0±0	0±0	0±0	0±0	0±0	0±0	0±0	0±0
		0±0	0±0	0.02±0.04	0±0	0±0	0±0	0±0	0±0	0±0	0±0	0±0	0±0	0±0	0±0	0±0	0±0	0±0
Crustacea	Ostracoda V	0±0	0±0	0±0	0±0	0±0	0±0	0±0	0±0	0±0	0±0	0±0	0±0	0.17±0.41	0±0	0±0	0±0	0±0
		0±0	0±0	0±0	0±0	0±0	0±0	0±0	0±0	0±0	0±0	0±0	0±0	0.05±0.12	0±0	0±0	0±0	0±0
Crustacea	Ostracoda VI	0±0	0±0	0±0	0±0	0±0	0±0	0±0	0±0	0±0	0±0	0±0	0±0	0±0	0±0	0±0	0.33±0.58	0±0
		0±0	0±0	0±0	0±0	0±0	0±0	0±0	0±0	0±0	0±0	0±0	0±0	0±0	0±0	0±0	0.09±0.15	0±0
Crustacea	*Pleuroprion frigidum*	0±0	0±0	0±0	0±0	0±0	0±0	0±0	0±0	0±0	0±0	0±0	0±0	0.33±0.82	0±0	0±0	0±0	0±0
		0±0	0±0	0±0	0±0	0±0	0±0	0±0	0±0	0±0	0±0	0±0	0±0	3.4±8.33	0±0	0±0	0±0	0±0
Crustacea	Tanaidacea I	0±0	0±0	0±0	0±0	0±0	0±0	0±0	0±0	0±0	0±0	0±0	0±0	0±0	0±0	0±0	0±0	0±0
		0±0	0±0	0±0	0±0	0±0	0±0	0±0	0±0	0±0	0±0	0±0	0±0	0±0	0±0	0±0	0±0	0±0
Crustacea	Tanaidacea III	0±0	0±0	0±0	0±0	0±0	0±0	0±0	0±0	0±0	0±0	0±0	0±0	0±0	0±0	0±0	0±0	0±0
		0±0	0±0	0±0	0±0	0±0	0±0	0±0	0±0	0±0	0±0	0±0	0±0	0±0	0±0	0±0	0±0	0±0
Crustacea	*Thorkelius sp.*	0±0	0.33±0.58	0.25±0.5	0±0	1±1	0±0	0±0	0±0	0±0	0±0	0±0	0±0	0±0	0±0	0±0	0±0	0±0
		0±0	0.02±0.03	0.02±0.05	0±0	0.09±0.14	0±0	0±0	0±0	0±0	0±0	0±0	0±0	0±0	0±0	0±0	0±0	0±0
Crustacea	*Typhlotanais sp.*	0±0	0±0	0±0	0±0	0±0	0±0	0±0	0±0	0±0	0±0	0±0	0±0	0±0	0.33±0.58	0±0	0±0	0±0
		0±0	0±0	0±0	0±0	0±0	0±0	0±0	0±0	0±0	0±0	0±0	0±0	0±0	0.02±0.03	0±0	0±0	0±0
Echinodermata	*Ctenodiscus crispatus*	0±0	0±0	0±0	0±0	0±0	0±0	0±0	0±0	0±0	0±0	0±0	0±0	0±0	0±0	0.33±0.58	0.33±0.58	0±0
		0±0	0±0	0±0	0±0	0±0	0±0	0±0	0±0	0±0	0±0	0±0	0±0	0±0	0±0	8.66±15	1924.2±3332.81	0±0
Echinodermata	*Ophiocten sericeum*	0±0	0±0	0±0	0±0	0±0	0±0	0±0	0±0	0±0	0±0	0±0	0±0	0.67±0.82	0.33±0.58	0±0	0±0	0±0
		0±0	0±0	0±0	0±0	0±0	0±0	0±0	0±0	0±0	0±0	0±0	0±0	333.69±596.1	1.95±3.37	0±0	0±0	0±0
Echinodermata	*Ophiopleura borealis*	0±0	0±0	0±0	0±0	0±0	0±0	0.33±0.58	0±0	0±0	0±0	0±0	0±0	0±0	0±0	0±0	0±0	0±0
		0±0	0±0	0±0	0±0	0±0	0±0	1016±1759.76	0±0	0±0	0±0	0±0	0±0	0±0	0±0	0±0	0±0	0±0
Echinodermata	*Ophiopus arcticus?*	0±0	0±0	0.25±0.5	0±0	0±0	0±0	0±0	0±0	0±0	0±0	0.33±0.58	0±0	0.5±0.84	0±0	0±0	0±0	0±0
		0±0	0±0	0.49±0.98	0±0	0±0	0±0	0±0	0±0	0±0	0±0	0.73±1.27	0±0	0.32±0.74	0±0	0±0	0±0	0±0
Echinodermata	Ophiuroid indef	0±0	0±0	0±0	0±0	0.33±0.58	0±0	0±0	0±0	0±0	0±0	0±0	0±0	0±0	0±0	0±0	0±0	0±0
		0±0	0±0	0±0	0±0	30.7±53.17	0±0	0±0	0±0	0±0	0±0	0±0	0±0	0±0	0±0	0±0	0±0	0±0
Echinodermata	*Pourtalesia jeffreysi gibbosa*	0±0	0±0	0±0	0±0	0.33±0.58	0±0	0±0	0±0	0±0	0±0	0±0	0±0	0±0	0±0	0±0	0±0	0±0
		0±0	0±0	0±0	0±0	237.17±410.78	0±0	0±0	0±0	0±0	0±0	0±0	0±0	0±0	0±0	0±0	0±0	0±0
Mollusca	*Astarte montagui*	0±0	0±0	0±0	0±0	0±0	0±0	0±0	0±0	0±0	0±0	0±0	0±0	0.33±0.82	0±0	0±0	0±0	0±0
		0±0	0±0	0±0	0±0	0±0	0±0	0±0	0±0	0±0	0±0	0±0	0±0	4.23±10.35	0±0	0±0	0±0	0±0
Mollusca	*Bathyarca pectunculoides*	0±0	0±0	0±0	0.33±0.58	1±0	0±0	0±0	0±0	0.33±0.58	0.33±0.58	0±0	1±1	0±0	0.33±0.58	0.33±0.58	0±0	0.33±0.58
		0±0	0±0	0±0	0.48±0.83	0.53±0.39	0±0	0±0	0±0	0.01±0.02	0.98±1.69	0±0	0.93±1.39	0±0	0.47±0.81	0.92±1.6	0±0	0.01±0.02
Mollusca	Bivalvia juv.	4±2.65	0.33±0.58	0.5±0.58	0±0	0±0	0±0	0±0	0±0	0±0	0±0	0±0	0±0	0±0	0±0	0±0	0±0	0±0
		0.37±0.51	0.03±0.05	0.01±0.01	0±0	0±0	0±0	0±0	0±0	0±0	0±0	0±0	0±0	0±0	0±0	0±0	0±0	0±0
Mollusca	Caudofoveata I	0±0	0.33±0.58	0.5±0.58	0±0	0±0	0±0	0±0	0±0	0±0	0±0	0±0	0±0	0±0	0±0	0±0	0±0	0±0
		0±0	0.33±0.57	56.42±110.33	0±0	0±0	0±0	0±0	0±0	0±0	0±0	0±0	0±0	0±0	0±0	0±0	0±0	0±0
Mollusca	Caudofoveata II	0±0	0.33±0.58	0±0	0±0	0±0	0±0	0±0	0±0	0±0	0±0	0±0	0±0	0±0	0±0	0±0	0±0	0±0
		0±0	0.33±0.57	0±0	0±0	0±0	0±0	0±0	0±0	0±0	0±0	0±0	0±0	0±0	0±0	0±0	0±0	0±0

Table A.3 – continued

Phylum	Taxon	19-4	36-2	45-4	76-2	69-1	84-1	68-1	85-1	93-2	105-1	115-2	107-1	122-1 129-1	125-2	139-3	139-2	154-1
Mollusca	Cuspidaria juv.	0±0	0±0	0±0	0±0	0±0	0±0	0±0	0±0	0±0	1±0	0±0	0±0	0±0	0±0	0±0	0±0	0±0
		0±0	0±0	0±0	0±0	0±0	0±0	0±0	0±0	0±0	1.26±1.92	0±0	0±0	0±0	0±0	0±0	0±0	0±0
Mollusca	*Cuspidaria sp. I*	0±0	0±0	0±0	0±0	0.33±0.58	0±0	0±0	0±0	0±0	0±0	0±0	0±0	0±0	0±0	0±0	0±0	0±0
		0±0	0±0	0±0	0±0	4.04±7	0±0	0±0	0±0	0±0	0±0	0±0	0±0	0±0	0±0	0±0	0±0	0±0
Mollusca	*Cuspidaria sp. II*	0±0	0±0	0±0	0.33±0.58	0±0	0±0	0±0	0±0	0±0	0±0	0±0	0±0	0±0	0±0	0±0	0±0	0±0
		0±0	0±0	0±0	0.49±0.85	0±0	0±0	0±0	0±0	0±0	0±0	0±0	0±0	0±0	0±0	0±0	0±0	0±0
Mollusca	*Cyclopecten hoskynsi*	0±0	0±0	0±0	0.33±0.58	0±0	0±0	0±0	0±0	0±0	0±0	0±0	0±0	0±0	0±0	0±0	0±0	0±0
		0±0	0±0	0±0	2.28±3.95	0±0	0±0	0±0	0±0	0±0	0±0	0±0	0±0	0±0	0±0	0±0	0±0	0±0
Mollusca	*Dacrydium vitreum*	0±0	0±0	0±0	1.33±1.53	0±0	0±0	0±0	0±0	0±0	0±0	0±0	0±0	0.5±0.55	0.33±0.58	0±0	0.33±0.58	0.33±0.58
		0±0	0±0	0±0	1.45±2.06	0±0	0±0	0±0	0±0	0±0	0±0	0±0	0±0	1.64±3.94	0.29±0.51	0±0	0.22±0.38	0.5±0.86
Mollusca	*Ennucula tenuis*	0±0	0.33±0.58	0±0	0±0	0±0	0±0	0±0	0±0	0±0	0±0	0±0	0±0	0±0	0±0	0±0	0±0	0±0
		0±0	0.05±0.08	0±0	0±0	0±0	0±0	0±0	0±0	0±0	0±0	0±0	0±0	0±0	0±0	0±0	0±0	0±0
Mollusca	Gastropoda juv.	0.33±0.58	0±0	0±0	0±0	0±0	0±0	0±0	0±0	0±0	0±0	0±0	0±0	0±0	0±0	0±0	0±0	0±0
		0.02±0.04	0±0	0±0	0±0	0±0	0±0	0±0	0±0	0±0	0±0	0±0	0±0	0±0	0±0	0±0	0±0	0±0
Mollusca	*Limatula cf. subauriculata*	0±0	0±0	0±0	0.33±0.58	0±0	0±0	0±0	0±0	0.67±1.15	0±0	0±0	0±0	0±0	0±0	0±0	0±0	0±0
		0±0	0±0	0±0	0.03±0.06	0±0	0±0	0±0	0±0	0.13±0.22	0±0	0±0	0±0	0±0	0±0	0±0	0±0	0±0
Mollusca	*Limatula subauriculata*	0±0	0±0	0±0	0±0	0±0	0±0	0±0	0±0	0±0	0±0	0±0	0.33±0.58	0±0	0±0	0±0	0±0	0±0
		0±0	0±0	0±0	0±0	0±0	0±0	0±0	0±0	0±0	0±0	0±0	37.87±65.59	0±0	0±0	0±0	0±0	0±0
Mollusca	*Macoma cf calcarea*	0±0	2±3.46	0±0	0±0	0±0	0±0	0±0	0±0	0±0	0±0	0±0	0±0	0.33±0.52	0±0	0±0	0.33±0.58	0±0
		0±0	0.49±0.86	0±0	0±0	0±0	0±0	0±0	0±0	0±0	0±0	0±0	0±0	0.05±0.08	0±0	0±0	0.21±0.37	0±0
Mollusca	*Margarites helicinus*	0±0	0±0	0±0	0±0	0±0	0±0	0±0	0±0	0±0	0±0	0±0	0±0	0.17±0.41	0±0	0±0	0±0	0±0
		0±0	0±0	0±0	0±0	0±0	0±0	0±0	0±0	0±0	0±0	0±0	0±0	0.18±0.45	0±0	0±0	0±0	0±0
Mollusca	*Philine sp.*	0±0	0±0	0±0	0.33±0.58	0.33±0.58	0±0	0±0	0±0	0±0	0±0	0±0	0±0	0.33±0.52	0.33±0.58	0±0	0±0	0±0
		0±0	0±0	0±0	0.08±0.14	1.48±2.56	0±0	0±0	0±0	0±0	0±0	0±0	0±0	0.02±0.05	0.06±0.1	0±0	0±0	0±0
Mollusca	Solenogastres	0±0	0±0	0.25±0.5	0±0	0±0	0±0	0±0	0±0	0±0	0±0	0±0	0±0	0.17±0.41	0±0	0±0	0±0	0±0
		0±0	0±0	0.57±1.14	0±0	0±0	0±0	0±0	0±0	0±0	0±0	0±0	0±0	0.01±0.02	0±0	0±0	0±0	0±0
Mollusca	*Yoldiella annenkovae*	0±0	0±0	0±0	0±0	0±0	0±0	0±0	0±0	0±0	0±0	0.67±1.15	0±0	0.33±0.82	0±0	1.33±1.15	0±0	0±0
		0±0	0±0	0±0	0±0	0±0	0±0	0±0	0±0	0±0	0±0	0.88±1.53	0±0	0.19±0.47	0±0	0.67±0.7	0±0	0±0
Mollusca	*Yoldiella frigida*	0±0	0±0	0±0	0±0	0±0	0±0	0±0	0±0	0±0	0±0	0±0	0±0	1.33±1.03	0±0	0.67±1.15	0±0	0±0
		0±0	0±0	0±0	0±0	0±0	0±0	0±0	0±0	0±0	0±0	0±0	0±0	0.42±0.36	0±0	0.19±0.34	0±0	0±0
Mollusca	Yoldiella juv.	0±0	0±0	0.5±1	0.33±0.58	0.33±0.58	0±0	0±0	0±0	0±0	0±0	0±0	0±0	0±0	0±0	0±0	0±0	0±0
		0±0	0±0	0.16±0.32	0.14±0.24	0.05±0.08	0±0	0±0	0±0	0±0	0±0	0±0	0±0	0±0	0±0	0±0	0±0	0±0
Mollusca	*Yoldiella lenticula*	0±0	0±0	0.25±0.5	0±0	0.67±1.15	0±0	1.33±1.15	0±0	0±0	0±0	0.33±0.58	0±0	0.5±0.84	0±0	0±0	0±0	0±0
		0±0	0±0	0.48±0.95	0±0	0.49±0.84	0±0	5.98±5.55	0±0	0±0	0±0	0.88±1.53	0±0	0.35±0.61	0±0	0±0	0±0	0±0
Mollusca	*Yoldiella propinqua*	0±0	0±0	0±0	0±0	1±1	0±0	1±1.73	0±0	0±0	0±0	0±0	0±0	0±0	0±0	0±0	0±0	0±0
		0±0	0±0	0±0	0±0	8.52±13.14	0±0	9.93±17.2	0±0	0±0	0±0	0±0	0±0	0±0	0±0	0±0	0±0	0±0
Mollusca	*Yoldiella solidula*	0±0	0±0	0.25±0.5	0±0	0±0	0±0	0.67±1.15	0±0	0±0	0±0	0±0	0±0	0±0	0±0	0±0	0±0	0±0
		0±0	0±0	0.48±0.95	0±0	0±0	0±0	3.65±6.32	0±0	0±0	0±0	0±0	0±0	0±0	0±0	0±0	0±0	0±0
Mollusca	*Yoldiella sp.*	0±0	0±0	0.5±1	1±1	0±0	0±0	0.33±0.58	0±0	0±0	0±0	0±0	0±0	0±0	0±0	0±0	0±0	0±0
		0±0	0±0	0.86±1.72	1.68±2.52	0±0	0±0	2.33±4.04	0±0	0±0	0±0	0±0	0±0	0±0	0±0	0±0	0±0	0±0
Nemertea	*Micrura sp. ?*	0±0	0±0	0±0	0±0	0±0	0±0	0±0	0±0	0±0	0±0	0±0	0±0	0.17±0.41	0±0	0±0	0±0	0±0
		0±0	0±0	0±0	0±0	0±0	0±0	0±0	0±0	0±0	0±0	0±0	0±0	45.27±110.88	0±0	0±0	0±0	0±0
Porifera	Porifera? I	0±0	0.33±0.58	0.25±0.5	0±0	0±0	0±0	0±0	0±0	0±0	0±0	0±0	0±0	0±0	0±0	0.33±0.58	0±0	0±0
		0±0	1.82±3.15	0±0	0±0	0±0	0±0	0±0	0±0	0±0	0±0	0±0	0±0	0±0	0±0	5.62±9.73	0±0	0±0
Porifera	Porifera? II	0±0	0±0	0±0	0±0	0±0	0±0	0±0	0±0	0±0	0±0	0±0	0±0	0±0	0±0	0±0	0±0	0.33±0.58
		0±0	0±0	0±0	0±0	0±0	0±0	0±0	0±0	0±0	0±0	0±0	0±0	0±0	0±0	0±0	0±0	0.48±0.83
Sipuncula	*Nephasoma diaphanes*	1±1.73	1±1	0.75±0.96	0.33±0.58	0.33±0.58	0±0	1±1	0.33±0.58	0.33±0.58	0±0	0.33±0.58	0.67±1.15	0.33±0.52	0.67±1.15	1.33±2.31	0±0	1.33±0.58
		1.14±1.98	0.22±0.2	0.27±0.31	0.32±0.55	0.18±0.32	0±0	5.59±9.56	2.84±4.92	1.39±2.4	0±0	0.1±0.18	4.76±8.24	0.27±0.63	0.31±0.53	0.74±1.29	0±0	0.29±0.31
Sipuncula	*Nephasoma lilljeborgi*	0±0	0±0	0±0	0±0	0±0	0±0	1±1.73	0±0	0±0	0±0	0±0	0±0	0.33±0.82	0±0	0.33±0.58	0±0	0±0
		0±0	0±0	0±0	0±0	0±0	0±0	23.94±41.47	0±0	0±0	0±0	0±0	0±0	1.12±2.74	0±0	0.62±1.07	0±0	0±0
Sipuncula	*Nephasoma sp.*	0±0	0±0	0±0	0±0	0±0	0±0	0±0	0±0	0±0	0±0	0±0	0±0	0±0	0±0	0.33±0.58	0±0	0±0
		0±0	0±0	0±0	0±0	0±0	0±0	0±0	0±0	0±0	0±0	0±0	0±0	0±0	0±0	0.01±0.02	0±0	0±0
Sipuncula	*Onchesoma stenrupii*	0±0	0.33±0.58	0.25±0.5	0±0	0±0	0.33±0.58	0±0	0±0	0.33±0.58	0.33±0.58	0±0	0±0	0±0	0±0	0±0	0±0	0±0
		0±0	0.08±0.13	0.03±0.06	0±0	0±0	0.06±0.1	0±0	0±0	0.53±0.92	0.32±0.55	0±0	0±0	0±0	0±0	0±0	0±0	0±0
Sipuncula	Sipuncula indef	0.33±0.58	0±0	1±2	0±0	0±0	0±0	0±0	0.33±0.58	0±0	0±0	0±0	0.33±0.58	0±0	0±0	0.33±0.58	0±0	0±0
		0±0.01	0±0	0.07±0.14	0±0	0±0	0±0	0±0	0.23±0.39	0±0	0±0	0±0	0.82±1.42	0±0	0±0	0.3±0.51	0±0	0±0
Sipuncula	Sipuncula indef II	0±0	0±0	0±0	0±0	0±0	0±0	0±0	0±0	0±0	0±0	0±0	0±0	0±0	0±0	0.33±0.58	0±0	0±0
		0±0	0±0	0±0	0±0	0±0	0±0	0±0	0±0	0±0	0±0	0±0	0±0	0±0	0±0	0.03±0.06	0±0	0±0
Sipuncula	Sipuncula juv.	0±0	0±0	0±0	0.33±0.58	0±0	0±0	0±0	0±0	0.33±0.58	0±0	0±0	0±0	0.17±0.41	0±0	1±1.73	0±0	0±0
		0±0	0±0	0±0	0.02±0.03	0±0	0±0	0±0	0±0	0±0	0±0	0±0	0±0	0.01±0.03	0±0	0.77±1.33	0±0	0±0

Table A.3 – continued

Phylum	Taxon	19-4	36-2	45-4	76-2	69-1	84-1	68-1	85-1	93-2	105-1	115-2	107-1	122-1 129-1	125-2	139-3	139-2	154-1
	indef	0±0 0±0	0±0 0±0	0±0 0±0	0±0 0±0	0.67±1.15 0±0	0±0 0±0	0±0 0.05±0.09	0±0 0±0	0±0 0±0	0±0 0±0	0±0 0±0	0±0 0±0	0.33±0.52 1.32±2.86	0±0 1.46±2.53	0±0 4.92±1.48	0±0 0±0	0±0 0±0
Foraminifera																		
Foraminifera	Astrorhiza sp.	0.33±0.58 0±0	0±0 0±0	10.75±7.18 0±0	0±0 0±0	0.67±1.15 0±0	0±0 0±0	0±0 0±0	0±0 0±0	0±0 0±0	0.33±0.58 0±0	0±0 0±0	0±0 0±0	2.83±3.25 0±0	1.33±1.53 0±0	0±0 0±0	4.33±4.16 0±0	0±0 0±0
Foraminifera	*Cassidulina teretis*	0±0 0±0	0±0 0±0	0±0 0±0	0±0 0±0	0±0 0±0	0±0 0±0	0±0 0±0	0±0 0±0	0±0 0±0	0±0 0±0	0±0 0±0	0±0 0±0	0.5±0.84 0±0	0±0 0±0	0±0 0±0	0±0 0±0	0±0 0±0
Foraminifera	*Cibicidoides lobatulus*	0±0 0±0	0±0 0±0	33.25±15.17 0±0	0.33±0.58 0±0	0±0 0±0	0±0 0±0	0.33±0.58 0±0	0±0 0±0	0.67±1.15 0±0	0.33±0.58 0±0	0.33±0.58 0±0	0±0 0±0	16.33±10.39 0±0	1.67±2.08 0±0	0±0 0±0	0±0 0±0	0±0 0±0
Foraminifera	*Cribrostomoides subglobosum*	0±0 0±0	0±0 0±0	0±0 0±0	0±0 0±0	0±0 0±0	0±0 0±0	0±0 0±0	0±0 0±0	2.67±2.08 0±0	9±1 0±0	10.33±3.06 0±0	0±0 0±0	4.17±1.17 0±0	14±5.29 0±0	0±0 0±0	49.67±18.58 0±0	2.33±1.15 0±0
Foraminifera	*Crithionina granum*	0±0 0±0	0±0 0±0	0±0 0±0	0±0 0±0	8±13.86 0±0	0±0 0±0	0±0 0±0	0±0 0±0	0±0 0±0	0±0 0±0	0±0 0±0	0±0 0±0	0±0 0±0	0±0 0±0	0±0 0±0	0±0 0±0	0±0 0±0
Foraminifera	*Crithionina hispida*	0±0 0±0	0±0 0±0	0±0 0±0	0±0 0±0	0±0 0±0	0±0 0±0	0±0 0±0	0±0 0±0	1.33±1.53 0±0	4.33±3.21 0±0	2.33±2.52 0±0	0±0 0±0	0±0 0±0	0±0 0±0	0±0 0±0	0±0 0±0	0±0 0±0
Foraminifera	*Crithionina pisum*	0.33±0.58 0±0	0±0 0±0	0±0 0±0	0±0 0±0	0±0 0±0	0±0 0±0	0±0 0±0	0±0 0±0	0±0 0±0	0.67±1.15 0±0	0.33±0.58 0±0	0±0 0±0	0.17±0.41 0±0	0±0 0±0	0±0 0±0	0±0 0±0	4±1.73 0±0
Foraminifera	*Cuneata arctica*	0±0 0±0	0±0 0±0	0±0 0±0	7.33±3.79 0±0	0±0 0±0	0.33±0.58 0±0	0±0 0±0	0.33±0.58 0±0	4±3.61 0±0	6.33±1.15 0±0	2.67±2.31 0±0	0±0 0±0	14.33±6.95 0±0	16±6.56 0±0	0±0 0±0	26.33±7.37 0±0	11±4.58 0±0
Foraminifera	*Dentalina frobischerensis*	0±0 0±0	0±0 0±0	1±2 0±0	0±0 0±0	0±0 0±0	0±0 0±0	0±0 0±0	0±0 0±0	0±0 0±0	0±0 0±0	0±0 0±0	0±0 0±0	0±0 0±0	0±0 0±0	0±0 0±0	0±0 0±0	0±0 0±0
Foraminifera	*Elphidium excavatum*	0±0 0±0	0±0 0±0	0±0 0±0	0±0 0±0	0±0 0±0	0±0 0±0	0±0 0±0	0±0 0±0	0±0 0±0	0±0 0±0	0±0 0±0	0±0 0±0	8±5.22 0±0	2.67±4.62 0±0	0±0 0±0	0±0 0±0	0±0 0±0
Foraminifera	*Hormosinella guttifer*	0±0 0±0	0.33±0.58 0±0	5±10 0±0	0±0 0±0	0±0 0±0	0±0 0±0	0±0 0±0	0±0 0±0	0±0 0±0	0±0 0±0	0±0 0±0	0±0 0±0	0±0 0±0	0±0 0±0	0±0 0±0	0±0 0±0	0±0 0±0
Foraminifera	*Hyalinea baltica*	0±0 0±0	0±0 0±0	0±0 0±0	0±0 0±0	0±0 0±0	0±0 0±0	0±0 0±0	0±0 0±0	0±0 0±0	0±0 0±0	0.33±0.58 0±0	0±0 0±0	0±0 0±0	0±0 0±0	0±0 0±0	0±0 0±0	0±0 0±0
Foraminifera	*Hyperammina sp.*	2.33±1.53 0±0	9.67±5.51 0±0	11.75±11.09 0±0	0±0 0±0	1.67±2.08 0±0	0±0 0±0	0±0 0±0	0±0 0±0	0±0 0±0	0±0 0±0	0±0 0±0	0±0 0±0	1±1.26 0±0	0±0 0±0	0±0 0±0	0±0 0±0	0±0 0±0
Foraminifera	*Islandiella norcrossi*	0±0 0±0	0±0 0±0	0±0 0±0	0±0 0±0	0±0 0±0	0±0 0±0	0±0 0±0	0±0 0±0	0±0 0±0	0±0 0±0	0±0 0±0	0±0 0±0	0±0 0±0	0.33±0.58 0±0	0±0 0±0	0±0 0±0	0±0 0±0
Foraminifera	Komokioidea	13.33±10.79 5.85±4.89	3.33±5.77 1.13±1.97	0±0 0±0	0±0 0±0	0±0 0±0	0±0 0±0	2±1 1.2±0.23	0±0 0±0	1±1.73 0.1±0.17	3.33±3.51 7.25±10.49	1±1 2.54±2.71	0±0 0±0	0.5±0.55 0.09±0.16	0±0 0±0	6±0 10.07±5.44	0.67±0.58 3.78±6.02	0±0 0±0
Foraminifera	*Labrospira crassimargo*	0±0 0±0	0±0 0±0	195.5±94.89 0±0	0±0 0±0	0±0 0±0	0±0 0±0	0±0 0±0	0±0 0±0	0.67±1.15 0±0	0±0 0±0	0±0 0±0	0±0 0±0	0±0 0±0	0±0 0±0	0±0 0±0	0±0 0±0	0±0 0±0
Foraminifera	*Nonion sp.*	0±0 0±0	0±0 0±0	0±0 0±0	0±0 0±0	0±0 0±0	0±0 0±0	0±0 0±0	0±0 0±0	0±0 0±0	0±0 0±0	0±0 0±0	0±0 0±0	4±6.2 0±0	0±0 0±0	0±0 0±0	0±0 0±0	0±0 0±0
Foraminifera	*Oolina sp.*	0±0 0±0	0±0 0±0	0±0 0±0	1.33±1.53 0±0	0±0 0±0	1.33±0.58 0±0	0±0 0±0	0±0 0±0	0±0 0±0	0±0 0±0	0±0 0±0	0±0 0±0	0±0 0±0	0±0 0±0	0±0 0±0	0±0 0±0	0±0 0±0
Foraminifera	*Pullenia sp.*	0±0 0±0	0±0 0±0	0±0 0±0	4±3.46 0±0	3.67±4.04 0±0	0±0 0±0	2.67±4.62 0±0	0±0 0±0	2±0 0±0	3.33±0.58 0±0	0±0 0±0	0±0 0±0	1±1.26 0±0	0.67±0.58 0±0	0±0 0±0	0±0 0±0	0.33±0.58 0±0
Foraminifera	*Pyrgo sp.*	0±0 0±0	0±0 0±0	1±2 0±0	2.67±1.53 0±0	25±20.66 0±0	1.67±2.08 0±0	0±0 0±0	0±0 0±0	0.33±0.58 0±0	2.67±1.15 0±0	0±0 0±0	0±0 0±0	4.67±4.89 0±0	0±0 0±0	0±0 0±0	0±0 0±0	0±0 0±0
Foraminifera	*Quinqueloculina sp.*	0±0 0±0	0±0 0±0	2±2.31 0±0	5±4.58 0±0	102.33±118.32 0±0	2.33±7.77 0±0	126.67±100.58 0±0	41.67±6.43 0±0	8.33±2.08 0±0	10±2.65 0±0	2.67±0.58 0±0	0±0 0±0	1.67±1.63 0±0	1.33±1.53 0±0	0±0 0±0	0±0 0±0	0±0 0±0
Foraminifera	*Reophax nodulosus*	0±0 0±0	0±0 0±0	0±0 0±0	0±0 0±0	0±0 0±0	0±0 0±0	0±0 0±0	0±0 0±0	0.33±0.58 0±0	0±0 0±0	0±0 0±0	0±0 0±0	0±0 0±0	0±0 0±0	0±0 0±0	0±0 0±0	0±0 0±0
Foraminifera	*Rhabdammina sp.*	0±0 0±0	0±0 0±0	0±0 0±0	5.33±3.06 0±0	1.33±2.31 0±0	0±0 0±0	3.33±1.15 0±0	2.67±1.53 0±0	14.67±5.03 0±0	7.33±1.15 0±0	1±0 0±0	0±0 0±0	2.17±1.72 0±0	10.33±4.73 0±0	0±0 0±0	1.33±0.58 0±0	0±0 0±0
Foraminifera	*Rupertina stabilis*	0±0 0±0	0±0 0±0	0±0 0±0	0±0 0±0	0±0 0±0	0±0 0±0	0±0 0±0	0±0 0±0	0±0 0±0	0±0 0±0	0±0 0±0	0±0 0±0	0±0 0±0	0±0 0±0	0±0 0±0	0±0 0±0	5.33±5.13 0±0
Foraminifera	*Saccammina sp.*	0±0 0±0	0±0 0±0	4±5.66 0±0	3.67±2.52 0±0	31.67±20.5 0±0	3.33±2.52 0±0	0±0 0±0	0±0 0±0	0±0 0±0	4.67±5.69 0±0	0±0 0±0	0±0 0±0	0.17±0.41 0±0	0±0 0±0	0±0 0±0	2±1 0±0	0±0 0±0
Foraminifera	Saccamminidae	0±0 0±0	0±0 0±0	0±0 0±0	0±0 0±0	0±0 0±0	0±0 0±0	5.33±6.11 0±0	0.33±0.58 0±0	0±0 0±0	0±0 0±0	0±0 0±0	0±0 0±0	0±0 0±0	0±0 0±0	0±0 0±0	0±0 0±0	0±0 0±0
Foraminifera	Saccorhiza ramosa	0±0 0±0	0±0 0±0	6±7.66 0±0	0±0 0±0	4.33±3.51 0±0	1.33±2.31 0±0	0±0 0±0	0±0 0±0	2.67±1.53 0±0	2.33±4.04 0±0	2.67±3.79 0±0	0±0 0±0	4.83±4.22 0±0	9.67±8.5 0±0	0±0 0±0	0±0 0±0	0±0 0±0
Foraminifera	*Vaginulina linearis*	0±0 0±0	0±0 0±0	0±0 0±0	0±0 0±0	0±0 0±0	0±0 0±0	0±0 0±0	0±0 0±0	0±0 0±0	0±0 0±0	0±0 0±0	0±0 0±0	0.17±0.41 0±0	0.33±0.58 0±0	0±0 0±0	0±0 0±0	0±0 0±0
Foraminifera	Foram indef	0±0 0±0	0.33±0.58 0±0	0±0 0±0	0.67±0.58 0±0	3.33±4.16 0±0	0.33±0.58 0±0	0±0 0±0	0.33±0.58 0±0	0±0 0±0	0±0 0±0	0±0 0±0	0±0 0±0	0±0 0±0	0±0 0±0	0±0 0±0	0±0 0±0	0±0 0±0

Table A.3 – continued

Phylum	Taxon	19-4	36-2	45-4	76-2	69-1	84-1	68-1	85-1	93-2	105-1	115-2	107-1	122-1 129-1	125-2	139-3	139-2	154-1
Foraminifera	Foram indef II	0±0	0±0	0±0	0±0	0±0	0±0	0±0	0±0	0±0	0±0	0±0	0±0	0±0	0.33±0.58	0±0	0±0	0±0
		0±0	0±0	0±0	0±0	0±0	0±0	0±0	0±0	0±0	0±0	0±0	0±0	0±0	0±0	0±0	0±0	0±0
Foraminifera	Foram indef. III	0±0	0±0	0±0	0±0	0±0	0±0	0±0	0±0	0±0	0±0	0±0	0±0	0±0	0±0	0±0	0±0	4.33±4.51
		0±0	0±0	0±0	0±0	0±0	0±0	0±0	0±0	0±0	0±0	0±0	0±0	0±0	0±0	0±0	0±0	0±0